

**Spectra of Atmospheric Motions in the Upper-Troposphere and  
Lower-Stratosphere over North America and Australia:  
Experimental Results and Theoretical Considerations**

By

Robert F. Abbey, Jr.

Department of Atmospheric Science  
Colorado State University  
Fort Collins, Colorado



**Department of  
Atmospheric Science**

Paper No. 211

SPECTRA OF ATMOSPHERIC MOTIONS IN THE UPPER-TROPOSPHERE AND  
LOWER-STRATOSPHERE OVER NORTH AMERICA AND AUSTRALIA:  
EXPERIMENTAL RESULTS AND THEORETICAL CONSIDERATIONS

by

Robert F. Abbey, Jr.

This report was prepared with support under  
Contract AT(11-1)-1340 with U.S. Atomic Energy Commission.

Principal Investigator: E. R. Reiter

Atmospheric Science Paper No. 211

Department of Atmospheric Science

Colorado State University

Fort Collins, Colorado

July 1972

## ABSTRACT

Spectrum analysis of the 200- and 300-mb wind components for 127 North American stations and of the 30-, 35-, and 40,000 ft-level winds for 10 Australian stations, using one and five years of data respectively, reveal distinct geographical variations of spectral densities at particular frequencies. Maximum spectral energies occur at periodicities 4.9- and 3.4-days which are representative of the time-scale for synoptic disturbances. Generally, the meridional spectral values exceed the zonal ones. Wide variations in spectra for different years occur over Australia, probably due to a lack of an orographic anchoring effect. Since corresponding latitudes in the Northern and Southern Hemispheres did not have the same spectral characteristics, interhemispheric comparisons of spectra were made along the subtropical jet-stream axis, used as a "natural-coordinate" axis. These comparisons indicate that cyclones with periodicities of 3-6 days account for relatively more meridional transport of energy in the Southern than in the Northern Hemisphere. The strong horizontal gradients of the kinetic energy spectra in frequency space determined in this study suggest that a regional treatment of the multivariate kinetic energy equation will have to contend with a careful evaluation of boundary flux terms.

#### ACKNOWLEDGEMENTS

The author is deeply indebted to Dr. Elmar R. Reiter for his never ceasing flow of ideas and seemingly inexhaustible supply of new approaches to meteorological problems. Without his guidance and advice this study may have never come to full fruition.

The programming abilities of Carroll Underwood and Alice Fields, the typing of Juanita Veen, and the drafting of the figures by Dana Wooldridge are sincerely appreciated. Acknowledgement is also made to the National Center for Atmospheric Research, Boulder, Colorado, for permitting my use of their excellent computing facilities in handling the vast amount of data necessary in this investigation. Above all, to my family and especially my wife, Mary Kay, whose patience was taxed to the extreme but whose encouragement never waned, a heartfelt "thank you" seems inadequate to express my feelings.

## TABLE OF CONTENTS

	Page
TITLE PAGE.....	i
ABSTRACT.....	iii
ACKNOWLEDGEMENTS.....	iv
LIST OF TABLES.....	vii
LIST OF FIGURES.....	viii
1.0 INTRODUCTION.....	1
2.0 NATURE OF SPECTRUM ANALYSIS.....	5
2.1 Mathematical Formalism.....	5
2.2 Basic Considerations and Problems in Interpreting Spectra.....	8
3.0 SELECTION AND USE OF DATA.....	16
3.1 Determination of Seasons.....	18
4.0 SPECTRA OF WIND COMPONENTS - EXPERIMENTAL RESULTS.....	27
4.1 Resultant Mean Winds.....	27
4.2 Variance Distributions.....	31
4.3 General Considerations of Spectral Peaks.....	36
4.4 Latitudinal Analyses.....	39
4.5 Analyses of Seasonal Spectra.....	45
4.6 Australian Spectra.....	52
4.7 Interhemispheric Comparisons.....	70
4.8 Conclusions.....	76
5.0 SPECTRA OF WIND COMPONENTS - THEORETICAL CONSIDERATIONS.....	78
5.1 Numerical and Analytical Models.....	78
5.2 Horizontal Wave-number Spectra.....	91
5.3 Conversion from Frequency to Wave-number Domain.....	94

TABLE OF CONTENTS - Continued

	Page
6.0 SUMMARY AND CONCLUSIONS.....	99
REFERENCES.....	102
APPENDIX.....	108
A.1 Mean Zonal and Meridional Wind Speeds.....	108
B.1 Periodicity of 18.5 Days.....	112
B.2 Periodicities of 10.6 and 9.25 Days.....	116
B.3 Periodicity of 6.17 Days.....	120
B.4 Periodicity of 4.93 Days.....	123
B.5 Periodicity of 3.70 Days.....	124
B.6 Periodicity of 3.36 Days.....	129
C.1 General Conclusions from Periodicity Distributions.....	133

LIST OF TABLES

Table	Page
4.5-1 Variances and mean wind speeds for the various seasons at Nantucket, Oakland and Jackson.....	46
4.6-1 Yearly and five-year variances and the mean wind speeds for seven Australian stations at the 30,000 ft., 35,000 ft., and 40,000 ft. levels.....	58-60
4.7-1 Zonal spectral densities at selected periodicities for stations located along the Northern Hemispheric subtropical jet stream and the Southern Hemispheric STJ....	74
5.1-1 Categorization and synthesis of barotropic and baroclinic theoretical models. (Modified from Paegle, 1969).....	79-80
5.1-2 Periods for the kinetic energy oscillation found in the computations by Aihara (1961).....	83
5.2-1 Categorization and synthesis of previous studies done in the wave-number or space domain. (Modified from Paegle, 1969).....	92-93
5.3-1 Phase speed from a divergent and non-divergent barotropic model, and group velocity from a divergent barotropic model for different wavelengths (after Paegle, 1969).....	96

LIST OF FIGURES

<u>Figure</u>	<u>Page</u>
2.2-1 An example of aliasing: two functions with exactly the same values at a uniform sampling interval. Once the sample has been taken, it is impossible to know which was the original function.....	11
2.2-2 Nyquist folding of a spectrum. The sampling rate is $F$ . Spectral analysis of the sampled function shows all of the spectrum folded into the range $0 \leq f = F/2$ . (After Gauss, 1970).....	12
3.0-1 Most of the North American radiosonde data network used in this study. Stations indicated by a square comprise the basic network used in defining seasons and arriving at seasonal analyses.....	17
3.0-2 Australian stations used in this investigation.....	17
3.1-1 Time intervals and locations when wind speeds were greater than 50 m/sec at the (a) 200 mb and (b) 300 mb constant pressure level.....	20
3.1-2 Time intervals and locations when wind speeds were greater than 30 m/sec at the (a) 200 mb and (b) 300 mb constant pressure levels.....	21
3.1-3 Semimonthly mean zonal wind speed profiles in m/sec at 700 mb for the western portion of the Northern Hemisphere for February 13-26, 1968 (solid line), February 28-March 13, 1968 (dashed line), and March 13-27, 1968 (dash-dot line). (After Dickson, 1968).....	23
3.1-4 Schematic diagram indicating the partitioning of the data year into seasons using the (a) winter-short and spring-long and (b) winter-long and spring short definitions.....	26
4.1-1 Resultant mean winds at the 200 mb pressure level for (a) summer, (b) fall, (c) winter <sub>S</sub> , (d) winter <sub>L</sub> , (e) spring <sub>L</sub> and (f) spring <sub>S</sub> .....	28-30
4.2-1 The zonal wind variance distribution across North America at the (a) 200 mb and (b) 300 mb pressure levels.....	32
4.2-2 The meridional wind variance distribution across North America at the (a) 200 mb and (b) 300 mb pressure levels.....	33

LIST OF FIGURES - Continued

<u>Figure</u>	<u>Page</u>
4.2-3 Generalized tracks taken by (a) many lows or cyclones and (b) many highs or anticyclones; width of line suggests relative abundance. (After Visher, 1954.....	34
4.3-1 The distribution of peak energy densities summed over all North American stations examined per frequency interval for the (a) zonal and (b) meridional spectra at the 200 mb (solid line) and 300 mb (dashed line) levels.....	37
4.4-1 Zonal spectral densities at selected frequencies for stations located along 32°N: 10.6 days (solid line), 5.69 days (dashed line), 4.9 days (dash-two dot line), 3.36 days (dash-dot line).....	40
4.4-2 Meridional spectral densities at selected frequencies for stations located along 32°N: 9.25 days (solid line), 6.17 days (dashed line), 4.9 days (dash-two dot line), 3.2 days (dash-dot line).....	40
4.4-3 Spectra of the (a) 200 mb heights and (b) 500 mb heights for Amarillo, Texas (35° 14'N 101° 42'W), for the data record 7/1/67-6/30/68.....	43
4.5-1 Schematic representation of the possible effects on the wind variance by terminating the data record at different points in time.....	49
4.5-2 Winter-long (solid line) and winter-short (dashed line) spectra at the 200 mb level for the Nantucket (a) zonal and (b) meridional wind components.....	50
4.5-3 Spring-short (solid line) and spring-long (dashed line) spectra at the 200 mb level for the Nantucket (a) zonal and (b) meridional wind components.....	51
4.5-4 Spring-short (solid line) and spring-long (dashed line) spectra at the 200 mb level for the Oakland (a) zonal and (b) meridional wind components.....	53
4.5-5 Spring-short (solid line) and spring-long (dashed line) spectra at the 200 mb level for the Jackson (a) zonal and (b) meridional wind components.....	54
4.5-6 Winter-long (solid line) and winter-short (dashed line) spectra at the 300 mb level for the Oakland meridional wind component.....	55

LIST OF FIGURES - Continued

<u>Figure</u>	<u>Page</u>
4.6-1 Comparison of pressure-level statistics with height level statistics using the standard deviation of relative density. (After Essenwanger, private communication.).....	57
4.6-2 Monthly mean latitudes of the Southern Hemispheric 200 mb subtropical jet stream axis between 110°E and 170°E for 1956-1961. (After Weinert, 1968.).....	61
4.6-3 Annual variations of the mean latitude of the Southern Hemispheric 200 mb subtropical jet stream axis at 120°E for 1956-1961. (After Weinert, 1968.).....	62
4.6-4 Seasonal change in the mean latitudes of the Southern Hemispheric 200 mb subtropical jet stream axis from 110°E to 170°E for 1956-1961. (After Weinert, 1968.)....	63
4.6-5 Annual variations in the Alice Springs spectra for the (a) zonal and (b) meridional wind components for the years: 1958 (solid line), 1959 (dashed line), 1960 (dash-two dot line), and 1961 (dash-dot line).....	65
4.6-6 Height variations in the (a) zonal and (b) meridional spectra for Townsville, 1959: 30,000 ft. (solid line), 30,000 ft. (dashed line), and 40,000 ft. (dash-dot line).	66
4.6-7 Height variations in the (a) 1958 and (b) 1961 zonal and meridional spectra for Eagle Farm (Brisbane): 30,000 ft. (solid line), 35,000 ft. (dashed line), and 40,000 ft. (dash-dot line).....	67-68
4.7-1 Comparison of the (a) zonal and (b) meridional spectra between the 200 mb level at Midland, Texas (31°56'N), (solid line) and the 40,000 ft. level at Guildford (31°56'S) (dashed line).....	71
A.1-1 Geographic distributions of the mean zonal wind speeds at the (a) 200 mb and (b) 300 mb constant pressure levels for 7/1/67 - 6/30/68.....	109
A.1-2 Geographic distributions of the mean meridional wind speeds at the (a) 200 mb and (b) 300 mb constant pressure levels for 7/1/67 - 6/30/68.....	110
B.1-1 Geographic distributions of the zonal spectral densities at a period of 18.5 days at the (a) 200 mb and (b) 300 mb constant pressure levels.....	113

LIST OF FIGURES - Continued

<u>Figure</u>	<u>Page</u>
B.1-2 Geographic distributions of the meridional spectral densities at a period of 18.5 days at the (a) 200 mb and (b) 300 mb constant pressure levels.....	114
B.2-1 Geographic distributions of the zonal spectral densities at a period of 10.6 days at the (a) 200 mb and (b) 300 mb constant pressure levels.....	118
B.2-2 Geographic distributions of the meridional spectral densities at a period of 9.25 days at the (a) 200 mb and (b) 300 mb constant pressure levels.....	119
B.3-1 Geographic distributions of the zonal spectral densities at a period of 6.17 days at the 300 mb constant pressure level.....	121
B.3-2 Geographic distributions of the meridional spectral densities at a period of 6.17 days at the (a) 200 mb and (b) 300 mb constant pressure levels.....	122
B.4-1 Geographic distributions of the zonal spectral densities at a period of 4.93 days at the (a) 200 mb and (b) 300 mb constant pressure levels.....	125
B.4-2 Geographic distributions of the meridional spectral densities at a period of 4.93 days at the (a) 200 mb and (b) 300 mb constant pressure levels.....	126
B.4-3 Mean kinetic energies per unit volume [ $\text{kg m}^{-1} \text{sec}^{-2}$ for (a) January, (b) April, (c) July and (d) October. (After Lahey, et al., 1960).....	127
B.6-1 Geographic distributions of the zonal spectral densities at a period of 3.36 days at the (a) 200 mb and (b) 300 mb constant pressure levels.....	130
B.6-2 Geographic distributions of the meridional spectral densities at a period of 3.36 days at the (a) 200 mb and (b) 300 mb constant pressure levels.....	131

## 1.0 INTRODUCTION

Since the development of spectrum or harmonic analysis and the recognition of its value in understanding the behavior of meteorological parameters, many studies have been performed. Reiter (1969) gives an extensive bibliography of the work related to spectrum considerations in atmospheric transport processes. Convenient lists of previous efforts have been compiled by Shapiro and Ward (1963) and Vinnichenko (1969, 1970).

Two important problems characterize the previous work in this area. These difficulties arose out of the necessity to deal with relatively small data samples. With the exception of Chiu (1960), who analyzed data of no less than sixteen months duration, and Wiin-Nielsen (1967), who analyzed one year of data, the length of data samples is quite short. Kahn (1962) used only two months of data; Benton and Kahn (1958) utilized two separate samples (winter and summer) each of only two months duration; Van Mieghem, et al. (1959) handled two data samples of four months in length. Yanai and Murakami (1970) also employed only four months of data.

By including only one-third of the year's data, and this being generally the winter period, significant deviations from an annual mean can occur. This shortcoming is in addition to the already known "sampling" error. Although much has been learned from the above spectral studies, the conclusions drawn are applicable only during that particular period under investigation and only at the particular station being considered. The present study uses one year of data from the North American upper wind network which are analyzed for two time intervals, and five

years of Australian data for ten stations. Seasonal analyses considering all seasons with varying lengths of record are also discussed.

The second basic inadequacy hindering several of the previous investigations relates to the sparsity of stations examined. Few stations were analyzed, yet either explicitly or implicitly the results were applied to the latitude circle of a given station. In other words, longitudinal variations were not taken into account. Wooldridge and Reiter (1970) recognized this problem and advocated not only a larger data sample, but also the analysis of additional stations in order to remove any local bias from their conclusions. Chiu (1960) and Vinnichenko (1969, 1970) analyzed the two longest data samples but they utilized only one and two stations respectively, i.e., Washington, D.C.; Belmar, N.J. and Cocoa, Fla.

With the exception of the tropical studies by Yanai (1968), and Yanai and Murakami (1970) and the above noted examinations, many of the investigations were not concerned with the upper-troposphere and lower-stratosphere. The pioneering work, dealt with spectra near the ground (Panofsky and McCormick, 1954; Van der Hoven, 1957). Results from such efforts will be noted when they have value to the present study. Many analyses also dealt with the 500-mb level, presumably because this was the highest reliable level of data available. Rather than considering actual winds, several investigators made use of pressure charts and consequently of the geostrophic assumption, such as the charts prepared by Brooks, et al. (1950), Crutcher and Halligan (1967), Heastie and Stephenson (1960), Lahey, et al. (1960) and Serebreny, et al. (1958). Whereas the geostrophic assumption may lead

to large errors in the lower troposphere, the actual wind regime in the upper-troposphere can be approximated closely by the geostrophic equation (Haltiner and Martin, 1957). Any significant departures of the spectra thus computed from those derived from the actual winds will be pointed out later.

The many different ways of calculating and presenting spectra provide some difficulty in comparing the previous work with this study as well as with other research efforts. Reiter (1972) and Vinnichenko (1970) have done much to alleviate one problem by indicating the connection between spectral estimates in time (frequency) domain with those in the space (wave number) domain. A second problem arises when comparisons are made between data derived from a certain pressure level as opposed to data collected at a constant height. Essenwanger (private communication) has shown that there exists a significant difference between statistical parameters computed at pressure levels versus those computed at constant height surfaces. This will be discussed in Chapter 4 in connection with the Australian spectra.

It is not unexpected to find considerable differences among the results of many of these observational studies. Since many of the discrepancies may be due to the aforementioned inadequacies, an attempt is made to resolve some of these inconsistencies by examining spectra from twelve months of twice daily data from 127 North American radiosonde stations.

Southern Hemispheric data sources are not only scarce but often-times inadequate. However, the Australian radiosonde network does lend itself, to a limited extent, to such an examination as mentioned previously. Consequently, a rather brief and preliminary investigation

is undertaken concerning the possible nature of the atmospheric disturbances and their roles over Australia. Comparisons are then made with the results obtained from the North American analyses.

As will be shown in this paper, there exists both a latitudinal and a longitudinal gradient of spectral densities over North America. The present work is a larger, more comprehensive study than has hitherto been undertaken in the attempt to determine hemispheric circulation characteristics based on real data.

## 2.0 NATURE OF SPECTRUM ANALYSIS

Power spectrum analysis partitions total variance among effects due to different frequencies. In the case of wind speed, the variance is proportional to the kinetic energy distributed between two frequencies. This investigation employs the spectral technique developed by Blackman and Tukey (1959). Only the general development and basic concepts of spectrum analysis are presented here; proofs and derivations of significant equations are included when they aid in the understanding of the mathematics involved. For a detailed treatment of spectrum analysis the reader should consult Bendat and Piersol (1968), Blackburn (1970), Gauss (1970), Hannan (1970), Jenkins and Watts (1969), Muller (1966); approaches from the mathematician's viewpoint are found in Goodman (1957), Grenander and Rosenblatt (1957), Kendall (1946) and Wiener (1930, 1949).

### 2.1 Mathematical Formalism

To describe the basic properties of random physical data, four main types of statistical functions are utilized (Bendat and Piersol, 1968; Essenwanger, 1970; Jenkins and Watts, 1969; Panofsky and Brier, 1963): (1) mean square values, (2) probability density functions, (3) auto-correlation functions, and (4) power spectral density functions.

The mean square value permits a simple description of the intensity of the wind fluctuations. The probability density function furnishes information concerning the properties of the data in the amplitude domain. Its principal application in the measurements of physical data is to establish a probabilistic description for the

instantaneous values of the data. The auto-correlation function and the power spectral density function yield similar information in the time and frequency domains, respectively. The power spectral density function technically supplies no new information over the auto-correlation function since the two are Fourier transform pairs (Blackman and Tukey, 1959; Jenkins and Watts, 1969; Muller, 1966). However, the information to be gleaned from each is presented in a different format. For our purpose the power spectral density function will be employed solely.

It is desirable to think of the wind velocities in terms of a combination of a static, time-invariant, component and a variable, fluctuating, component. The static component may be described by a mean value,  $\bar{v}_i$ , defined as:

$$\bar{v}_i = \lim_{T \rightarrow \infty} \frac{1}{T} \int_0^T v_i(t) dt \quad (1)$$

which is simply the average of the individual values,  $v_i(t)$ , at a given time,  $t$ , over the total time interval,  $T$ , where  $i = 1, 2, 3$  correspond to the  $x, y, z$  components of the velocity vector  $\vec{V}$ . These components are often referred to as the  $u, v$  and  $w$  components of the wind, respectively.

The variance, mean square value of the departures from the mean, defines the fluctuating component as

$$\sigma_i^2 = \lim_{T \rightarrow \infty} \frac{1}{T} \int_0^T [v_i(t) - \bar{v}_i]^2 dt \quad (2)$$

where  $\sigma_i^2$  denotes the variance of the ith wind component defined previously.

The time dependence of the values of the data can be represented by the auto-correlation function,  $R_i(\tau)$ . This function is simply determined by comparing the values of the data at time  $t$  and  $t + \tau$  in the following function,

$$R_i(\tau) = \lim_{T \rightarrow \infty} \frac{1}{T} \int_0^T v_i(t) v_i(t+\tau) dt \quad (3)$$

where  $\tau$  represents the time increment and  $T$  is the total observation time.  $R_i(\tau)$  is the value of the auto-correlation function of the ith-component of the wind over the lag time,  $\tau$ .

As mentioned previously, the power spectral density function describes the general frequency composition of the wind data in terms of the spectral density,  $S$ , of its mean square value. The power spectrum is a Fourier transform of the auto-correlation function,

$$R_i(\tau) = \int_{-\infty}^{\infty} S_i(f) e^{2\pi i f \tau} df \quad (4)$$

where  $S_i(f)$  represents the spectral density of the ith-component of the wind associated with the frequency,  $f$ . The mean square value is equal to the total area under a plot of  $f S_i(f)$  versus  $\ln f$ . The spectrum, then shows how the variance or average power of the wind data is distributed according to frequency.

The inverse relation to Eq. (4) is

$$S_i(f) = \int_{-\infty}^{\infty} R_i(\tau) e^{-2\pi i f \tau} d\tau \quad (5)$$

From the symmetry properties of the stationary correlation function, it follows that the power spectral density functions are real, non-negative, and even functions of  $f$ . (For further clarification, see Bendat and Piersol, 1968; Grenander and Rosenblatt, 1957; Jenkins and Watts, 1969; and Wiener, 1949).

The above relations, Eqs. (4) and (5) simplify to

$$R_i(\tau) = 2 \int_0^{\infty} S_i(f) \cos 2\pi f\tau df \quad (6)$$

$$S_i(f) = \int_{-\infty}^{\infty} R_i(\tau) \cos 2\pi f\tau d\tau = 2 \int_0^{\infty} R_i(\tau) \cos 2\pi f\tau d\tau \quad (7)$$

## 2.2 Basic Considerations and Problems in Interpreting Spectra

One fundamental consideration in the study of time series is that the variability is a function of the time lag used in smoothing (Munn, 1970). More generally, let  $x$  be a continuous variable having smoothed values  $x_1, x_2, \dots, x_k$  over consecutive intervals of time, each interval of constant width,  $\tau$ , called the time lag. The total length of record is, therefore,  $k\tau$ . Statistical properties are denoted by Eqs. (1) and (2). For illustrative purposes, consider the effect of doubling the time lag from  $\tau$  to  $2\tau$ . Because of the additional smoothing the variance is reduced. The largest possible reduction of variance is achieved when the  $x_i$ 's are drawn from a table of random numbers; a lesser reduction occurs when there is a certain correlation between  $x_i$  and  $x_{i+1}$ . In the limiting case of repetition of each  $x_i$  (i.e., the series  $x_1, x_1, x_2, x_2, \dots, x_{k-1}, x_{k-1}, x_k, x_k$ ) an increase from  $\tau$  to  $2\tau$  has no effect on the variance.

Therefore, the variance of a time series that possesses a certain auto-correlation decreases more slowly with an increase in lag time than it would for a set of random numbers. As  $\tau$  becomes smaller, the variance becomes larger because more and more of the fluctuations are retained. Since this study is concerned primarily with the large-scale features of the general circulation, it is desirable to have  $\tau$  as long as possible and yet still retain the ability to discern periodicities of the large-scale motions. Thus, for the major portion of this investigation,  $\tau$  has been chosen to be 24 hours. However, in the case of the seasonal analyses  $\tau$  is 12 hours in length, thereby retaining more fluctuations in the wind data.

The second basic consideration concerns the wide range of possible time lags contributing to atmospheric variability. Because such a wide range is prevalent, the abscissa along which are plotted the values of the frequencies is converted where appropriate to a logarithmic scale in the graphical presentations of the spectral values. Equal areas may be preserved by noting that

$$\int_{f_1}^{f_2} S_i(f) df = \int_{f_1}^{f_2} f S_i(f) d \ln f \quad (8)$$

Hence, the ordinate scale is properly chosen as  $fS(f)$  if the abscissa is  $\ln f$ . Both the standard as well as the equal area presentations are used in this study.

Thirdly, the frequency intervals that can be interpreted with significance within the limits of the data record need to be

determined. The Nyquist folding frequency limits the high frequency end of the spectra; this frequency,  $\frac{1}{2}$ , is discussed in the next section. Munn (1970) defines the practical low-frequency limit to be one cycle per  $N/5$ , where  $N$  is the number of observations. Some investigators prefer a value of one cycle per  $N/10$ . The limit one actually chooses depends on the reliability and the consistency of the data observations. This consideration leads to the primary problem in handling "real" data: the length of the actual data record.

In the various wind records under present consideration, it was found that no gap of missing data existed that was longer than three days. Blackman and Tukey (1959) maintain that these gaps can be filled by using either the linear interpolation technique or the spline function technique without affecting the spectrum if the number of missing data does not exceed 5% of the total number of observations. This criterion was not exceeded in the present investigation. Due to the short time interval that the gaps persisted, the linear interpolation technique was applied to fill in the missing data points.

Inherent in the spectral technique are three areas of major concern, aliasing, sampling, and the partitioning of energy into finite frequencies. A common example of aliasing is offered by the stroboscope.

An example of aliasing is shown in Fig. 2.2-1.

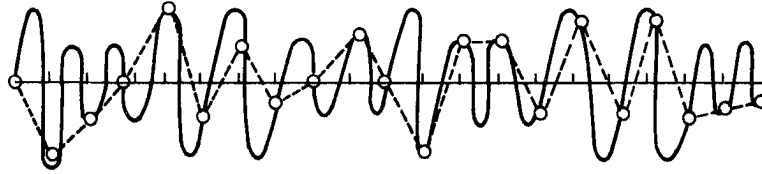


Fig. 2.2-1 An example of aliasing: two functions with exactly the same values at a uniform sampling interval. Once the sample has been taken, it is impossible to know which was the original function.

From the above figure it is clear that if the sample function is recorded at finite frequency intervals (circles) the resultant function (dashed line) may differ considerably from the original record (solid line). The higher frequency oscillation are simple ignored by this procedure.

When data are sampled at a frequency,  $f$ , the frequency about which folding takes place,  $f/2$ , is called the Nyquist folding frequency. The power in the nonresolvable frequencies greater than 1 cycle/2 days in this investigation is added to and cannot be distinguished from the real power in the resolvable frequencies less than 1 cycle/2 days. According to Oort (1969) the higher frequencies that are aliased into a resolvable frequency  $f$  are:

$$2f_n - f, 2f_n + f, 4f_n - f, 4f_n + f, 6f_n - f, 6f_n + f, \dots, (2k)f_n \pm f$$

where  $f_n$  is the Nyquist folding frequency.

Figure 2.2-2 illustrates the Nyquist folding of a spectrum (after Gauss, 1970; Muller, 1966).

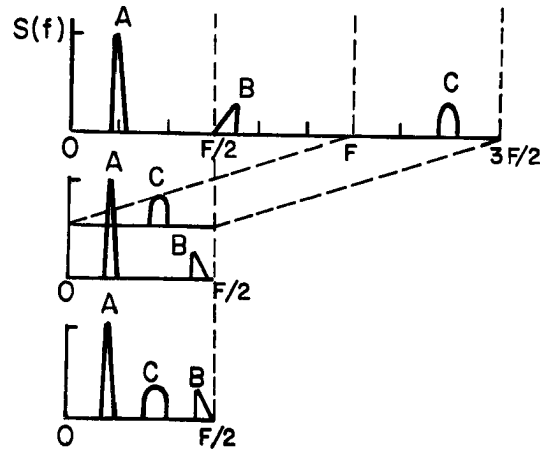


Fig. 2.2-2 Nyquist folding of a spectrum. The sampling rate is  $F$ . Spectral analysis of the sampled function shows all of the spectrum folded into the range  $0 \leq f = F/2$ . (After Gauss, 1970).

From the above diagram it is seen that frequencies less than  $f/2$  retain the spectral densities associated with them. Point A thus remains the same, not being affected by the folding of the spectrum. However, point B is "folded" about the frequency  $f/2$  and consequently shows up as a peak in the high frequency end of the resolvable spectrum. The same is also true of point C which is actually a high-frequency peak but appears in the resultant spectrum as a peak in the middle range of resolvable frequencies. Aliasing is avoided by using low-pass band filters on the data sample prior to applying the spectral analysis technique (Gauss, 1970; Holloway, 1958; Oort, 1969).

If it is assumed that the aliased portion of the spectrum, i.e., those frequencies less than the Nyquist frequency, resembles "white noise" whose power is independent of frequency, then the effect of aliasing will be to add to the true power at frequencies greater than the folding frequency a constant amount independent of frequency (Blackman and Tukey, 1959; Jenkins and Watts, 1969; Muller, 1966).

Aliasing is independent of the way in which the spectrum is presented (Oort, 1969). However, different representations of the spectrum might give different impressions of the effect of aliasing. For example, if one plots  $fS(f)$  along the ordinate and  $\ln f$  along the abscissa, the effects of aliasing will tend to show up near the folding frequency. If the true spectrum were to show a decrease of power with increasing frequency near the Nyquist frequency instead of being independent of frequency, the effects of aliasing would be still more concentrated near the frequency. The frequencies considered in this paper extend only to about 1/2.8 days.

Sampling fluctuations constitute another major concern when dealing with spectral analysis. A very "rough" graph results when plotting individual power spectral estimates versus frequency, i.e., many individual small peaks are evident. The location and magnitude of these peaks may be climatologically insignificant. They may be caused by sampling fluctuations rather than by any systematic physical phenomenon disturbing the wind regime. Consequently, it is highly desirable to average out these peaks to obtain a more useful and coherent presentation. The method applied here is known as "hanning" (Muller, 1966) in which

$$\begin{aligned} S_0 &= (s_0 + s_1) \\ S_k &= (s_{k-1} + 2s_k + s_{k+1}) \\ S_m &= (s_{m-1} + s_m), \end{aligned} \tag{9}$$

where  $s_k$  is the original and  $S_k$  is the smoothed spectral estimate,  $k = 1, 2, \dots, m$ .  $S_0$  and  $S_m$  correspond to the end point spectral estimates.

The third major problem in interpreting spectra involves the partitioning of the kinetic energy into finite frequency components dictated by the length of the data record and the number of time lags used. A simple formula for determining the finite frequencies is

$$f_n = \frac{n}{2m \tau} \quad (10)$$

where  $f_n$  is the finite frequency,  $m$  corresponds to the maximum number of time lags used,  $\tau$  is the time interval between observations, and  $n = 1, 2, \dots, m$ . A phenomenon may have a periodicity between the finite frequency intervals defined by (10); this phenomenon will then contribute to the spectral estimates corresponding to the nearest frequencies defined by (10).

Two other shortcomings exist regarding spectrum analysis. This technique determines the energy in a series of frequency bands and yields a root-mean-square average amplitude for each band. No information is provided, however, concerning the distribution of the amplitudes of the individual fluctuations. In other words, for a given frequency interval, the variance contribution may be the result of a few large fluctuations or many small ones.

Spectrum analysis also fails to detect phase shifts. A phase shift occurs when the peaks in the data record are displaced by a time interval which does not correspond to an integral multiple of the periodicity of the peaks. For example, if there is energy in a frequency band centered on 2 cycles per week, then a 7-day cycle that begins on Wednesday and another that begins on Sunday both contribute to the spectral density associated with the frequency of 2 cycles/week.

As another illustration, suppose a 3-day synoptic cycle dies out for a time but begins again out of phase with the original one. Spectrum analysis will not isolate this occurrence as having the same frequency.

Most of the aforementioned problems can be solved to a limited extent if one is aware of their existence. All of the above difficulties must be allowed for when interpreting spectra. Despite these inadequacies which limit the effectiveness of the spectral analysis technique, spectrum analysis still provides useful information in dealing with meteorological parameters.

### 3.0 SELECTION AND USE OF DATA

Figure 3.0-1 shows the 127 North American radiosonde stations which were subjected to spectrum analysis for the period July 1, 1967 through June 30, 1968. Those stations indicated by a square comprised the basic network which was used to define the seasons and to arrive at seasonal analyses of the data. The seasonal-definition problem, not considered by previous authors, will be discussed in the following section. Standard radiosonde ascents at 00- and 12-GMT provided the wind data for this study; only the 200- and 300-mb levels were examined.

Australian stations investigated are presented in Fig. 3.0-2. These ten stations were generally lacking in consistent data except at 00 GMT; consequently, this was the only observation time to be considered. Five years of good data were available for the years 1958-1962. Wind data from three heights were subjected to the spectrum analysis routine: 30,000, 35,000, and 40,000 foot levels. However, the data at constant height levels are not entirely consistent with the data obtained at constant pressure levels (Essenwanger, private communication); caution must therefore be exercised in the comparisons of the 30,000 foot with the 300 mb results and the 40,000 foot with the 200 mb results. This problem will be discussed in more detail when interpreting the Australian spectra in Chapter 4.

Winds were broken down into the zonal, u, and meridional, v, components. Each wind component for the individual stations was spectrum analyzed using one year of daily observations. Two sets of spectra were compiled from analyses of the North American data,

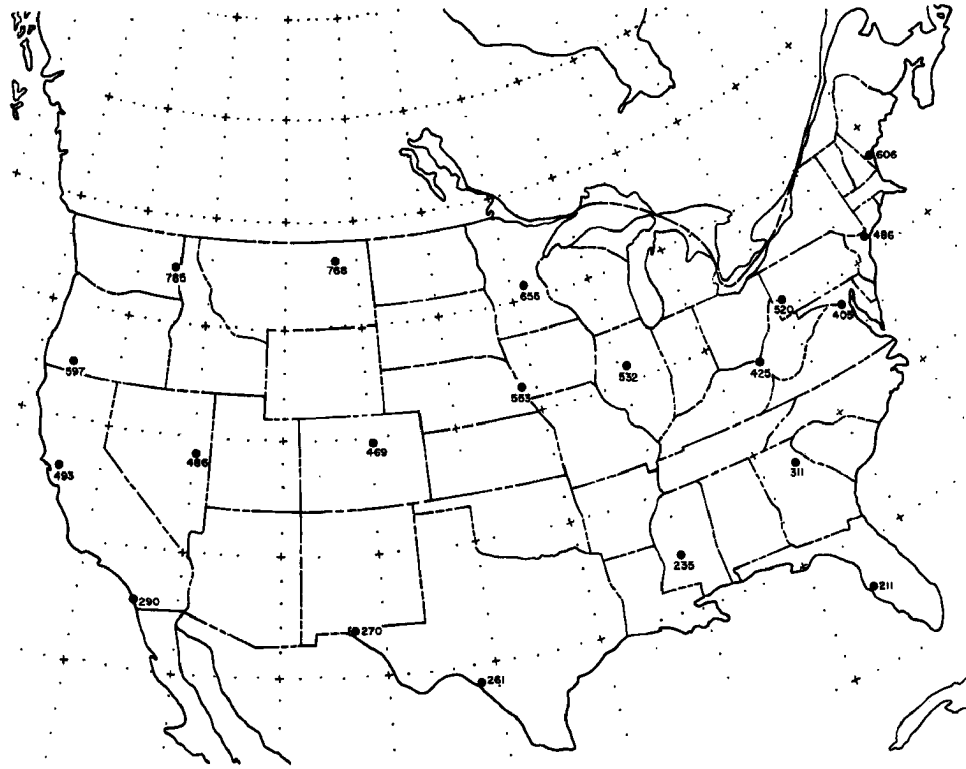


Fig. 3.0-1 Most of the North American radiosonde data network used in this study. Stations indicated by a square comprise the basic network used in defining seasons and arriving at seasonal analyses.

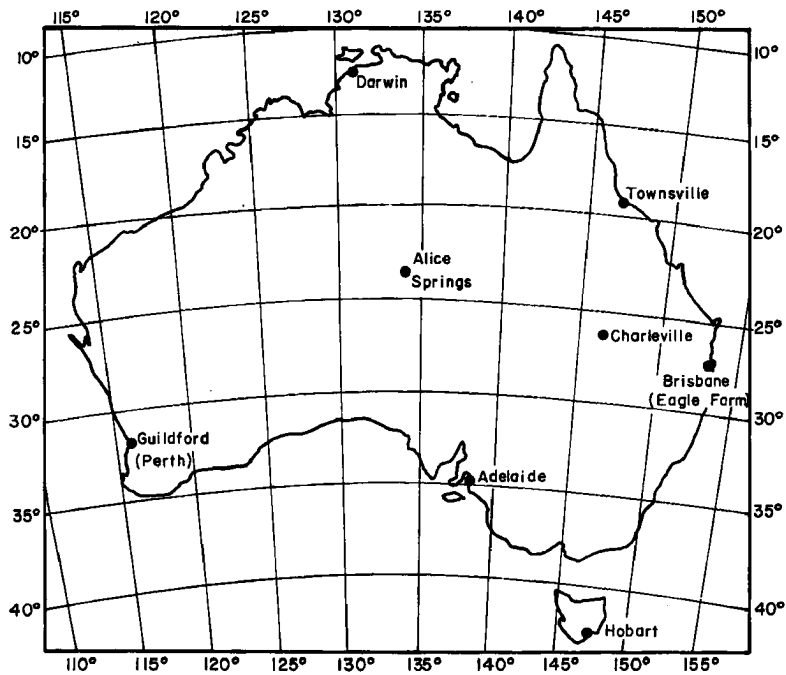


Fig. 3.0-2 Australian stations used in this investigation.

one set corresponding to each observation time. The separation of the two data collection time periods served to filter out the diurnal effects which were not of particular interest in this investigation (see previous discussion, Chapter 2.0). Only in the seasonal spectra were the two observation times combined. This was necessitated by the lack of a sufficient number of data points in a given season if only one time period with observations every 24 hours had been considered. Interhemispheric comparisons are made between the annual spectra derived from the 00 GMT data only.

The spectral density value at a given frequency for each station was plotted on a geographic map; isolines of constant spectral density were then drawn for every  $100 \text{ m}^2 \text{ day sec}^{-2}$ . Also shown on these maps are the values of  $fS(f)$  for each isoline. These distributions are found in the Appendix.

### 3.1 Determination of Seasons

Previous investigators have been content to use the standard or accepted guidelines for determining the limits of the season they desire to examine (Benton and Kahn, 1958; Henry and Hess, 1958; Horn and Bryson, 1963; Julian, et al, 1970; Kahn, 1962; Kubota, 1959; Kubota and Iida, 1954; Rosenthal, 1960; Saltzman and Fleisher, 1962; Wallace and Chang, 1969; White and Cooley, 1956; Wiin-Nielsen, 1967; Yanai and Murakami, 1970; Yanai, et al, 1968) i.e. winter, January-March; spring, April-June; summer, July-September; autumn, October-December. Those investigations which considered only two seasons defined winter to be January-June, and summer to be July-December. These time intervals were probably convenient, but the synoptic

weather patterns do not behave according to these definitions. To determine the accurate spectral representations for each season as defined by the wind regimes forms a significant portion of this study.

To gain more insight into the nature of the periodicities inherent in the yearly spectra of the individual stations, time sections of the wind distribution for twenty stations representative of the areal extent of the United States were made for the data period. Figure 3.0-1 shows these stations by a square. Time intervals in which the greatest and least amounts of variance were contained could then be identified from an analysis of these time sections. The definitions of the four seasons were determined solely on the basis of the upper-level wind distributions. The definitions of "season" which follow generally fit the behavior of the general circulation of the atmosphere at the 200- and 300-mb levels.

Using the time sections of wind distributions for each of the twenty representative stations, the 200- and 300-mb wind speeds were classified into three categories: 1) speeds in excess of 50 m/sec (Fig. 3.1-1); 2) speeds between 30 and 50 m/sec (Fig. 3.1-2); and 3) speeds less than 30 m/sec. If the wind speeds did not persist for at least four consecutive days with the same classification defined above, the wind speeds were classified according to the previous category. Thus, any wind speed to be reclassified had to persist for a minimum of four consecutive days. This procedure effectively filters out the short time-scale fluctuations which may or may not have been random in nature.

"Winter" was defined to commence with the onset of 30 m/sec winds at the 200- and 300-mb levels. November 26, 1967 marked this onset.

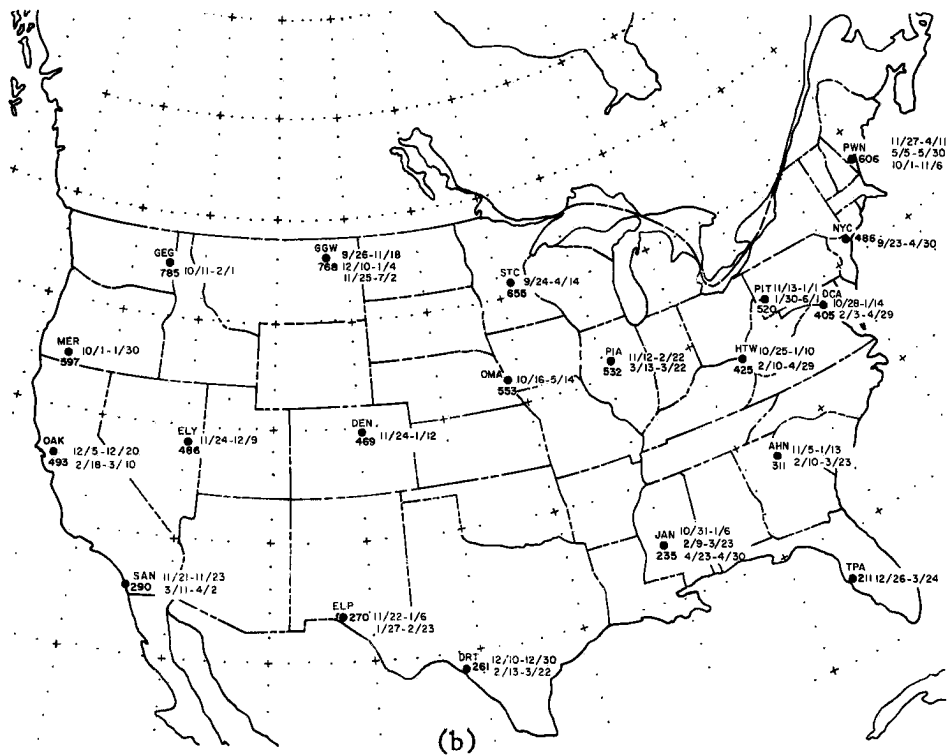
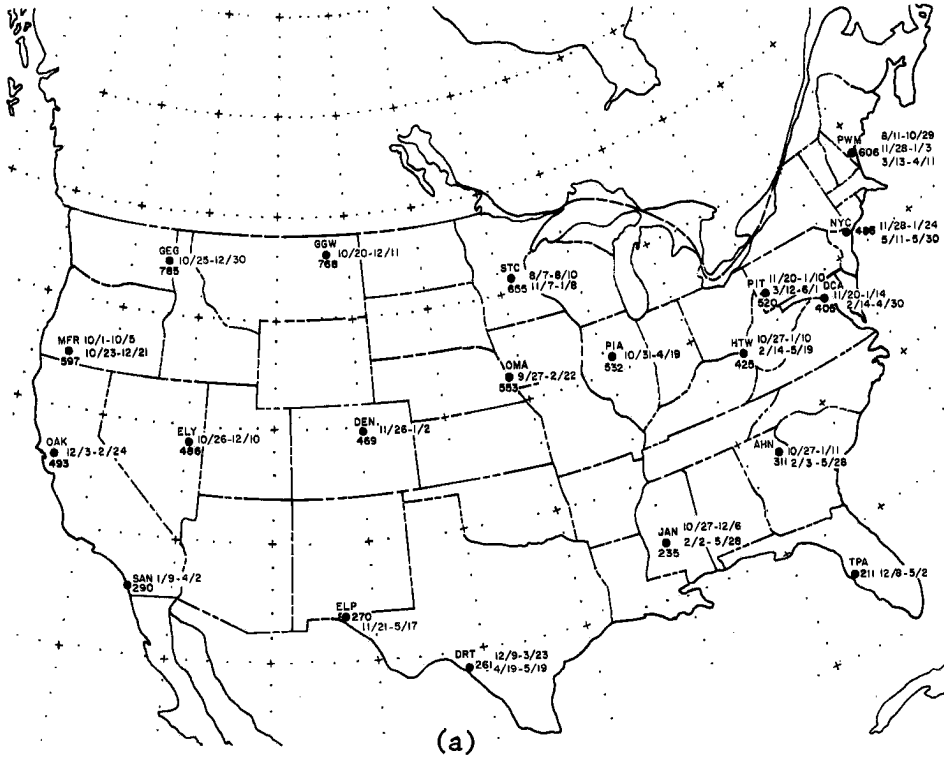


Fig. 3.1-1 Time intervals and locations when wind speeds were greater than 50 m/sec at the (a) 200 mb and (b) 300 mb constant pressure level.

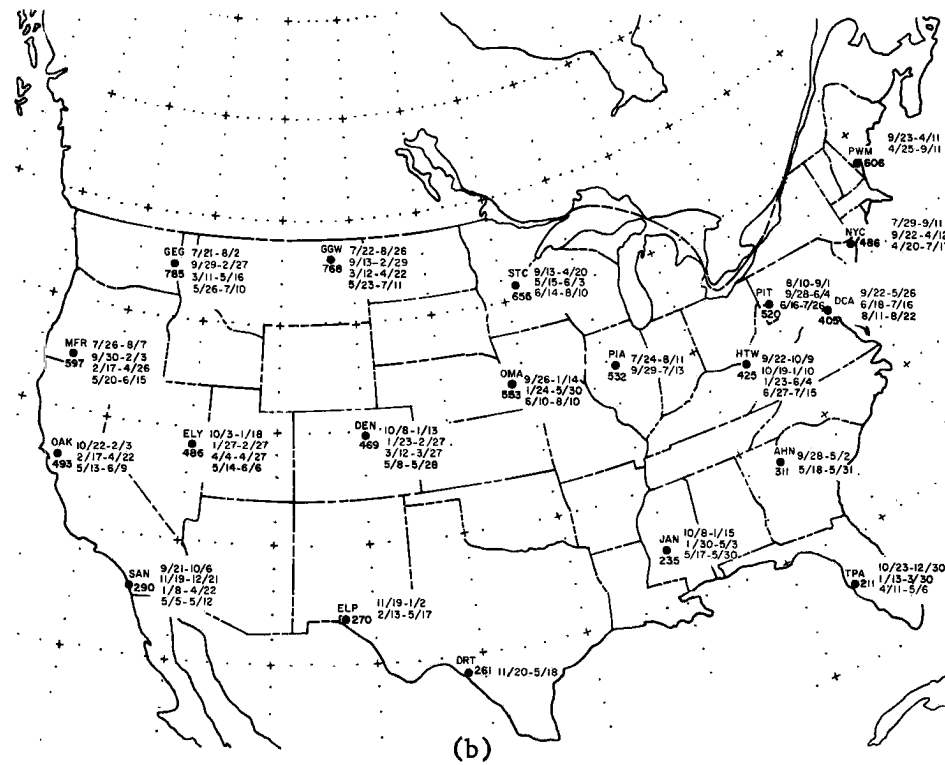
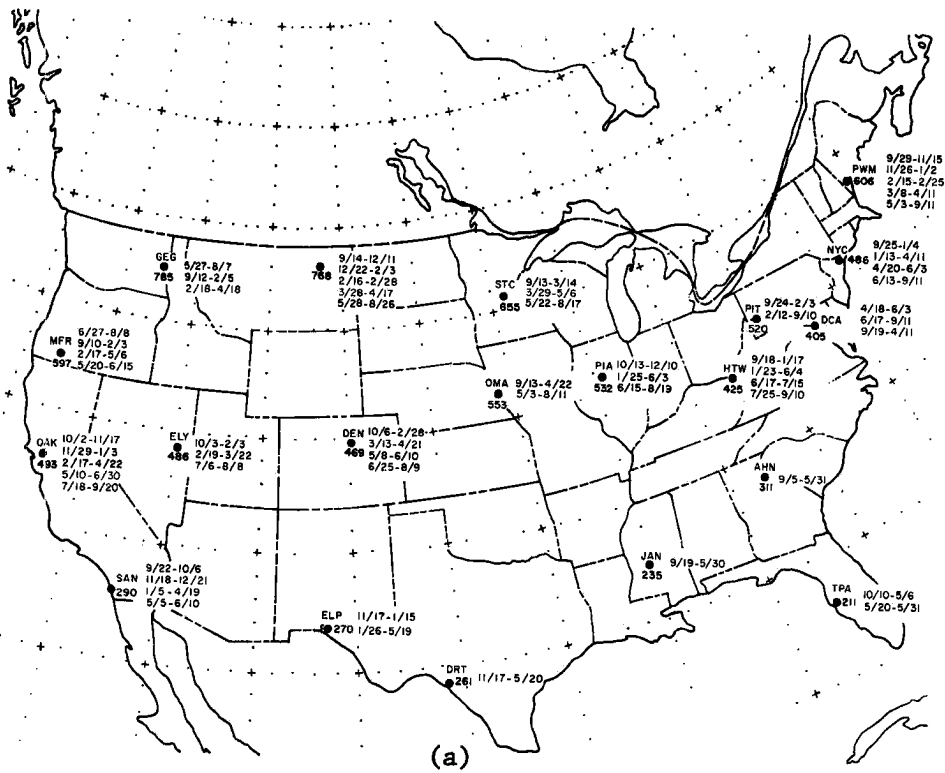


Fig. 3.1-2 Time intervals and locations when wind speeds were greater than 30 m/sec at the (a) 200 mb and (b) 300 mb constant pressure levels.

On this date wind speeds greater than 30 m/sec at these two pressure levels were observed over most of the United States. The poleward shift of the subtropical jet stream (STJ) was quite pronounced over the southern stations of San Diego, El Paso, Del Rio and Jackson (Krishnamurti, 1961a; Reiter, 1963). The northward migration of the STJ over the United States actually occurred on November 19, 1967. By November 26, 1967 all of the twenty stations examined were under the influence of wind speed regimes with speeds greater than 30 m/sec. It is interesting to note that the stations poleward of 40°N began to manifest characteristics of winter circulation patterns between September 13-30, 1967. These intrusions were usually of short duration and indicated the tendency of the polar-front jet stream (PFJ) to shift equatorward (Reiter, 1963). However, by November 26, 1967 these fluctuations were at a minimum and relatively high wind speeds were well established.

To determine the end of the wintertime wind speeds, "breaks" in the wind regimes were searched out. Two definite "breaks" with wind speeds less than the required minimum of 30 m/sec persisting for four days occurred in the data as shown in Fig. 3.1-2. The first recession of 30 m/sec winds commenced around February 26, 1968; the second break began approximately on March 24, 1968. Ninety percent (18 of 20) of the stations followed one or both of these dates. The actual weather maps at 700 mb for the months of February and March yielded the following information as presented in Fig. 3.1-3: (1) February 26, 1968 marked the time of maximum zonal wind speeds over the western portion of the Northern Hemisphere, from this date on the semimonthly average

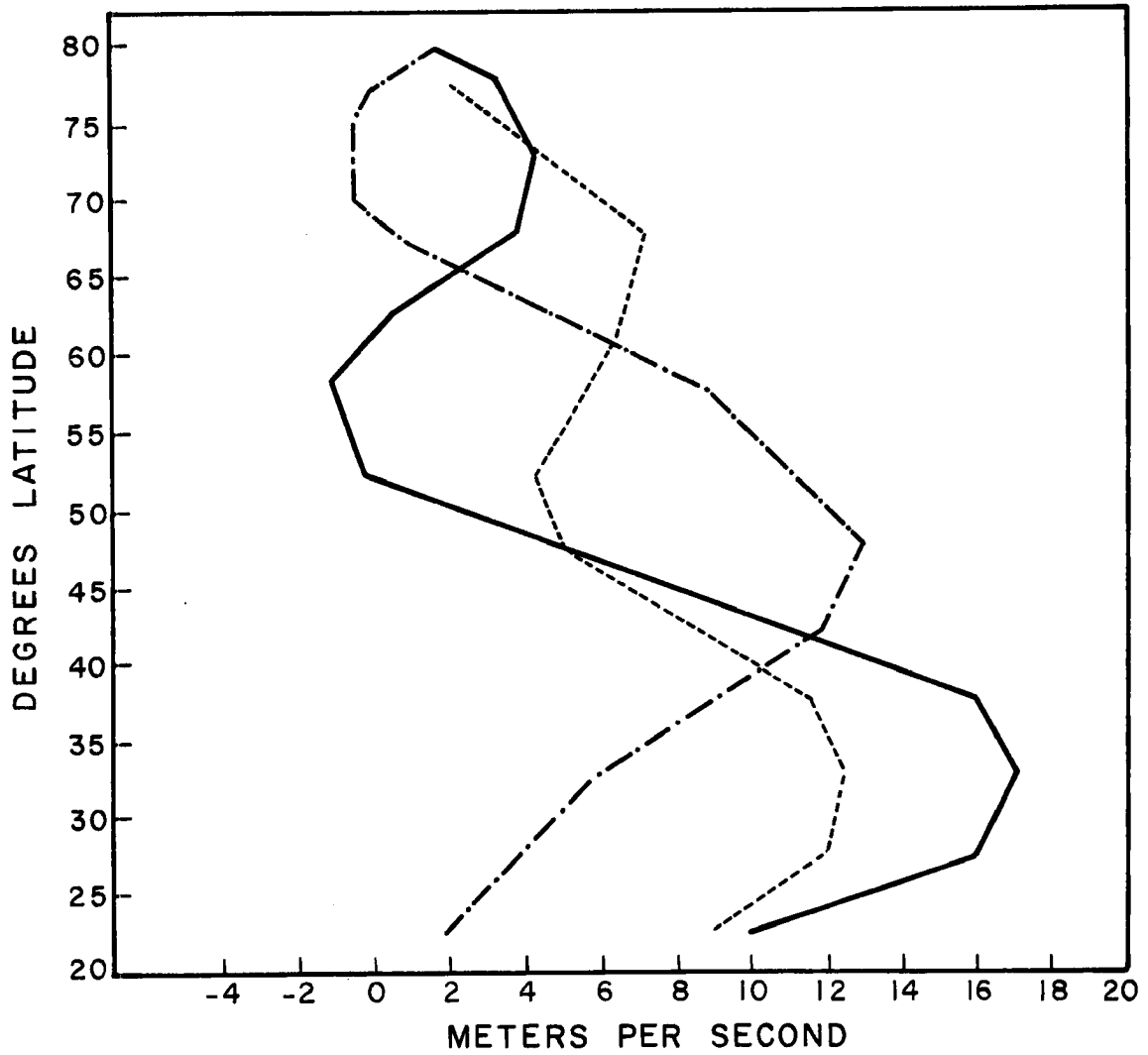


Fig. 3.1-3 Semimonthly mean zonal wind speed profiles in m/sec at 700 mb for the western portion of the Northern Hemisphere for February 13-26, 1968 (solid line), February 28-March 13, 1968 (dashed line), and March 13-27, 1968 (dash-dot line). (After Dickson, 1968).

wind speeds began to decline (Dickson, 1968); (2) February 26, 1968 maximum also corresponded to the southernmost average position of the mean zonal wind speed over the western portion of the Northern Hemisphere (Dickson, 1968); (3) the period February 27 - March 13, 1968 was a time of readjustment and transition, a decline in wind speeds and a poleward migration of the maximum winds; (4) the period March 14-26, 1968 witnessed an increase in wind speeds and the establishment of the maximum mean wind speeds around  $48^{\circ}\text{N}$  (Dickson, 1968); (5) after March 26, 1968 the winds lessened in intensity.

With the establishment of the mean maximum wind speeds at their southernmost position and greatest intensity, any diminution of these conditions would mark the end of "winter". Therefore, February 26, 1968 was chosen to terminate the wintertime wind regime. However, to ascertain the effect of defining winter in the above manner, the later date, March 24, 1968 was used alternatively as a termination point. Spectra of the winter season using both definitions were determined. Comparisons and results are presented in Chapter 4.5.

Spring was the longest of any season, February 26 - June 11, 1968. This was a period of transition and fluctuations in the upper-level wind speeds. When the winter season is extended to March 24, 1968, spring must of necessity be shortened by 27 days. The effect of this shortening procedure on the spectra can also be evaluated. Hereafter, the terms "winter-short" and "spring-long" will refer to the first definition mentioned above, i.e., November 26, 1967- February 26, 1968- June 11, 1968; "winter-long" and "spring-short" will refer to the delineation using November 26, 1967-March 24, 1968-June 11, 1968 as cut-off dates.

After June 11, 1968, the wind speeds in the United States at 300-mb were less than 30 m/sec with only occasional bursts of velocities in excess of this speed. Only the extreme northern United States stations of Portland (Maine), St. Cloud, Glasgow and Spokane exhibited times when the duration of these 30 m/sec winds lasted for at least four days on more than one or two occasions. This phenomenon can easily be explained by the proximity of these stations to the summertime polar-front jet stream (Reiter, 1963; Riehl, 1962).

The summer season had to commence with the beginning of the data record on July 1, 1967, rather than with the end of spring on June 11, 1968, in order not to bias the seasonal spectra. If the data were not used in this manner, cyclic permutations would be introduced into the spectra. Each year is different; if the seasons were allowed to use the data at both ends of the data record, then spectrum analysis would determine the periodicities of phenomena which have been assumed to be recurring each year. The above procedure rendered only 19 days useless. With the summer season generally characterized by light winds and fair weather conditions it is logical to mark the end of this period when the first inclinations of a transition and intensification of upper-level winds occur. September 9, 1967 indicated this tendency for the winds to increase and move equatorward.

After this date the wind speeds increased until, finally, on November 26, 1967 the 30 m/sec winds became established over four consecutive days. Thus autumn terminated on November 26, 1967. The transition from autumn to winter occurred much faster than the transition from winter to spring at the 300-mb level.

Ideally, the dates chosen to define the length of a season should fit the data of all stations; realistically, they do not. Thus the dates as selected above satisfy the data of as many stations as possible. Figure 3.1-4 schematically shows the partitioning of the year into seasons. The definitions chosen limited the length of winter and summer to approximately three months each. Whereas spring lasted for three and one-half months, autumn persisted for only two and one-half months. As mentioned earlier, the time interval between data observations was shortened to 12 hours. This allowed approximately 180 data points of wind values for each season to be used in the determination of the respective spectra.

Seasonal analyses were performed for Nantucket, Oakland, and Jackson for each of the seasons defined above at both the 200- and 300-mb levels. The results of this investigation are discussed in Chapter 4.5. The Australian stations were not analyzed by season; the lack of sufficient data collection throughout the day prohibited obtaining enough data points to make such spectra meaningful.

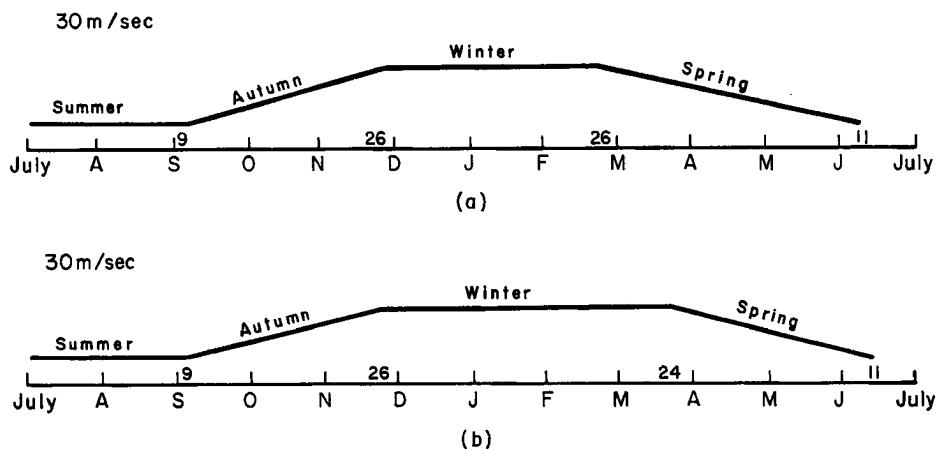


Fig. 3.1-4 Schematic diagram indicating the partitioning of the data year into seasons using the (a) winter-short and spring-long and (b) winter-long and spring-short definitions.

#### 4.0 SPECTRA OF WIND COMPONENTS - EXPERIMENTAL RESULTS

Several approaches were taken to discern the physical processes which contributed to the various spectral density peak values in the spectra of the individual stations described in Chapter 3. A composite analysis was performed using the results derived from baroclinic and barotropic theoretical investigations. Chapter 5 presents the conclusions thus determined. Several approaches were taken: 1. The resultant winds for the various seasons for each station were determined. 2. The variances of the wind speed for the 200- and 300-mb levels were computed and analyzed for the North American and Australian stations. 3. The North American geographic distributions of spectral densities at selected frequencies were determined and interpreted. 4. A latitudinal analysis of spectral characteristics for every  $4^{\circ}$  of latitude from  $20^{\circ}\text{N}$  to  $80^{\circ}\text{N}$  over North America was performed using the spectra of the individual stations. 5. Inter- and intra- seasonal comparisons were made using the results of spectrum analyses derived from wind data for three selected North American stations.

Interhemispheric comparisons were performed utilizing the spectral density values at selected frequencies for stations located along the subtropical jet stream axis over North America and Australia, respectively.

##### 4.1 Resultant Mean Winds

The resultant mean wind is defined as  $(u^2 + v^2)^{\frac{1}{2}}$ . The 200-mb values were computed and plotted as shown in Fig. 4.1-1 for each of the seasons defined in Chapter 3. Generally the winter resultant winds were greater than the winds of any other season, closely followed by the spring values. The corresponding resultant winds for summer and autumn were considerably less than those of winter and spring with the summer

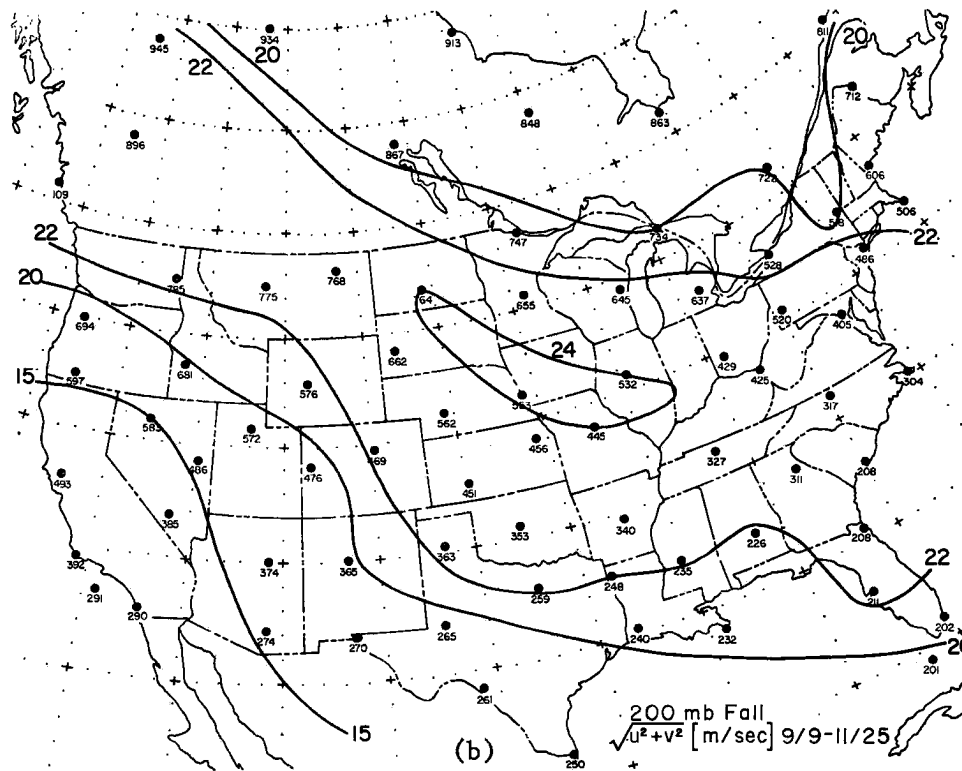
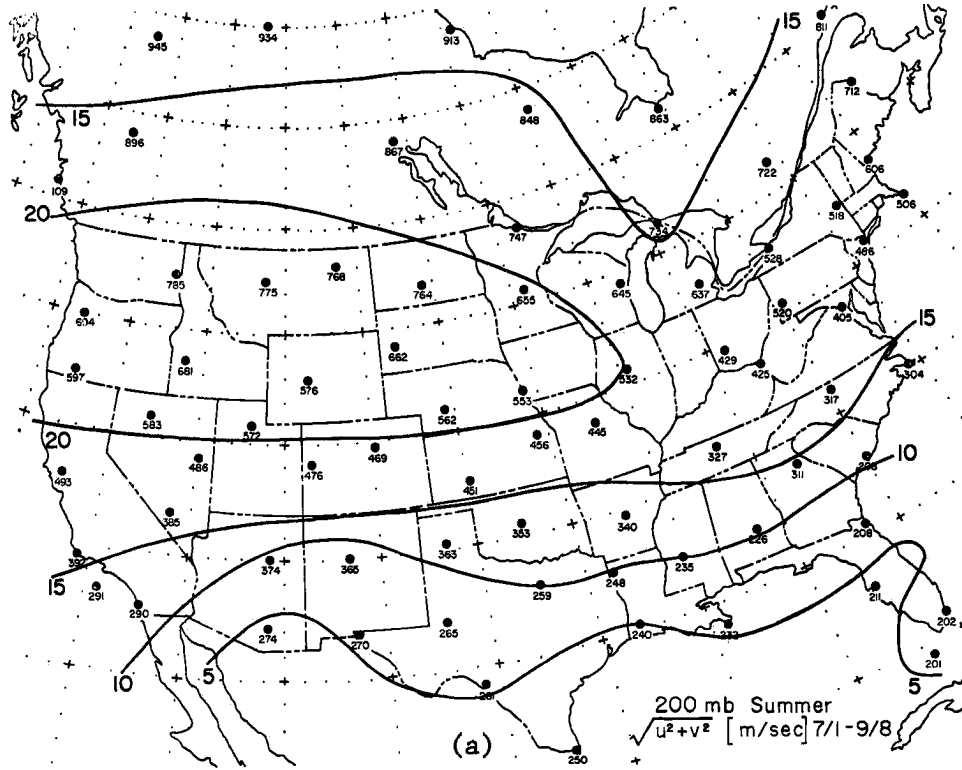
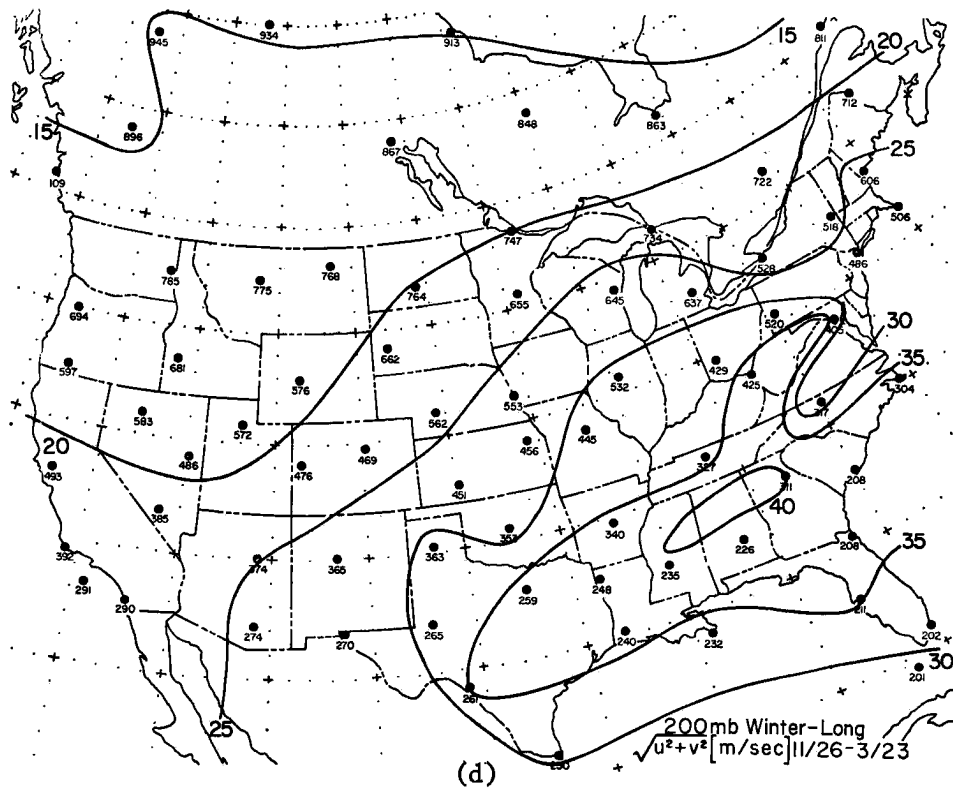
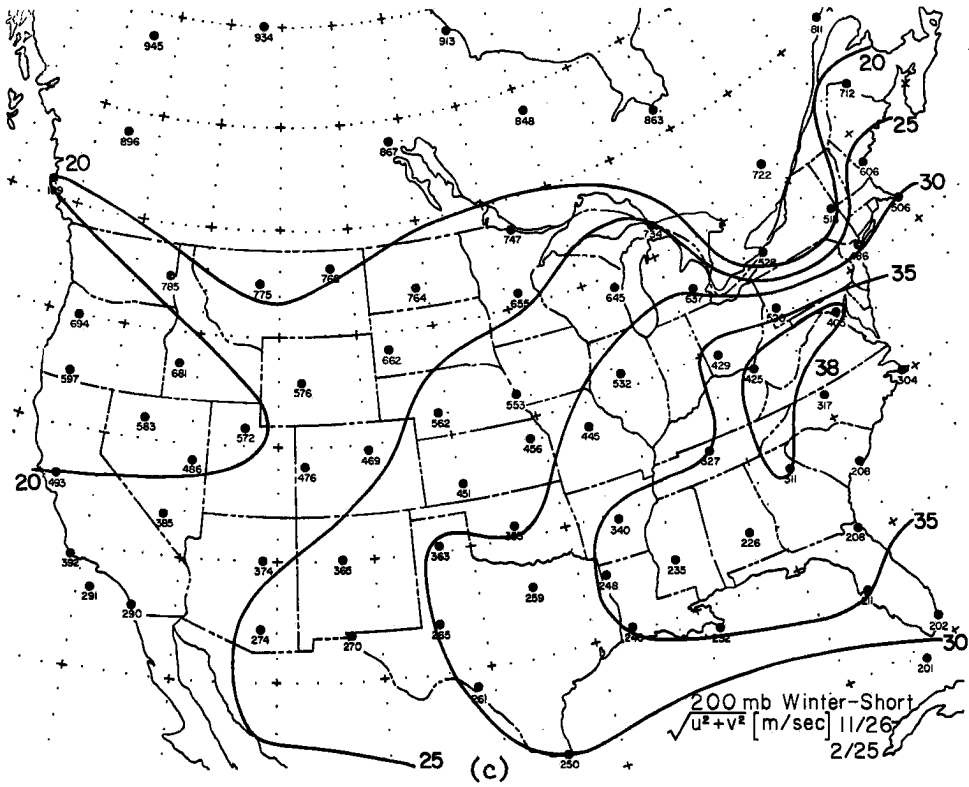
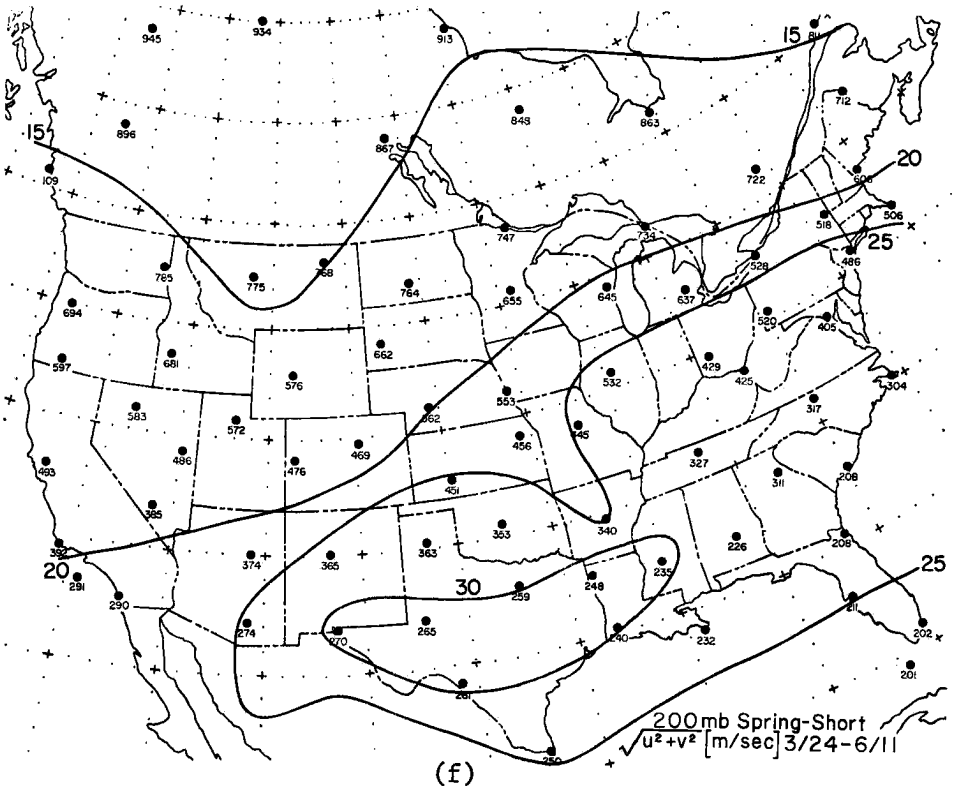
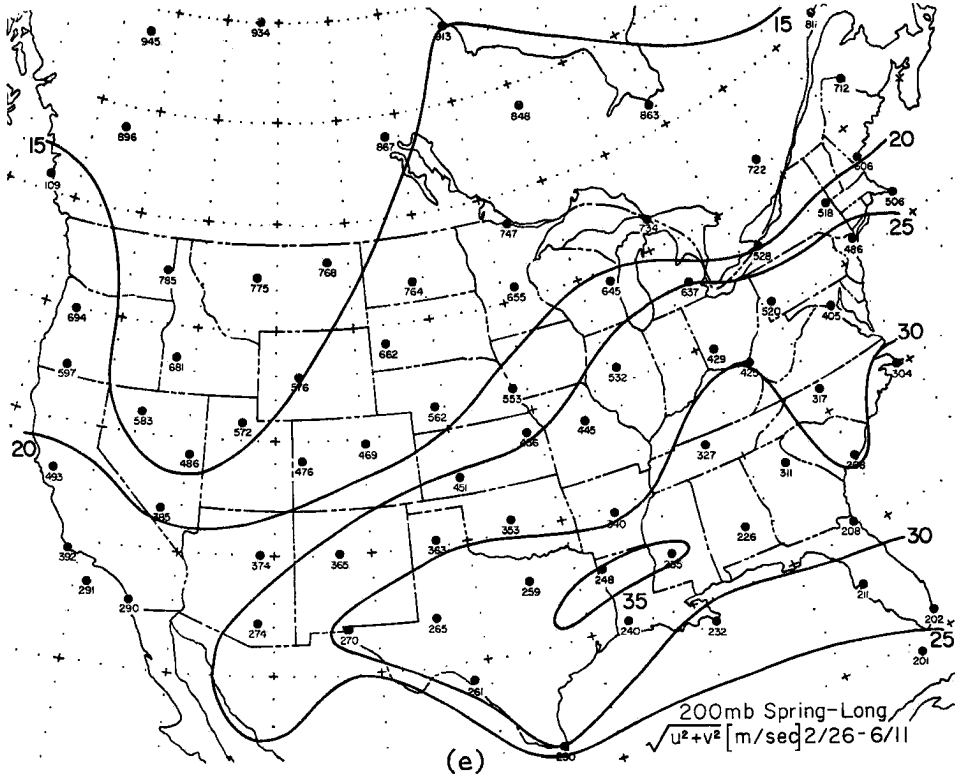


Fig. 4.1-1 Resultant mean winds at the 200 mb pressure level for (a) summer, (b) fall, (c) winter<sub>S</sub>, (d) winter<sub>L</sub>, (e) spring<sub>L</sub> and (f) spring<sub>S</sub>.





values being the smallest. The mean resultant winds clearly indicate the influence of the definitions of seasons discussed previously in Chapter 3. Particularly evident is the influence of the subtropical jet stream during the winter season. Also noticeable is the migration of the polar front jet stream in the middle latitudes.

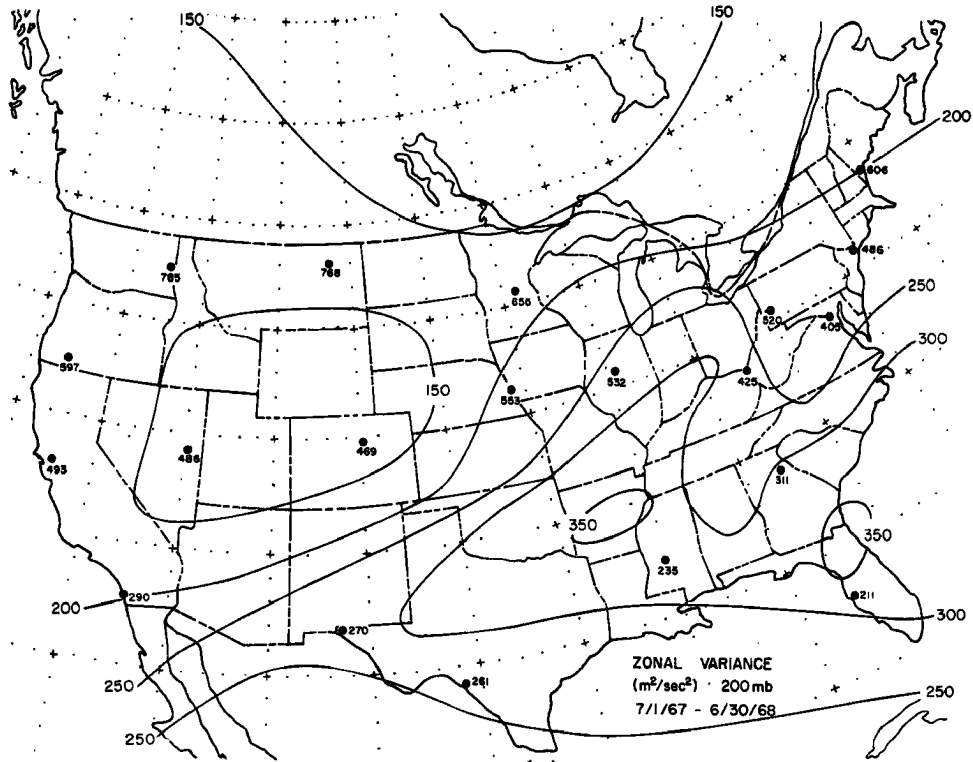
Annual mean winds for the 200- and 300-mb levels are found in the Appendix.

#### 4.2 Variance Distributions

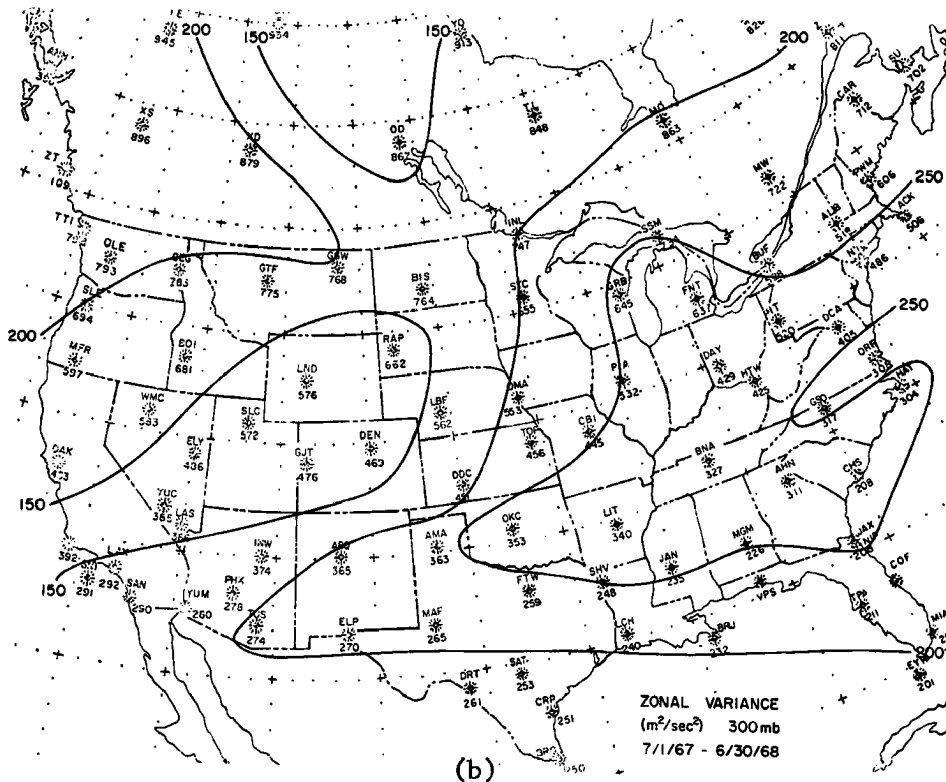
As noted in Chapter 2, the variance of wind speed is proportional to the kinetic energy distributed between two frequencies. Equation (2) defines variance in terms of the fluctuating components of wind velocity. The zonal and meridional wind variance distributions across North America for the 200- and 300-mb levels are shown in Figs. 4.2-1 and 4.2-2. The variance values were computed from daily wind speeds for the period July 1, 1967, through June 30, 1968.

The 200-mb zonal wind variances reveal an area of maximum values located in the southeast; especially high values occur in the Little Rock, Arkansas, and Jacksonville, Florida, regions. The influence of the subtropical jet stream over the southern United States accounts for this distribution (Reiter, 1963; Krishnamurti, 1961). A tight gradient of variance values extends northeastward from Texas to the eastern Great Lakes. This orientation corresponds to a primary storm track position indicated by Visher (1954) and Klein (1957).

An area of minimum variance occurs in the Great Basin region bordered on the east by North Platte. This region lies between the Cascades and Sierra Nevadas to the west and the Rockies to the east. The pattern indicates little zonal variation in the wind regimes flowing between these mountain ranges.



(a)



(b)

Fig. 4.2-1 The zonal wind variance distribution across North America at the (a) 200 mb and (b) 300 mb pressure levels.

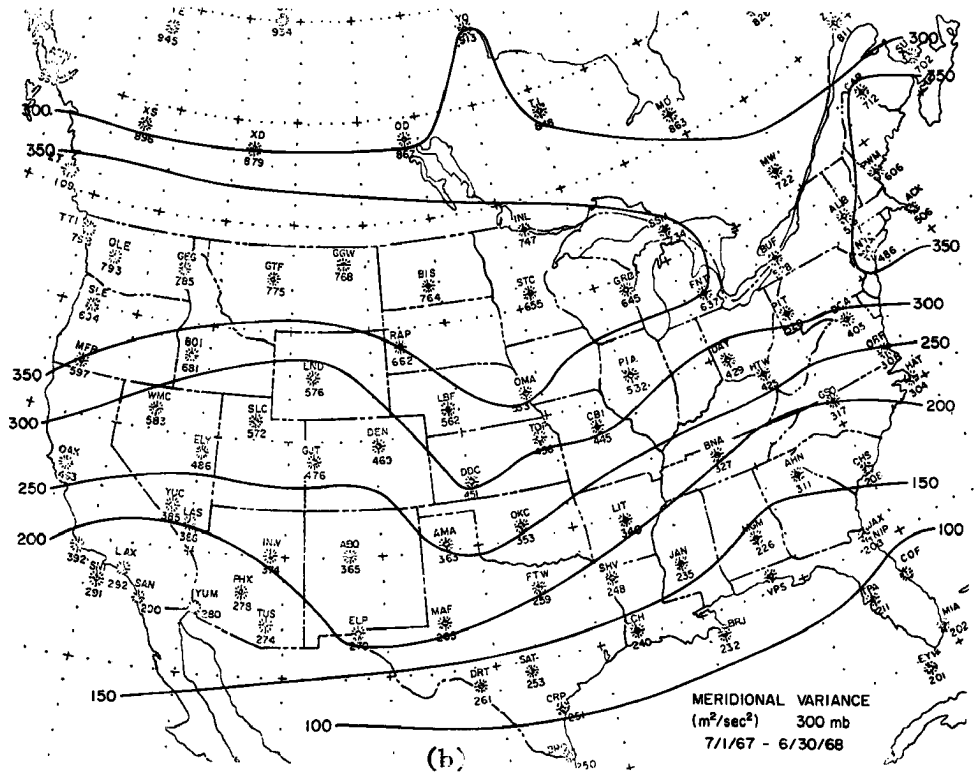
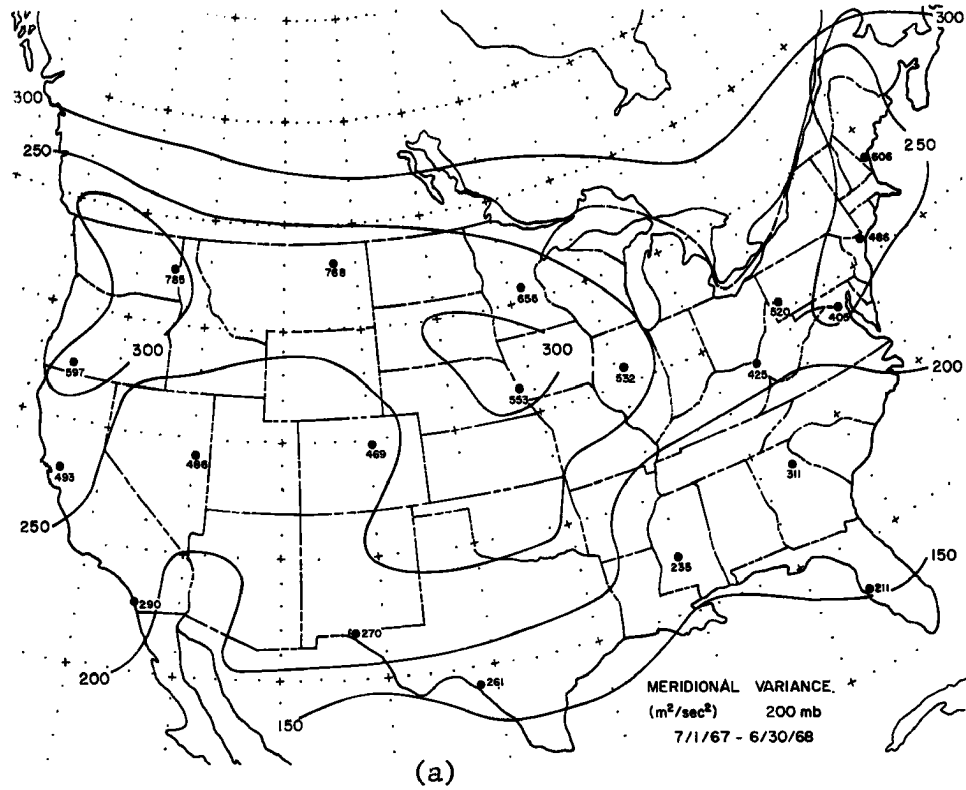


Fig. 4.2-2 The meridional wind variance distribution across North America at the (a) 200 mb and (b) 300 mb pressure levels.

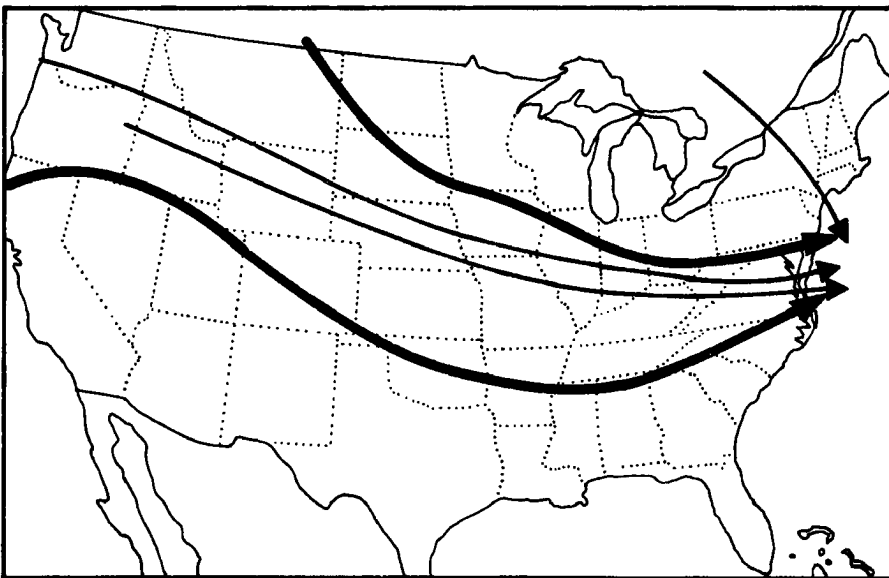
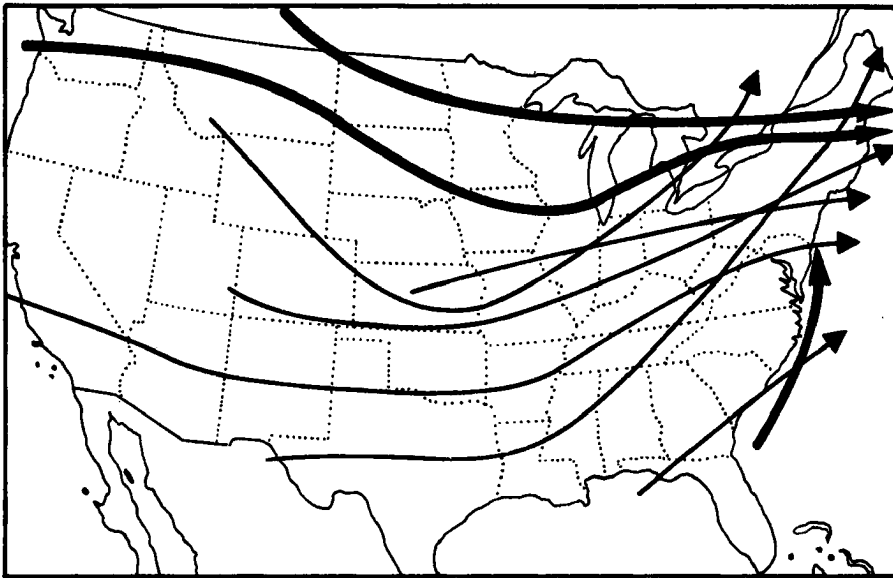


Fig. 4.2-3 Generalized tracks taken by (a) many lows or cyclones and (b) many highs or anticyclones; width of line suggests relative abundance. (After Visher, 1954)

Generally, the variance distribution at 300-mb agrees quite well with that at 200-mb. However, the 300-mb values are slightly lower than their 200-mb counterparts. Thus, the higher level zonal winds are more variable. The fluctuating height of the tropopause as a function of latitude and season (Reiter, 1963) probably accounts for this observation. Further evidence of this is suggested by the broad area of low variances poleward of  $50^{\circ}\text{N}$ . In this region the 200-mb level is in the stratosphere; consequently, the effects of tropospheric disturbances on the 200-mb wind speeds will be less than the corresponding effects on the 300-mb wind speeds.

The meridional variance distribution for the 200-mb level shows an elongated pattern which is oriented generally east-west with the orographic influence of the Rocky Mountains quite evident. Maximum values occur in three regions: Oregon-Washington; southeastern South Dakota-eastern Nebraska-western Iowa; New York-Connecticut-Massachusetts. The first and third areas appear to be the result of the shift of the long wave features of the general circulation; the second area of maximum variances is probably due to the perturbing influence of the Rocky Mountains upon the originally zonal current (Bolin, 1950; Reiter, 1963; Kasahara, 1966).

Over the United States there does not exist a closed region of minimum meridional variance unless the area south of  $30^{\circ}\text{N}$  is considered. Extremely low meridional variances are evident in the Caribbean area; values are typically in the neighborhood of  $30\text{-}40\text{ m}^2/\text{sec}^2$ . With no orographic influence generating meridional disturbances, small variance values result, at least in the latitude band  $18^{\circ}\text{-}25^{\circ}\text{N}$ . It might be pointed out that even the zonal variances are small; however, they are still generally twice as large as the meridional variances.

Values for the 300-mb variances are usually greater than the corre-

sponding ones for the 200-mb level. This is in contrast to the zonal distribution of variance with height. The meridional perturbations decrease with increasing height whereas the zonal variations become greater. The wind current does become more zonally oriented with height; the pulsating effects in the zonal current would then dominate over the directional shifts of the wind pattern.

With the tendency of the general circulation to produce troughs on the Atlantic and Pacific seaboards which alternate with ridges, the meridional variations in the flow pattern should be influenced by this tendency. This observation is substantiated by the fact that maximum meridional variances exist in the Pacific Northwest and in New England. With the lack of data over the oceans, it is possible that these areas of maximum variance cover a wider extent than presented here.

#### 4.3 General Considerations of Spectral Peaks

A "peak" in a spectrum was considered to be significant if its energy density exceeded the energy densities in the frequency bands immediately adjacent to it by a minimum of 5% of the central energy density value (Munn, 1970). To illustrate which periodicities are more common and, therefore, more significant than others, peaks at each frequency in both the zonal and meridional spectra of each individual station were counted respectively. The number of peaks at each frequency were then totaled for the zonal and meridional spectra separately. Figure 4.3-1 presents the distribution of peaks thus totaled from all the spectra of the North American stations per frequency interval. Thus, trends exhibited by the individual stations collectively became apparent.

The distribution of peaks in the zonal spectrum are shown in Fig. 4.3-1a. The most evident peak which existed in the spectra of many

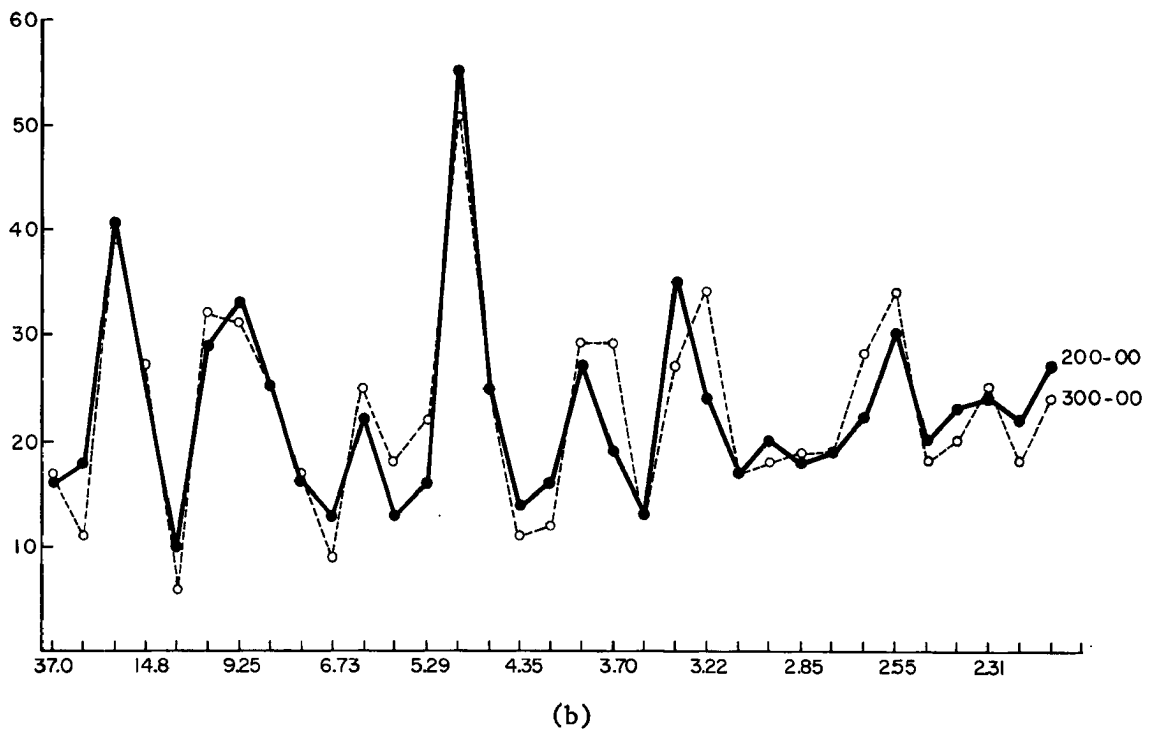
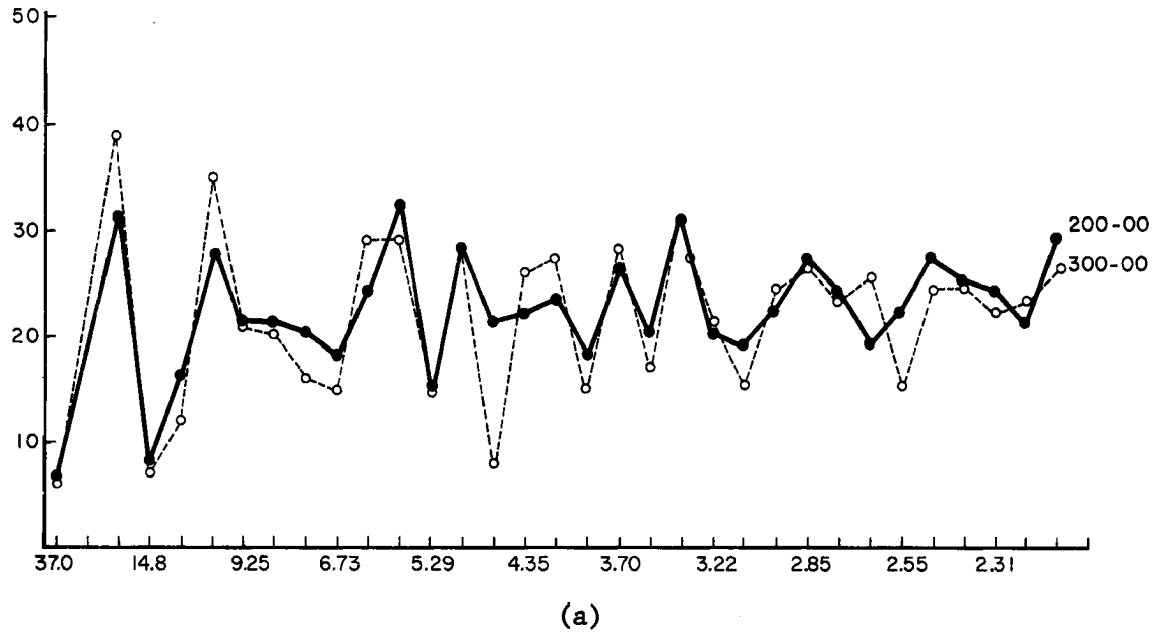


Fig. 4.3-1 The distribution of peak energy densities summed over all North American stations examined per frequency interval for the (a) zonal and (b) meridional spectra at the 200 mb (solid line) and 300 mb (dashed line) levels.

stations occurs with a periodicity of 18.5 days. However, only 39 of 117 stations (33%) possessed a peak at this periodicity. This illustrates the wide range of possible spectral representations of the zonal wind which exists over North America. Considering the wide areal extent of the stations involved, this may be a significant periodicity. Many stations also possessed peaks at frequencies of 10.6-, 6.17 or 5.69-, 4.93-, 3.70- and 3.36-days.

Figure 4.3-1b presents the number of stations having peaks in their meridional spectra at the various frequencies. Generally, the number of stations possessing a peak in their meridional spectra is greater than the corresponding number of stations having a peak in the zonal spectra. In addition the curves for the 200- and 300-mb representations correspond quite closely in general pattern and also in magnitude which was not necessarily true regarding the zonal distributions. Fifty-five stations observed a 4.93-day periodicity in their meridional spectra. This represents 48% of the stations examined. In addition to the major peak at 4.93-days, minor peaks occurred with periodicities of 18.5-, 9.25-, 6.17-, 3.89 or 3.70-, and 3.22-days.

A significant number of stations observed peaks at the same frequencies in both the zonal and meridional wind component spectra with two exceptions. The zonal spectra had a tendency to peak, generally, at periodicities of 10.6- and 3.36-days; whereas the meridional spectra for a number of stations exhibited peaks with periodicities of 9.25- and 3.22-days. This discrepancy of one frequency interval may be the result of the necessity to partition energy densities into finite frequency intervals, a problem previously discussed in Chapter 2. It appears, at least qualitatively, that the v-component of the wind

behaved more consistently than the u-component. This behavior may be partially accounted for by instrument errors.

Peaks with a periodicity of less than 2.96 days are not considered. The reasons for excluding these higher frequencies are threefold. Primarily, as pointed out in Chapter 2, the major effects of aliasing are found in this range of high frequencies limited by the Nyquist frequency. Secondly, no one particular frequency can be considered significant at frequencies greater than  $1/2.96$  day, at least no periodicity was observed by a large number of stations. Thirdly, it is not the purpose of this investigation to analyze these short-term fluctuations.

Since the geographic distributions of these spectral values associated with the above periodicities are secondary to this paper, they will be treated in the appendix.

The question of the peaks at the longer periodicities being harmonics of the higher frequency peaks was considered but dismissed as being negligible.

#### 4.4 Latitudinal Analyses

To show the possible inadequacies of averaging geostrophic winds around a given latitude circle and then spectrum-analyzing the resulting winds (Benton and Kahn, 1958; Horn and Bryson, 1963; Kahn, 1962; Kao and Bullock, 1964; Saltzman, 1958; Saltzman and Fleisher, 1962; Shapiro and Ward, 1963) this study contains spectra based on actual wind data for stations oriented along every  $4^{\circ}$  of latitude from  $20^{\circ}\text{N}$  to  $80^{\circ}\text{N}$  over North America. The ten stations located along  $32^{\circ}\text{N}$  are an illustrative example.

Figures 4.4-1 and 4.4-2 depict the zonal and meridional spectral densities at selected frequencies along  $32^{\circ}\text{N}$ , respectively. Considering

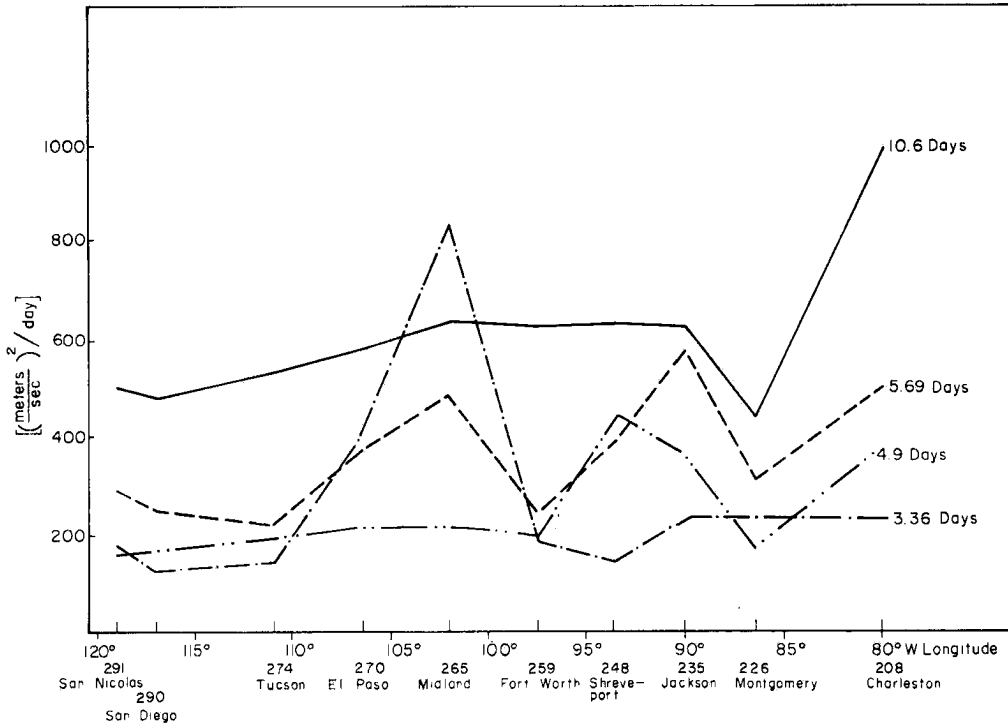


Fig. 4.4-1 Zonal spectral densities at selected frequencies for stations located along 32°N: 10.6 days (solid line), 5.69 days (dashed line), 4.9 days (dash-two dot line), 3.36 days (dash-dot line).

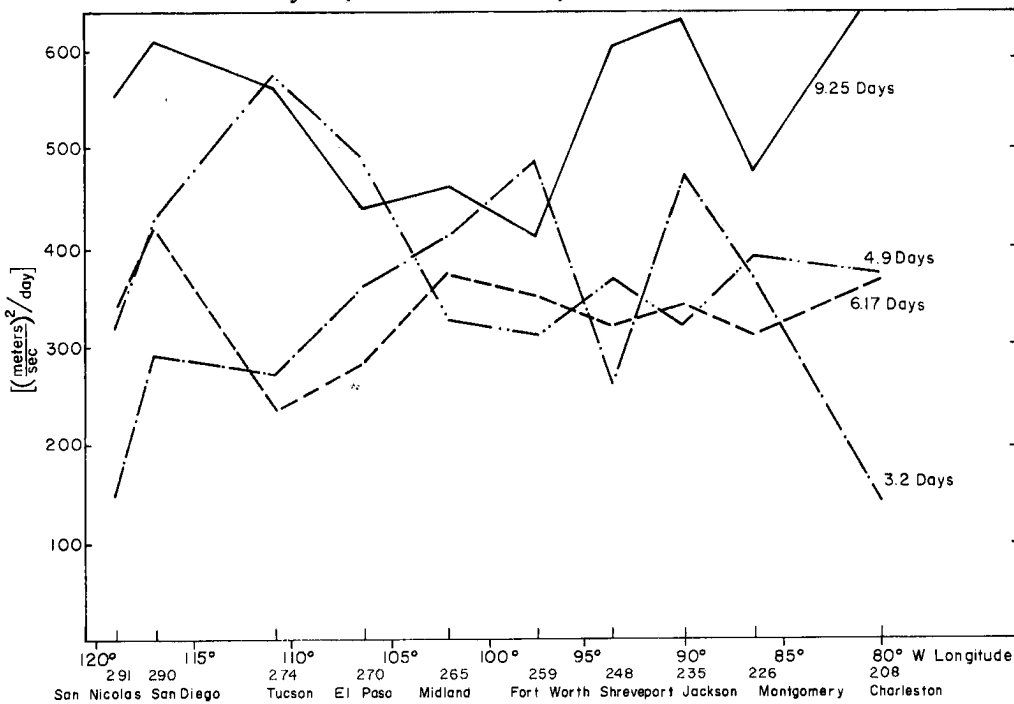


Fig. 4.4-2 Meridional spectral densities at selected frequencies for stations located along 32°N: 9.25 days (solid line), 6.17 days (dashed line), 4.9 days (dash-two dot line), 3.2 days (dash-dot line).

the zonal distribution first, the spectral values seem to be grouped in geographic regions. Selecting the spectra of any one station along this latitude as being representative of the latitude circle would be misleading. Charleston, perhaps, has the greatest spectral densities generally, closely followed by those values at Midland and Jackson.

The reason for this is that Charleston is located near favored positions of storm tracks as shown by Visher (1954) in Fig. 4.2-3. The intrusion of the subtropical jet stream during the winter months as outlined by Krishnamurti (1961) and discussed in Chapter 3.1 also contributed to the higher spectral densities at Charleston. The STJ does not enter at the west coast of North America and proceed along the 32nd meridian. The above three stations are 10-12° apart; their respective spectra indicate a possible wave-like structure in the STJ axis (Krishnamurti, 1961). The high spectral densities at Charleston were due also to the increase in kinetic energy from the influx of subtropical cyclones.

Fort Worth, Shreveport and El Paso displayed the same magnitude of spectral values, generally; these values can probably be attributed to the STJ. The reasons for Montgomery's spectral densities being less are unclear. The stations possessing the lowest spectral values were San Nicolas, San Diego and Tucson. They were far enough south from the effect of the northwest storms and too far west to receive the major effect of the changes in the long-wave circulation features as discussed previously.

A peak at 3.36 days existed at most of the stations. A maximum spectral density for this frequency was found at Midland. Only Jackson and Charleston did not possess this peak in their respective zonal spectra. The cyclogenesis which occurred at the Midland region in the

mean (Klein, 1957) probably accounted for this distribution. With the lack of such a prominent peak at Fort Worth, the track of these new cyclones must be directed sharply to the northwest.

Also within the frequency range of synoptic disturbances is the peak at 4.11 days. The maximum spectral density at this frequency occurred in the Fort Worth spectrum. Eastward from Shreveport this periodicity did not appear in any of the zonal spectra.

With the exclusion of Shreveport and Jackson, a slight peak was evident in the spectra of the remaining stations at 8-10 days. This peak in the spectra was due to small oscillations in the heights of constant pressure levels. The heights of the 200- and 500-mb levels for Amarillo were subjected to spectrum analysis with the results presented in Fig. 4.4-3. Evident in both spectra is the peak around nine days. This tendency to peak in the 8-10 day range apparently extended no farther eastward than Shreveport with Montgomery providing an exception.

Figure 4.4-2 presents the meridional spectral distribution along  $32^{\circ}\text{N}$  for selected frequencies. There is much closer agreement between meridional spectral values than existed in the zonal spectral distribution. An average peak spectral density exists in the Fort Worth region decreasing both eastward and westward. The east coast station, Charleston, has slightly greater spectral values than its west coast counterpart, San Nicolas; Charleston spectral densities are, however, less than the corresponding ones at San Diego. Fort Worth had the highest variance in the v-component of the wind along this latitude circle (Fig. 4.2-2). This could account for the slightly higher spectral densities at that station.

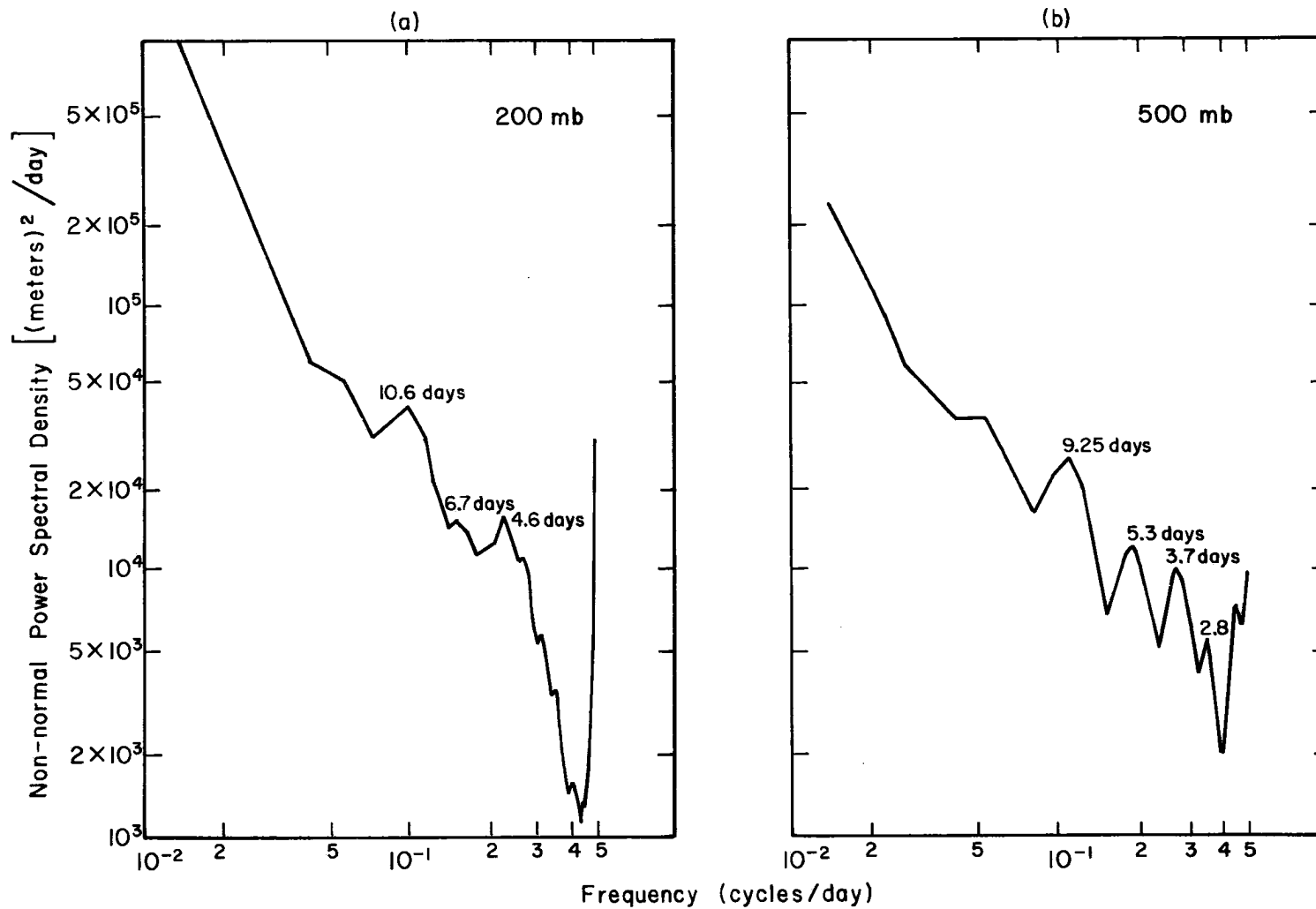


Fig. 4.4-3 Spectra of the (a) 200 mb heights and (b) 500 mb heights for Amarillo, Texas (35° 14'N 101° 42'W), for the data record 7/1/67-6/30/68.

A second development can be traced in the spectral values associated with a periodicity near 4.5 days. Tucson possesses the highest spectral density at this frequency. This periodicity does not have a peak at Shreveport or Jackson; it becomes displaced to a periodicity around 4.9 days in the Charleston spectrum. This frequency corresponds to the cyclone frequencies (Klein, 1957); many cyclones originated in the area where peak spectral values at 4.5 days occurred (Klein, 1957).

The peak in the meridional spectra at or near a period of 3 days is prevalent at all but two stations. The spectra of the two coastal stations, San Nicolas and Charleston, do not have this peak; the maximum spectral value at a 3-day periodicity occurs at Jackson with a smaller maximum at Fort Worth. This periodicity is within the range of the cyclone-anticyclone frequencies. The absence of this peak at San Nicolas and its appearance at San Diego is puzzling and remains unexplained. Charleston's lack of a spectral peak at this frequency indicated that major storm or anticyclone tracks bypassed this area. This was thought to be the reason for the absence of such a spectral peak at San Nicolas; but the proximity of the San Nicolas spectral peak to the peak present in the San Diego spectrum indicates more than just this.

The meridional spectra were generally greater in magnitude than the zonal spectral values at all the stations but Midland, Jackson and Charleston. The meridional spectral densities within the frequency range 12-25 days were greater than the zonal spectral values. But at higher frequencies, and especially at 3.36 days, the zonal spectral densities were greater in magnitude. Charleston was the only station along 32°N which portrayed the entire zonal spectrum greater in

magnitude than the meridional spectrum. The above generalizations indicate that the anisotropy of disturbances along  $32^{\circ}\text{N}$ , with the energy in the u-component exceeding that in the v-component, extended in the mean to those phenomena with frequencies greater than 1/18 days. Other results appear in the Appendix.

#### 4.5 Analyses of Seasonal Spectra

The wind data from Nantucket, Oakland and Jackson were subjected to seasonal spectrum analysis using the definitions described in Chapter 3. In the following discussion the subscripts L and S refer to the long and short seasons defined in Chapter 3. The effect of the seasonal definition on the calculations of variance and the determinations of spectra cannot be dismissed as insignificant; different conclusions may be reached depending on which definition is chosen.

Variances of the wind data and mean zonal and meridional wind speeds were calculated and plotted in Table 4.5-1. In all but two categories, the 200- and 300-mb level meridional wind spectra for Jackson, the variances for summer were the smallest of any season. In a little over half of the categories examined, the winter variances were the greatest. The variance values of the spring and autumn winds were often interchanged within the above extremes.

The Nantucket wind variances show interesting relationships in Table 4.5-1. The 200- and 300-mb zonal wind variances increase from summer to fall to spring  $L-S$  to winter  $L-S$ ; this alignment indicates that the zonal winds at Nantucket are the most variable in winter. The zonal wind fluctuations at 300-mb were predominant in spring; the meridional wind fluctuations were more pronounced in autumn. The 200-mb variance pattern is quite different. The autumn variance is less than

Table 4.5-1

Variances and mean wind speeds for the  
various seasons at Nantucket, Oakland and Jackson

	NANTUCKET				OAKLAND				JACKSON			
	506		300 mb		493		300 mb		235		300 mb	
	200 mb	300 mb	200 mb	300 mb	200 mb	300 mb	200 mb	300 mb	200 mb	300 mb	200 mb	300 mb
	var/ $\bar{u}$	var/ $\bar{v}$	var/ $\bar{u}$	var/ $\bar{v}$	var/ $\bar{u}$	var/ $\bar{v}$	var/ $\bar{u}$	var/ $\bar{v}$	var/ $\bar{u}$	var/ $\bar{v}$	var/ $\bar{u}$	var/ $\bar{v}$
	m <sup>2</sup> sec <sup>2</sup> /m/sec											
Summer	115/22	190/9	74/19	183/9	63/11	90/13	59/8	49/9	163/10	148/-3	79/8	89/-2
Autumn	147/20	285/6	206/18	386/8	262/13	269/-4	263/9	248/-3	242/23	224/-3	229/18	208/-2
Winter-L	330/38	229/-2	422/32	393/-8	306/20	260/-7	260/17	321/-5	353/39	232/5	265/31	257/4
Spring-S	226/24	288/-4	288/22	308/-3	141/17	162/-8	165/16	211/-8	226/32	113/-6	196/24	83/.9
Winter-S	367/30	227/-2	424/36	406/-1	318/19	236/-7	277/17	279/-6	321/36	206/5	244/29	234/4
Spring-L	214/24	276/-3	276/21	320/-2	176/19	209/-7	175/16	280/-7	308/35	168/1	254/27	148/1

that of spring  $S$ , but the spring  $L$  value is less than that of autumn. In both instances the transition seasons, autumn and spring, have the greatest amounts of variability at this level. The fluctuating position of the polar front jet stream during these seasons contributes to the higher variance of autumn and spring at Nantucket.

Oakland variances at the 200-mb level reveal that most of the wind variability occurred in the autumn and winter seasons. Summer and spring variance values are the smallest. The 200-mb zonal pattern shows the winter  $L-S$  variance values greater than those of autumn whereas the 200-mb meridional distribution indicates that the autumn variances are greater than those of winter  $L-S$ . As noted previously, the zonal variability in winter predominated over the meridional variability whereas the converse is true in autumn. The autumn and winter  $L$  zonal variances are similar at the 300-mb level; by shortening the winter season its variance became greater than that of autumn.

When considering the 300-mb meridional variances, the order of the seasons is changed depending upon the seasons chosen. This behavior can be attributed to the change in the length of the data record for winter and spring. This is an excellent example of the effect and importance of how a "season" is defined.

Variance values of the Jackson wind data illustrate still a different pattern of behavior. In every instance, the often mentioned effect of defining seasons is apparent. In most of the categories the summer variance is the least followed by the spring  $S$  values. Spring  $L$  variances of the zonal wind become greater than autumn at the 200- and 300-mb levels. In fact, at 300-mb spring  $L$  has the greatest variance whereas the spring  $S$  variance is only greater than summer. The

meridional variances for both constant pressure levels possess similar characteristics. The most variable meridionally are autumn and winter; winter variances are usually greater.

With Nantucket, the northernmost station of these three, the winter<sub>L</sub> variances were less than the winter<sub>S</sub> and the spring<sub>L</sub> values were less than the spring<sub>S</sub> variances. At Jackson, the southernmost station of these three, the opposite was true; winter<sub>S</sub> variances were less than winter<sub>L</sub> values and spring<sub>S</sub> values were less than spring<sub>L</sub> variances. Oakland exhibited both characteristics, one at each level. Thus the explanation for this behavior must lie in the relationship between the circulations characteristics of the various seasons and the effect of the lengthening of the definition of a season.

The above conclusions can be reached only when considering an inhomogeneous data record. Figure 4.5-1 illustrates the two situations described above. By terminating the data record at a given point, different statistical characteristics may result than had the data record been terminated at another point. However, the intricate complexities involved in determining variances are beyond the scope of this investigation.

Since we are specifically interested in the effect on the power spectra of lengthening or shortening the data record for a given season, all three stations were analyzed in this regard. Nantucket's spectra for winter<sub>L</sub> and winter<sub>S</sub> at both levels for both wind components show remarkable similarity (Fig. 4.5-2). The same holds true for the spring<sub>S</sub> and spring<sub>L</sub> spectra with the exception of the 200-mb zonal spectrum (Fig. 4.5-3). The change in the spring 200-mb zonal spectra was not unique to Nantucket. Both Oakland and Jackson had their 200-mb zonal

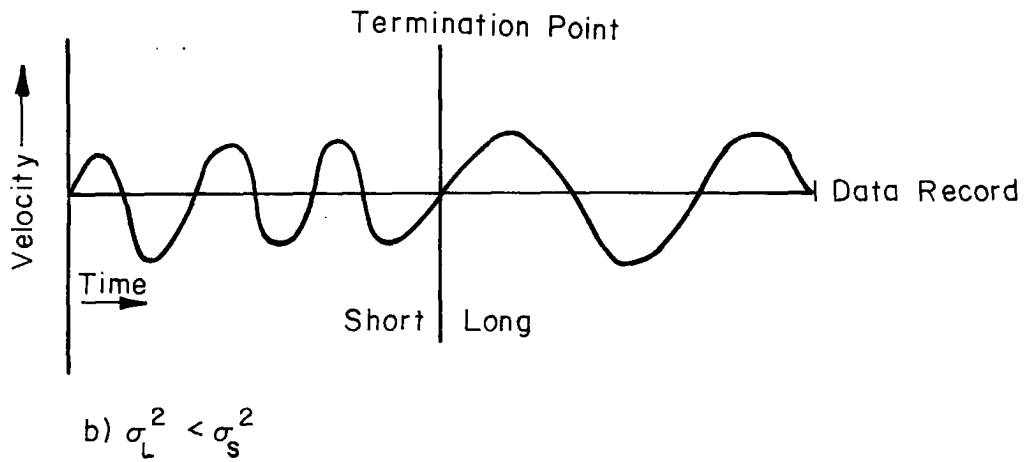
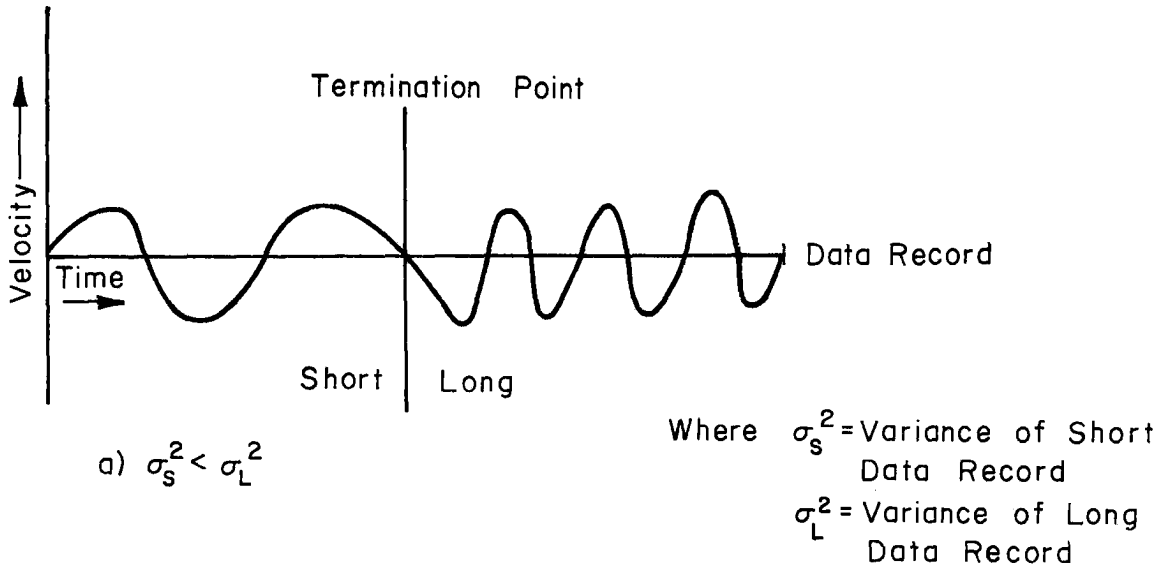


Fig. 4.5-1 Schematic representation of the possible effects on the wind variance by terminating the data record at different points in time.

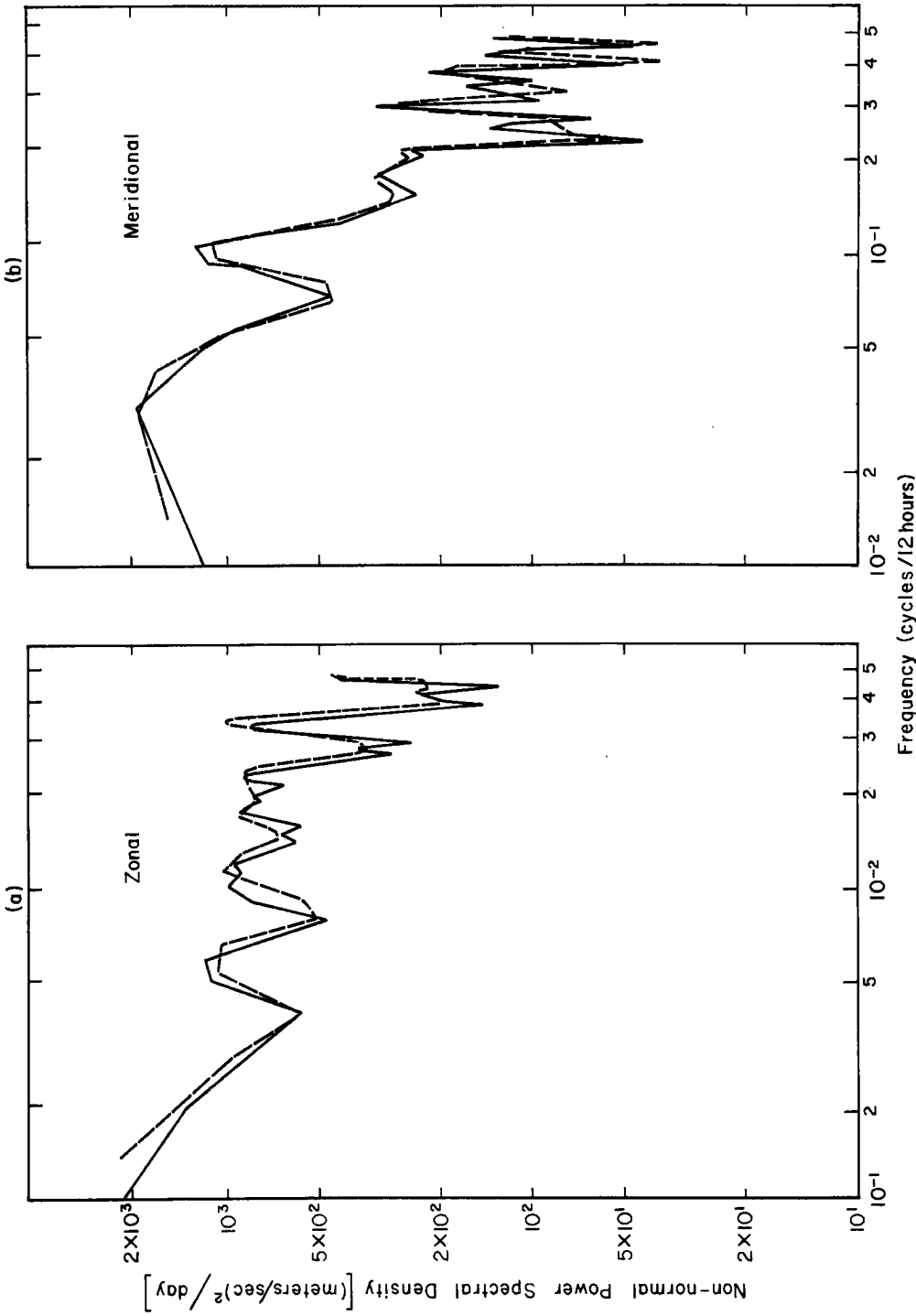


Fig. 4.5-2 Winter-long (solid line) and winter-short (dashed line) spectra at the 200 mb level for the Nantucket (a) zonal and (b) meridional wind components.

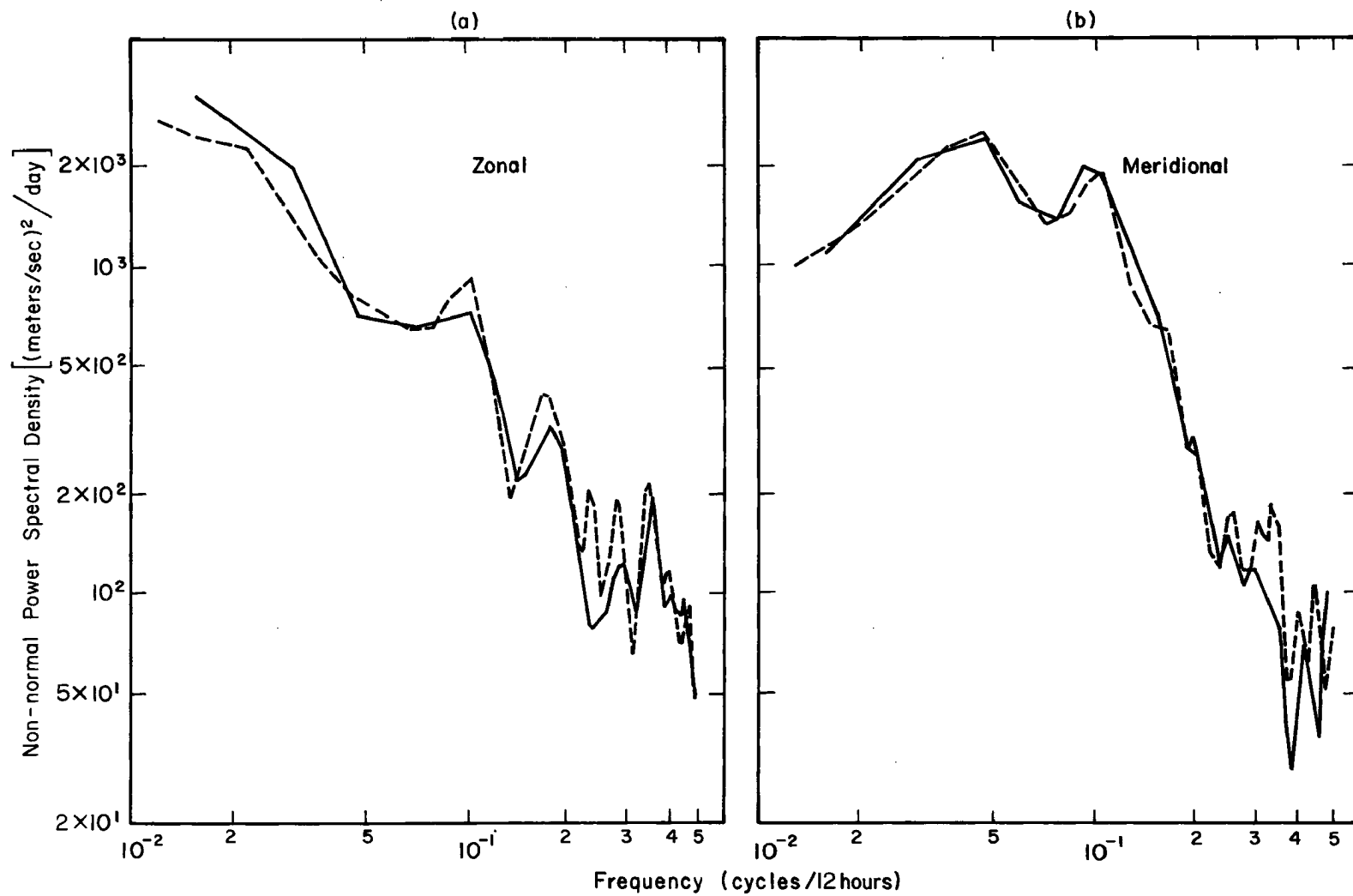


Fig. 4.5-3 Spring-short (solid line) and spring-long (dashed line) spectra at the 200 mb level for the Nantucket (a) zonal and (b) meridional wind components.

spring spectra altered by changing the length of the data record. The respective spectra of the aforementioned stations are presented in Figs. 4.5-4 and 4.5-5. As is evident from these two figures, the characters of the zonal circulation as represented by the power spectra for spring can be different depending on the length of the data record used.

Not only the zonal spectra but also the meridional spectra can be altered by defining the seasons differently. Evidence of this actually occurring is furnished by the 300-mb meridional winter spectra for Oakland which is presented in Fig. 4.5-6.

#### 4.6 Australian Spectra

Ten Southern Hemispheric stations (Fig. 3.0-2) were examined for the five year period, 1958-1962. Of these stations Cocos Island, Darwin and Lae were considered to be too far equatorward to be of value in this particular paper. Only two stations, Alice Springs and Charleville, were in a continental regime. The Australian continent lies between 12° and 37°S which is considerably equatorward of the United States where much more detailed analyses are possible. In making direct comparisons of the Australian spectra with the North American results obtained previously, much care needs to be exercised.

As mentioned in Chapter 3, the wind data from Australia were recorded at constant heights rather than at constant pressure levels. In a preliminary study comparing constant pressure-level statistics with constant height-level statistics Essenwanger (private communication) found that considerable discrepancies may result. His only comparison thus far used the standard deviation of relative density which is defined as  $\rho_r = \frac{\rho_i - \rho_s}{\rho_s}$  where  $\rho_s$  refers to the standard atmosphere density at a

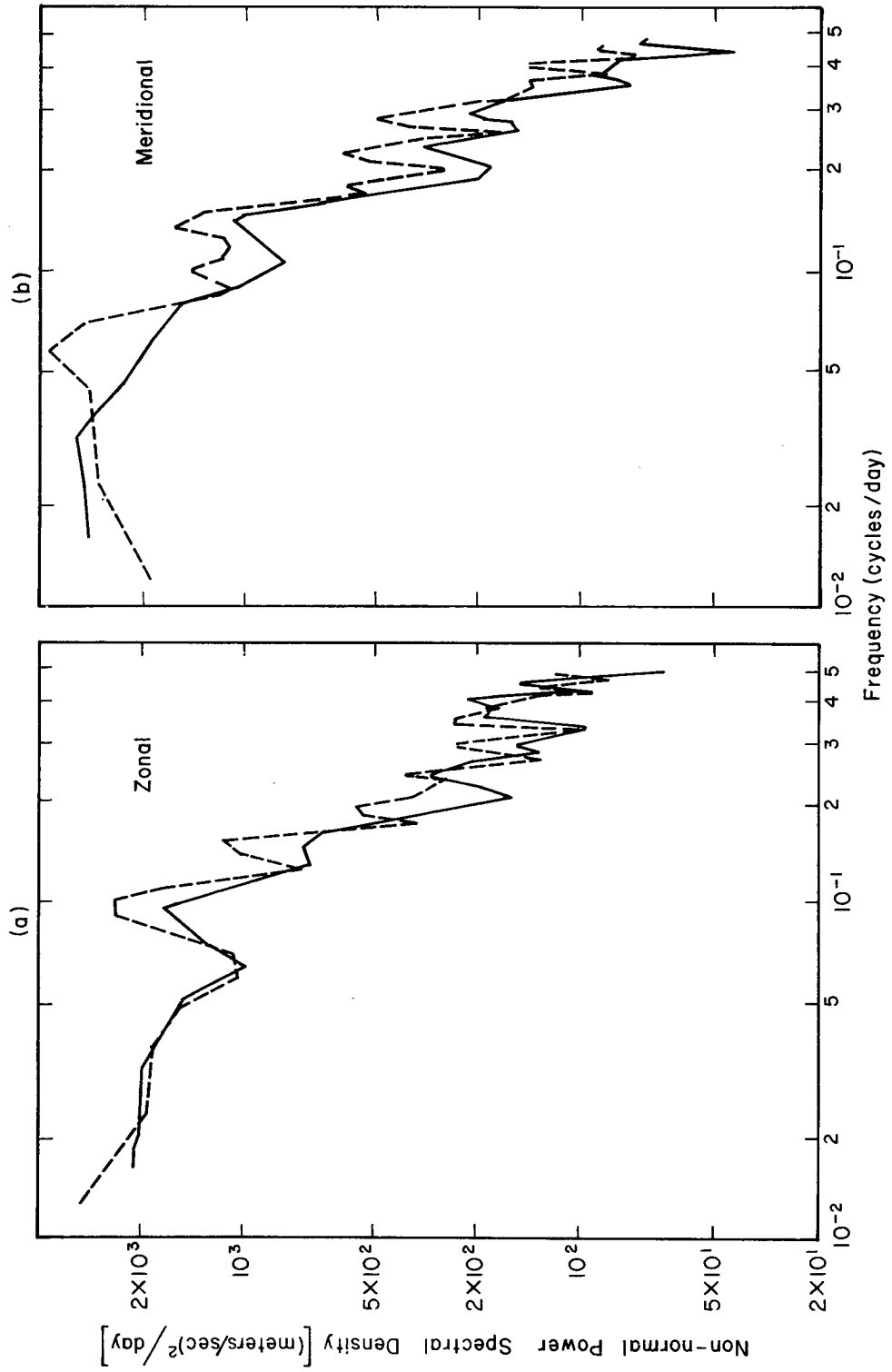


Fig. 4.5-4 Spring-short (solid line) and spring-long (dashed line) spectra at the 200 mb level for the Oakland (a) zonal and (b) meridional wind components.

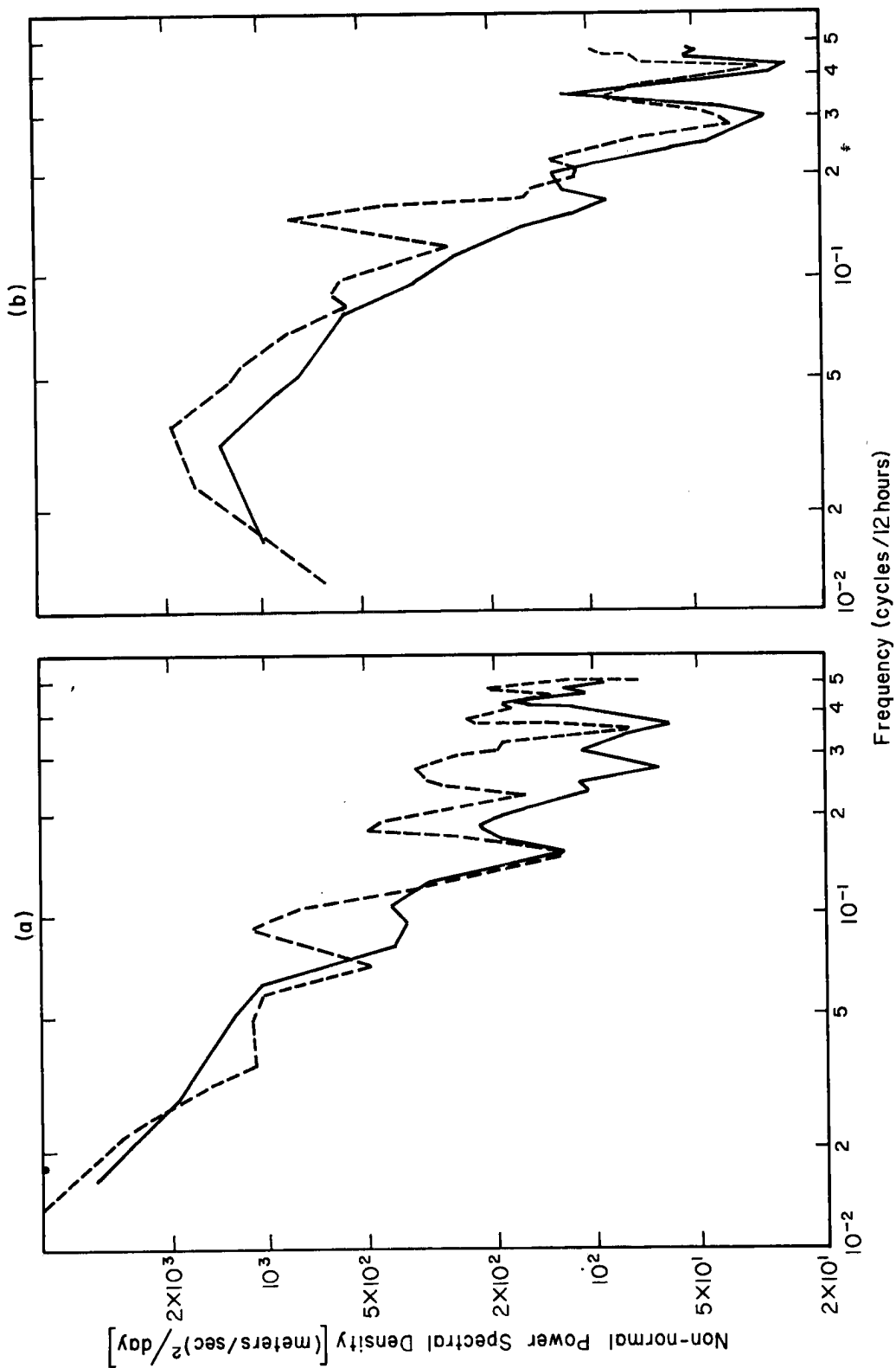


Fig. 4.5-5 Spring-short (solid line) and spring-long (dashed line) spectra at the 200 mb level for the Jackson (a) zonal and (b) meridional wind components.

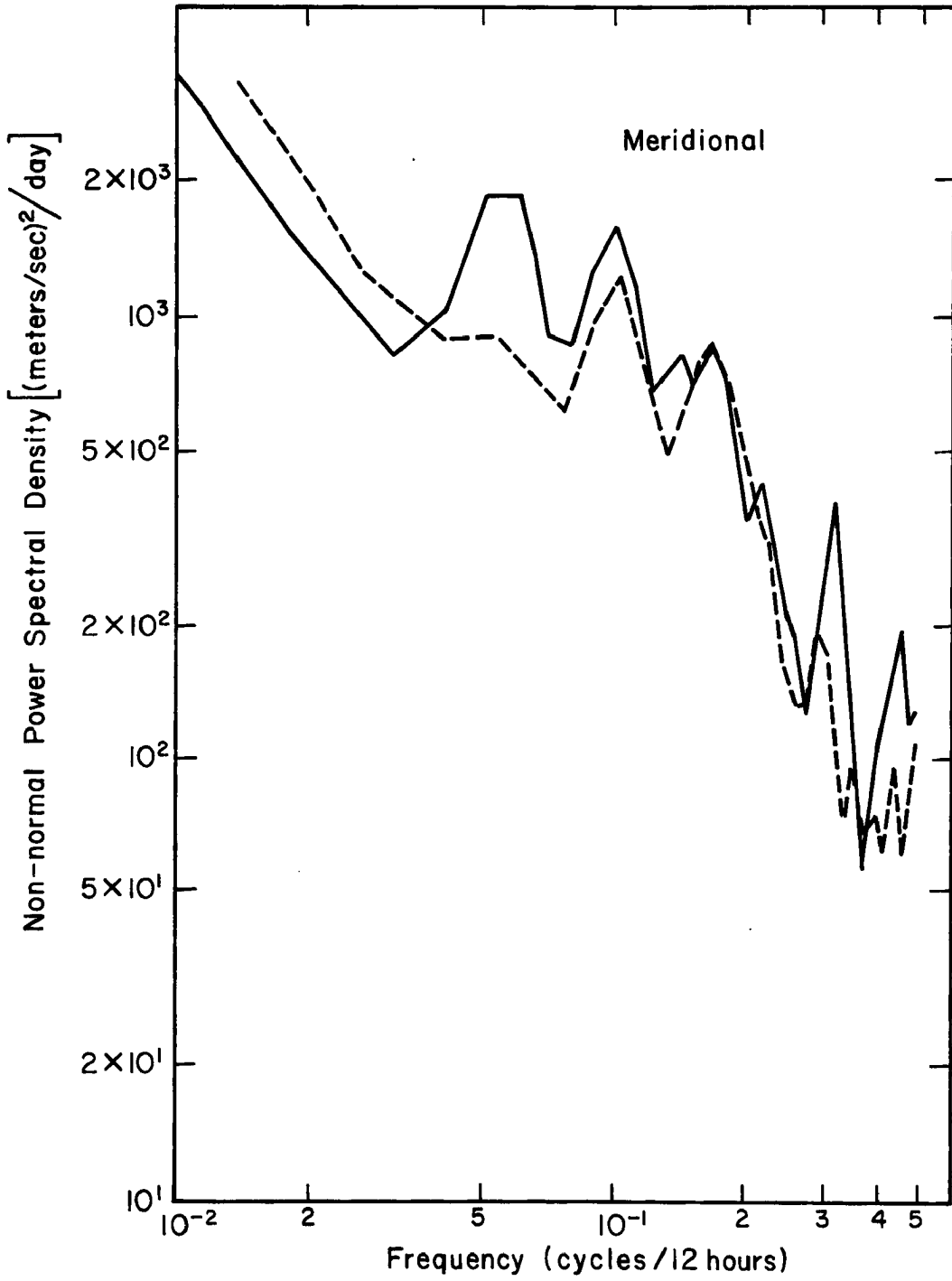


Fig. 4.5-6 Winter-long (solid line) and winter-short (dashed line) spectra at the 300 mb level for the Oakland meridional wind component.

particular height and  $\rho_i$  is the actual measured density. Fig. 4.6-1 shows the results he obtained. Essenwanger's investigation does not imply that wind statistics will be affected as much as the relative density, nor does it preclude this possibility. The actual comparison of these two methods of data recording and their effect upon statistical analyses will be the subject of a future report. A serious problem in the interpretation and comparison of atmospheric phenomenon may exist if the aforementioned conclusions prove to be true.

Table 4.6-1 summarizes the yearly and five-year variances and the mean zonal and meridional winds for each of the ten stations at the 30,000, 35,000, and 40,000 foot constant height levels. Wide variations exist from one year to the next, often by as much as 60%; the variations are not restricted to one level for a given station or one year for all stations. Anderssen (1965), Gibbs (1965; 1953), Radok and Grant (1957), Rubin and van Loon (1954), Taljaard (1967) and van Loon (1965; 1967) repeatedly pointed out the extreme variability of the Southern Hemispheric circulation and weather systems; this study reinforces their conclusions. Figure 4.6-2 graphically depicts the monthly mean latitudes of the Southern Hemispheric 200-mb subtropical jet stream axis from  $110^{\circ}$  to  $170^{\circ}$ E for the years 1956-1961 (Weinert, 1968). Weinert (1968) also determined the annual variation of the mean latitude of the Southern Hemispheric 200-mb subtropical jet stream axis at  $120^{\circ}$ E for the six years, 1956-1961. These annual variations are shown in Fig. 4.6-3. As a further illustration of the Southern Hemispheric variability, Weinert (1968) calculated the seasonal changes in the mean latitudes of the 200-mb subtropical jet stream axes from  $110^{\circ}$ E to  $170^{\circ}$ E for the same six year period (Fig. 4.6-4). The present investigation

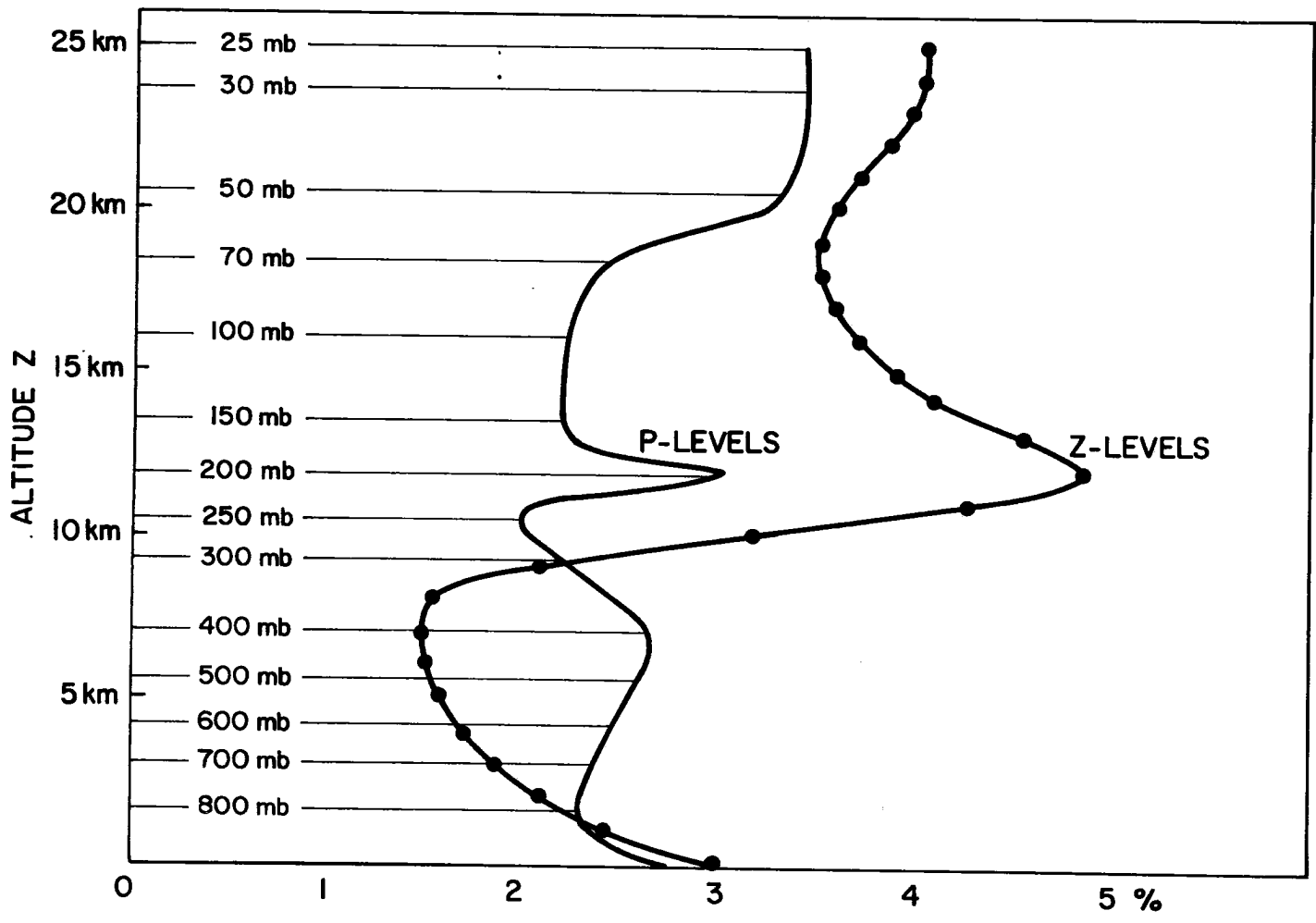


Fig. 4.6-1 Comparison of pressure-level statistics with height level statistics using the standard deviation of relative density. (After Essenwanger, private communication.)

Table 4.6-1

Yearly and five-year variances and the mean wind speeds  
for seven Australian stations at the 30,000 ft.,  
35,000 ft., and 40,000 ft. levels.

	1958	1959	1960	1961	1962	1958-1962	
	var/ $\bar{u}$						
	var/ $\bar{v}$						
Townville	167/22	174/22	199/21.5	127/22	170/23	168/22	40,000 ft.
	126/-2	148/-2	111/-0.001	141/-1.1	137/.91	134/-0.8	
	171/20	152/20	189/21	122/21	162/20	159/20	35,000 ft.
	102/-0.6	142/-1	90.5/.15	112/-0.47	107/1.3	111/-0.17	
	155/16	133/17	168/17.5	111/18	133/16	141/17	30,000 ft.
	82/.06	110/-0.5	69+.3	90/146	95/1.6	90/.4	
Alice Springs	234/32	213/30	398/34	230/32	246/32	266/32	40,000 ft.
	192.5/2	231/2.7	188/1.1	195/5	222/6.8	210/3.5	
	253/28	228/26	411/31	257/28	268/29	286/28	35,000 ft.
	158/2	186/3.3	164/1.1	161/4.7	177/6.1	172/3.4	
	237/22.5	214/20	396/26	260/21.5	231/22	272/22.5	30,000 ft.
	114/2	146/3.4	134/1.6	122/5.5	126/5.4	131/3.6	
Charleville	332/37	356/36	425/36	307/33	320/34	350/35	40,000 ft.
	187/2	276/1.8	208/4	260/2.0	218/3.3	230/2.7	
	354/34	333/31	445/33	364/29	317/30	365/31	35,000 ft.
	202/-0.9	300/1.7	170/3.4	235/2.75	207/3.6	224/2.5	
	324/26	297/25	375/27	316/22	290/25	323/25	30,000 ft.
	146/1.4	207/2.4	136/3	200/217	141/3.4	166/2.5	

Table 4.6-1 (Continued)

	1958	1959	1960	1961	1962	1958-1962	
	var/ $\bar{u}$						
	var/ $\bar{v}$						
Eagle Farm	305/38	337/35	451/40	308/34	322/35	349/36.5	40,000 ft.
	254/1	232/-.16	275/1.3	244/-3.1	267/-.58	253/-.45	
	317/33	363/31	437/36	362/31	368/32	372/32	35,000 ft.
	226/1	238/-.22	255/1.1	252/-2.6	247/.41	245/-.06	
	285/25	290/23	354/22	334/23	311/25	318/25	30,000 ft.
	169/1	155/-.16	180/.8	183/-1.1	168/.62	161/.29	
Guildford	493/35	310/37	403/37	389/35	366/37	393/36	40,000 ft.
	174/2	319/-.73	228/1.3	178/-1.1	181/.65	198/.44	
	423/27.5	283/32	379/32	382/29	410/32	377/31	35,000 ft.
	171/.8	221/-1.0	231/-.2	205/-1.1	216/-.01	209/-.24	
	284/22	241/25	276/24	260/21	307/25	276/23.5	30,000 ft.
	139/.4	179/-1.6	185/.23	147/-1.4	148/-.13	160/-.52	
Adelaide	354/30	305/25	272/29	297/24	357/29	323/27	40,000 ft.
	204/1	200/3.6	202/3.2	205/4.6	159/5.1	197/3.6	
	329/25	304/21	318/26	281/20	402/26	332/24	35,000 ft.
	207/1	206/2.7	243/2.5	201/4.3	191/4.1	211/2.9	
	235/20	249/17	256/20	189/16	276/21	244/19	30,000 ft.
	171/1	167/1.6	193/2.1	168/4	166/3.3	174/2.4	

Table 4.6-1 (Continued)

	1958	1959	1960	1961	1962	1958-1962	
	var/ $\bar{u}$						
	var/ $\bar{v}$						
Hobart	182/24	177/21	234/20	219/18	214/21	209/21	40,000 ft.
	210/-.8	226/-.1	193/-.1	219/1.9	203/-.64	212/.081	
	238/23	226/19	271/18	246/16	244/20	250/19	35,000 ft.
	273/-1	299/-.41	278/-.7	262/1.3	252/-1.1	273/-.36	
	235/21	219/17	255/16	225/15	193/18	230/17	30,000 ft.
	256/-1.4	256/-.64	268/-1.0	243/1.0	258/-1.1	257/-.63	



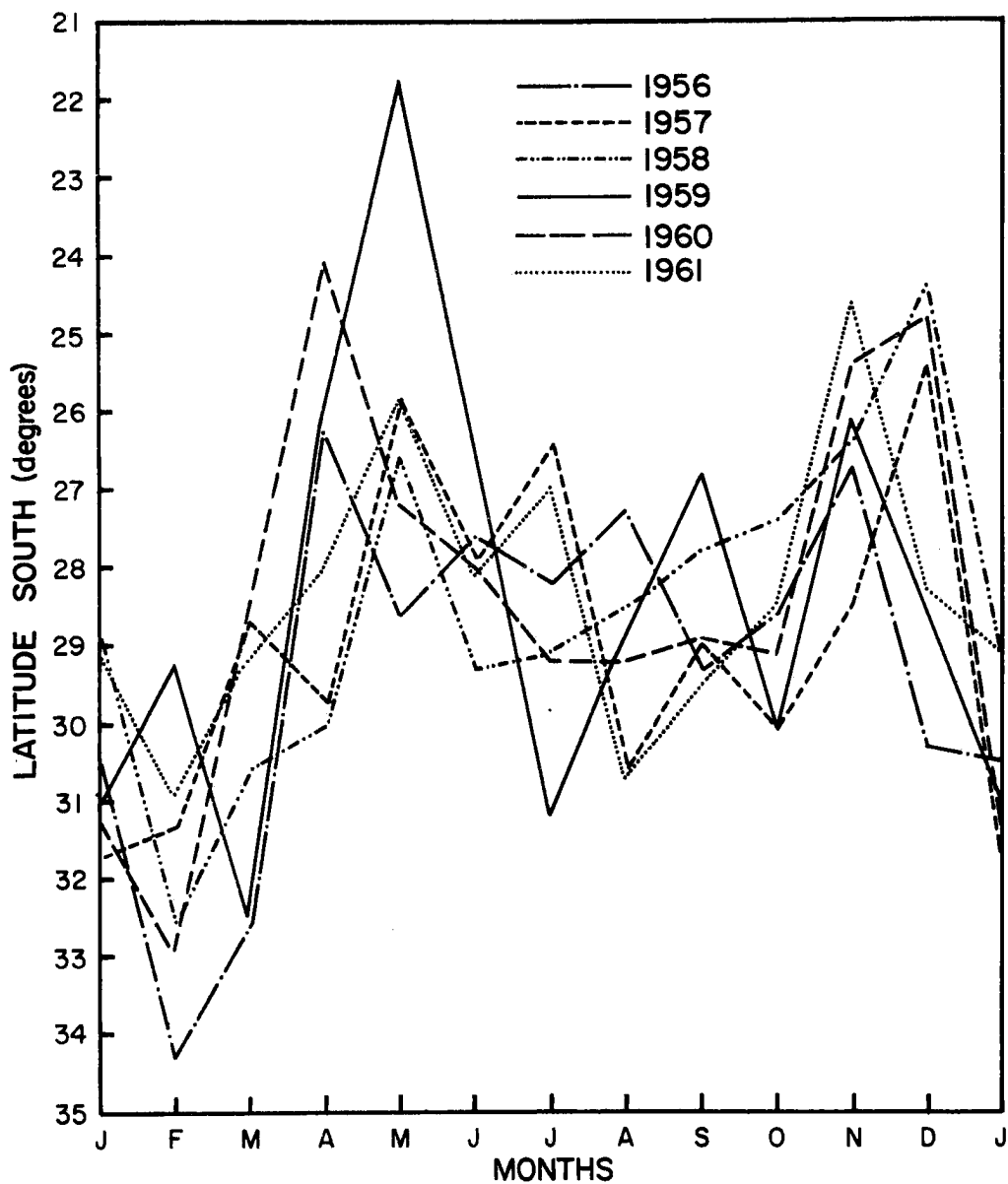


Fig. 4.6-3 Annual variations of the mean latitude of the Southern Hemispheric 200 mb subtropical jet stream axis at 120°E for 1956-1961. (After Weinert, 1968.)

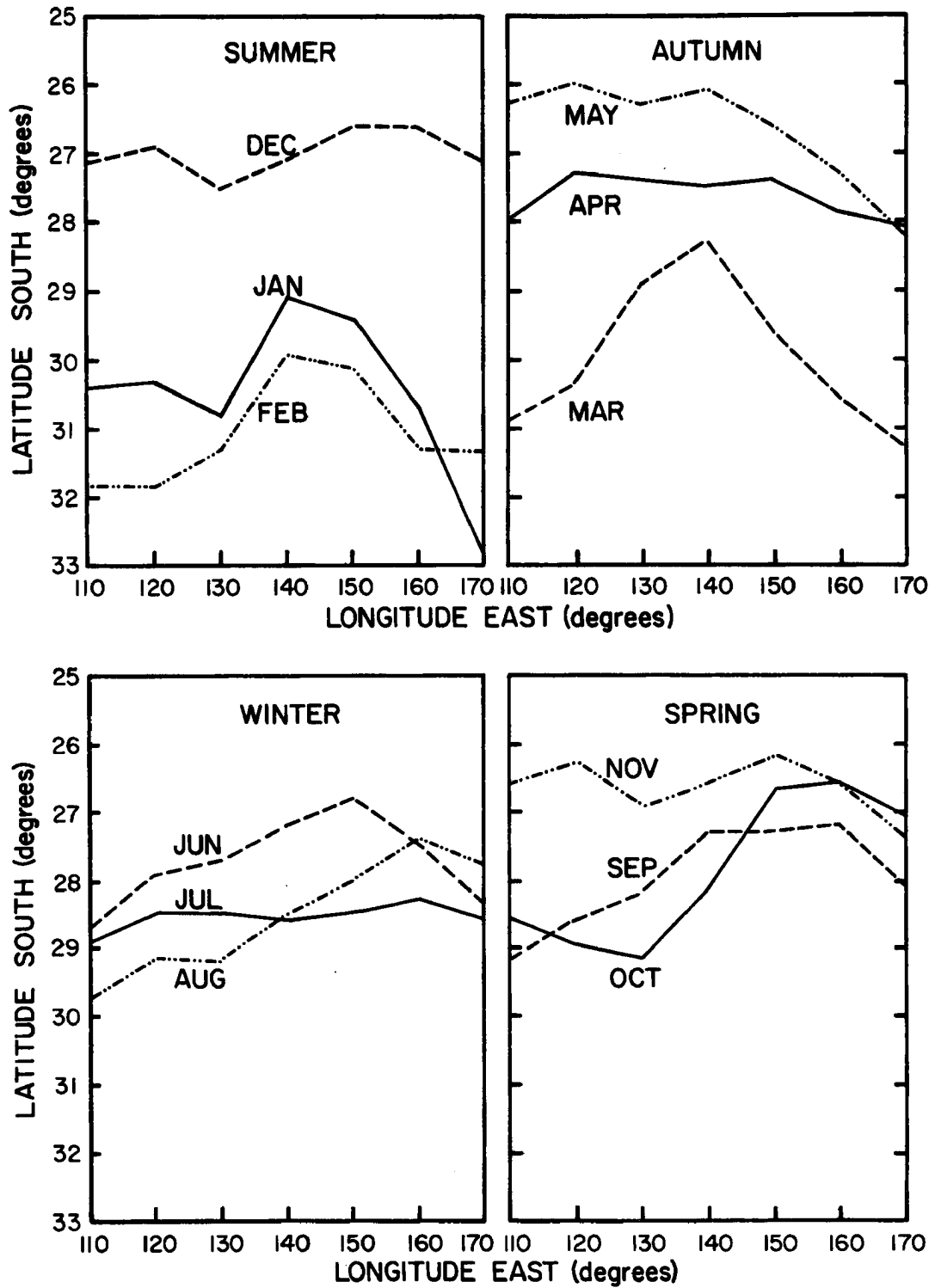


Fig. 4.6-4 Seasonal change in the mean latitudes of the Southern Hemispheric 200 mb subtropical jet stream axis from 110°E to 170°E for 1956-1961. (After Weinert, 1968.)

deals with the years 1958-1962, therefore Weinert's statistics may be considered relevant.

To illustrate the wide range of values in the spectral representations Alice Springs was selected. Figure 4.6-5 provides this comparison. As can easily be seen, each year portrays a different spectral distribution; a spectral peak one year and a minimum value the next year may occur at a given frequency. In the zonal spectra, the only spectral peak common to all years is around a periodicity of 3.2 days. The above statements are also applicable to the meridional spectra. Three years have a spectral peak near 3.6 days with the 1959 spectrum providing an exception. The above results demonstrate that individual spectra are indicative only of the data period subjected to analysis.

Representing the variation with height of both the zonal and meridional spectra, Figs. 4.6-6 and 4.6-7 present the spectra of Townsville for 1959 and Eagle Farm (Brisbane) for 1958 and 1961, respectively. The zonal spectra of Townsville remains essentially unaltered as a function of height, both in magnitude and slope. The 40,000 foot level has the highest spectral densities over most of the spectrum while the lowest spectral densities occur at the lowest level, 30,000 feet. Good agreement is also found among the three levels in the meridional spectra of Townsville. The 40,000 foot spectrum has the higher spectral densities at the lower frequencies; the 35,000 foot spectrum has the higher values at the middle frequencies and the 30,000 foot spectrum generally has the lowest spectral densities. The most obvious feature of these spectra is the peak at all levels at 9.25 days. As discussed in Chapter 4.4, this periodicity in the Northern Hemisphere corresponded to small height changes in the

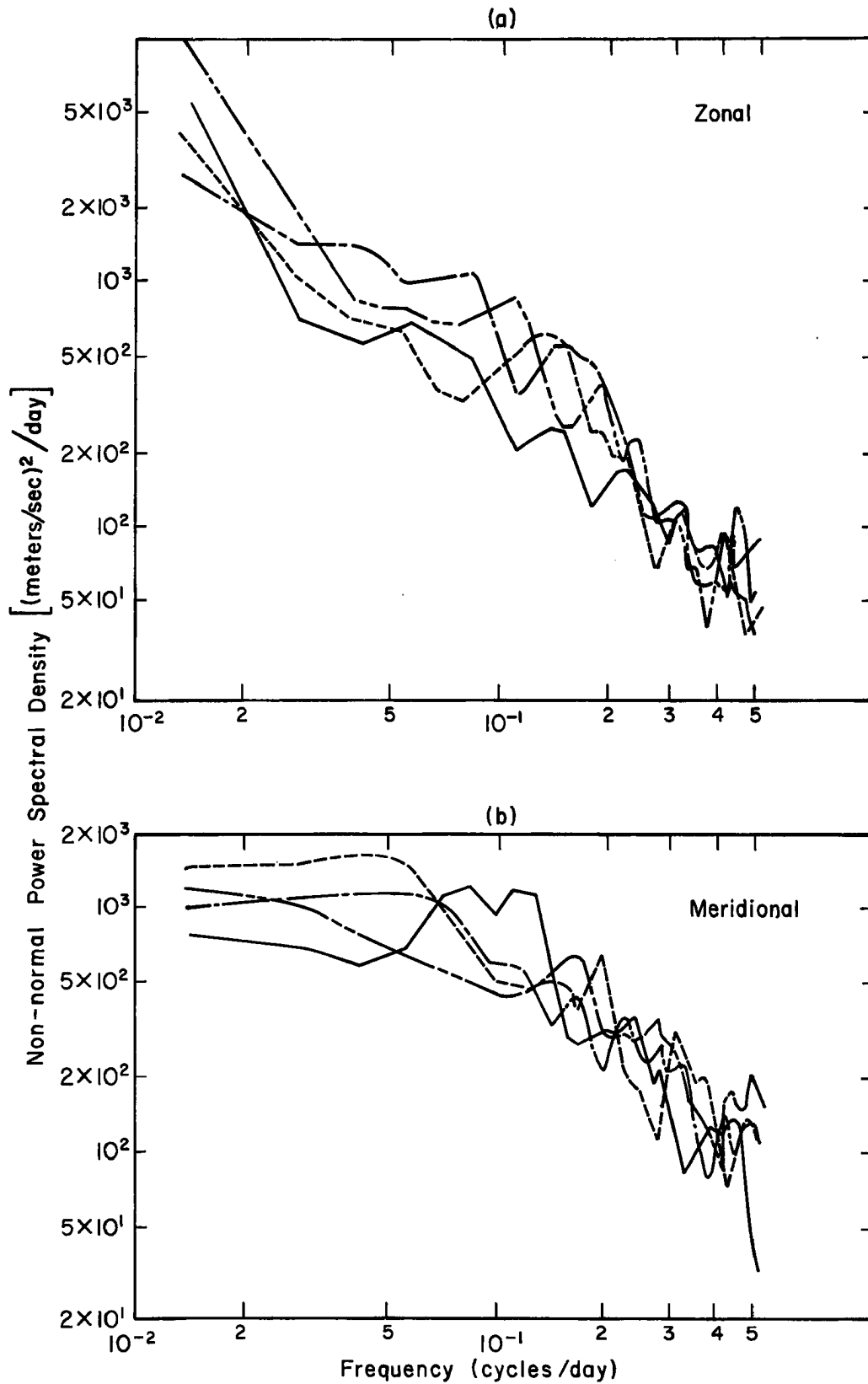


Fig. 4.6-5 Annual variations in the Alice Springs spectra for the (a) zonal and (b) meridional wind components for the years: 1958 (solid line), 1959 (dashed line), 1960 (dash-two dot line), and 1961 (dash-dot line).

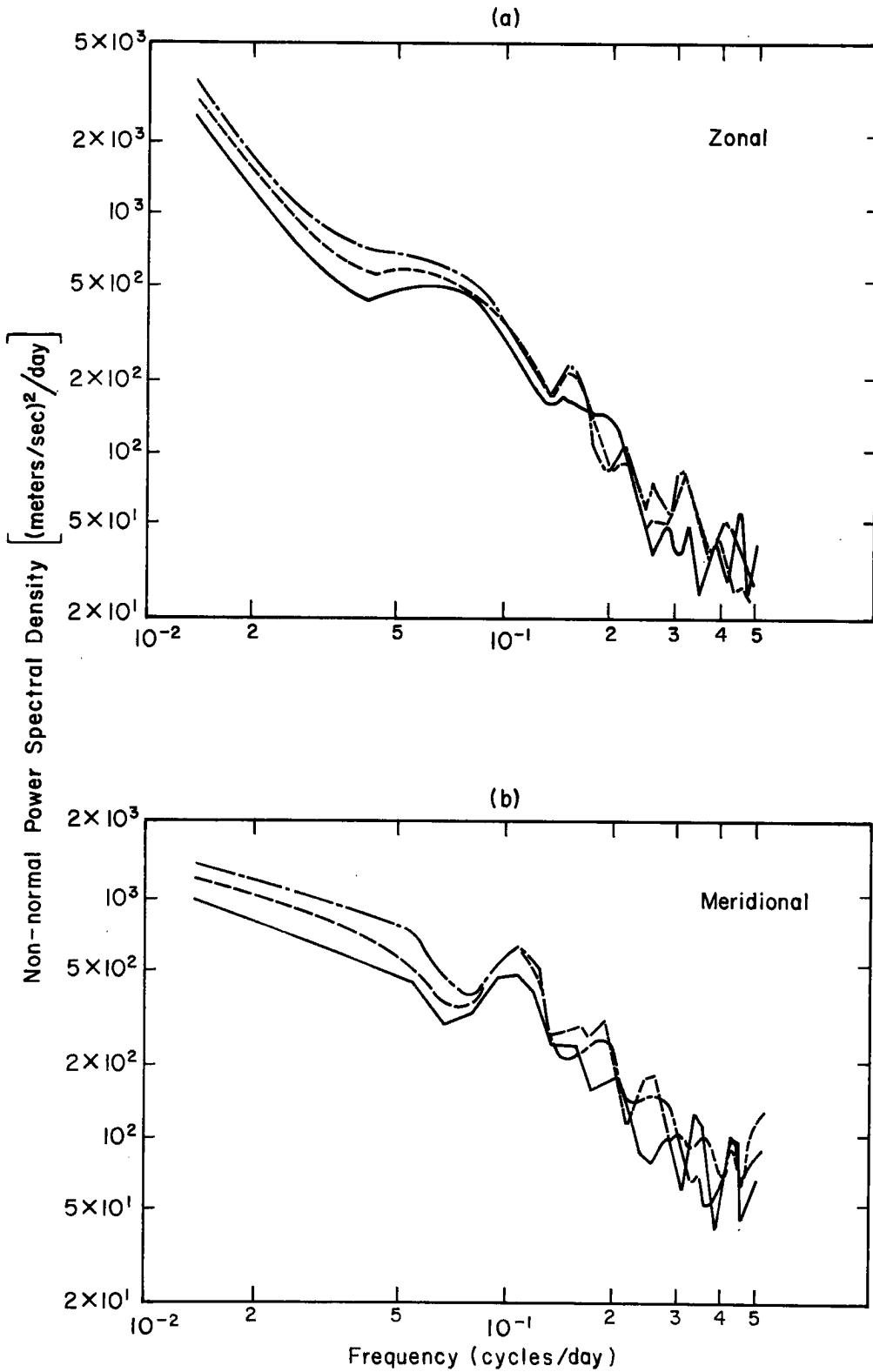


Fig. 4.6-6 Height variations in the (a) zonal and (b) meridional spectra for Townsville, 1959: 30,000 ft. (solid line), 35,000 ft. (dashed line), and 40,000 ft. (dash-dot line).

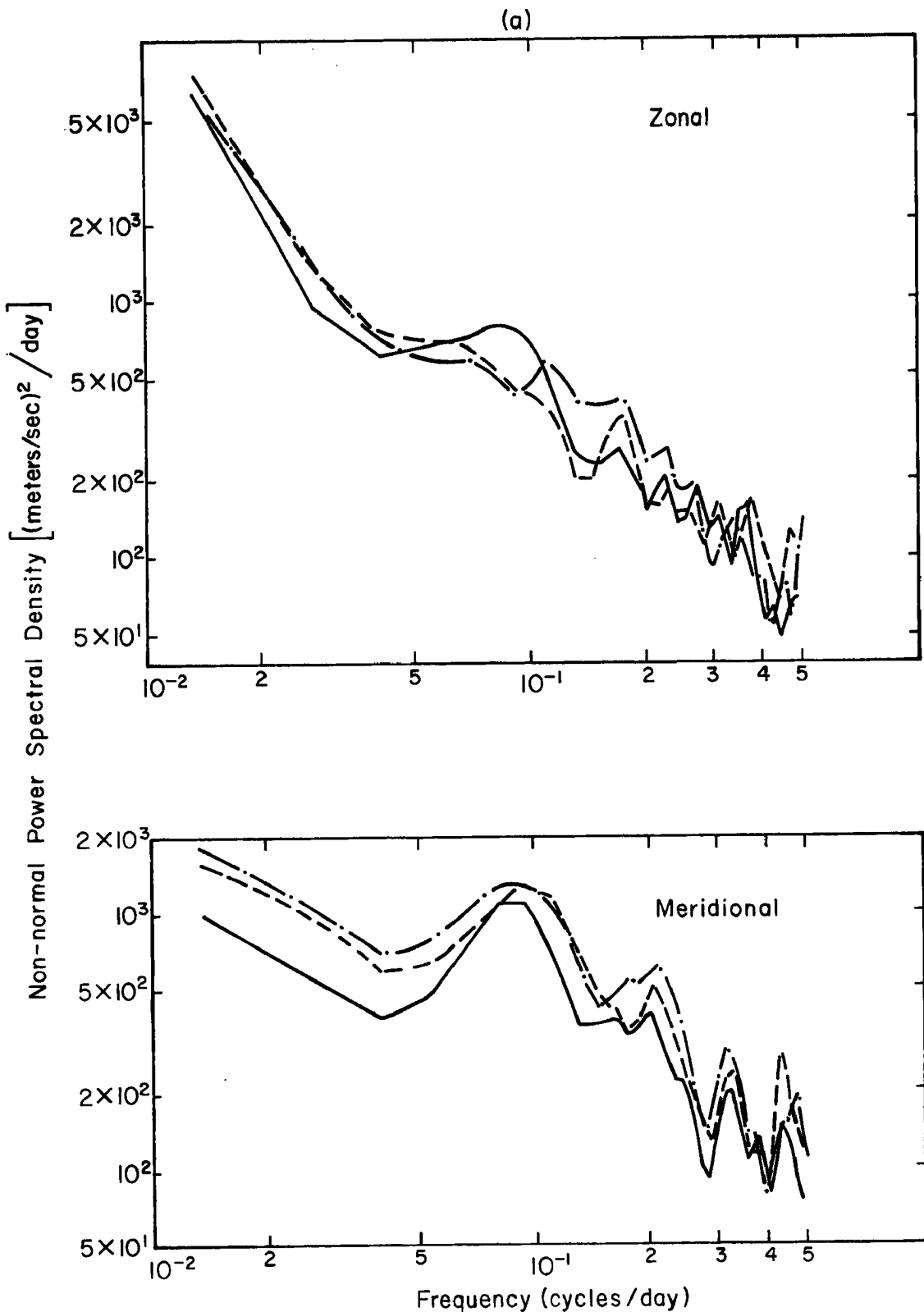
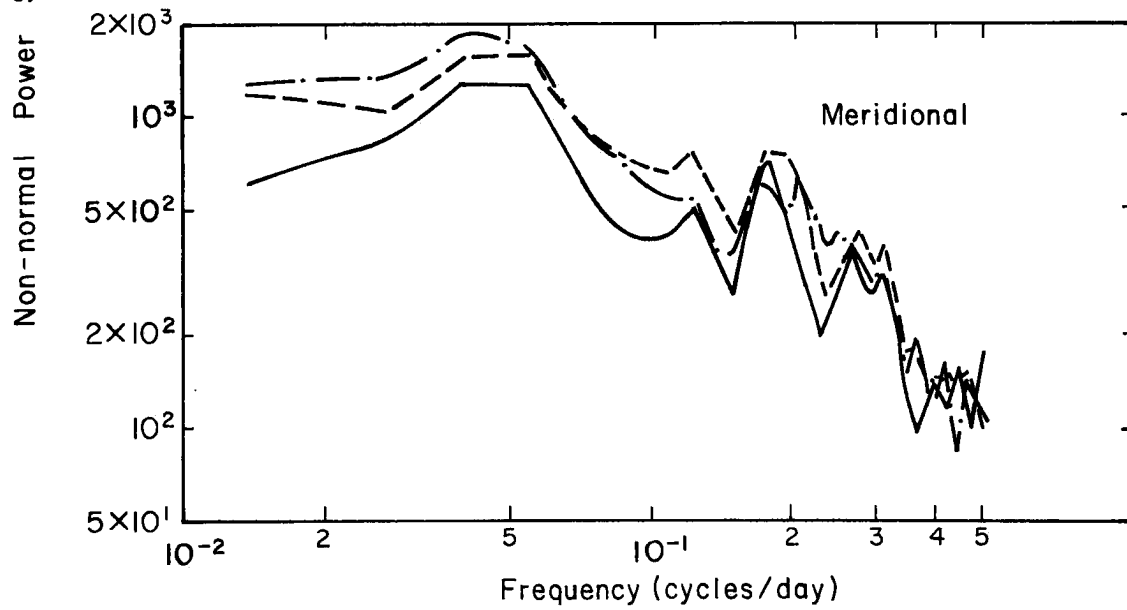
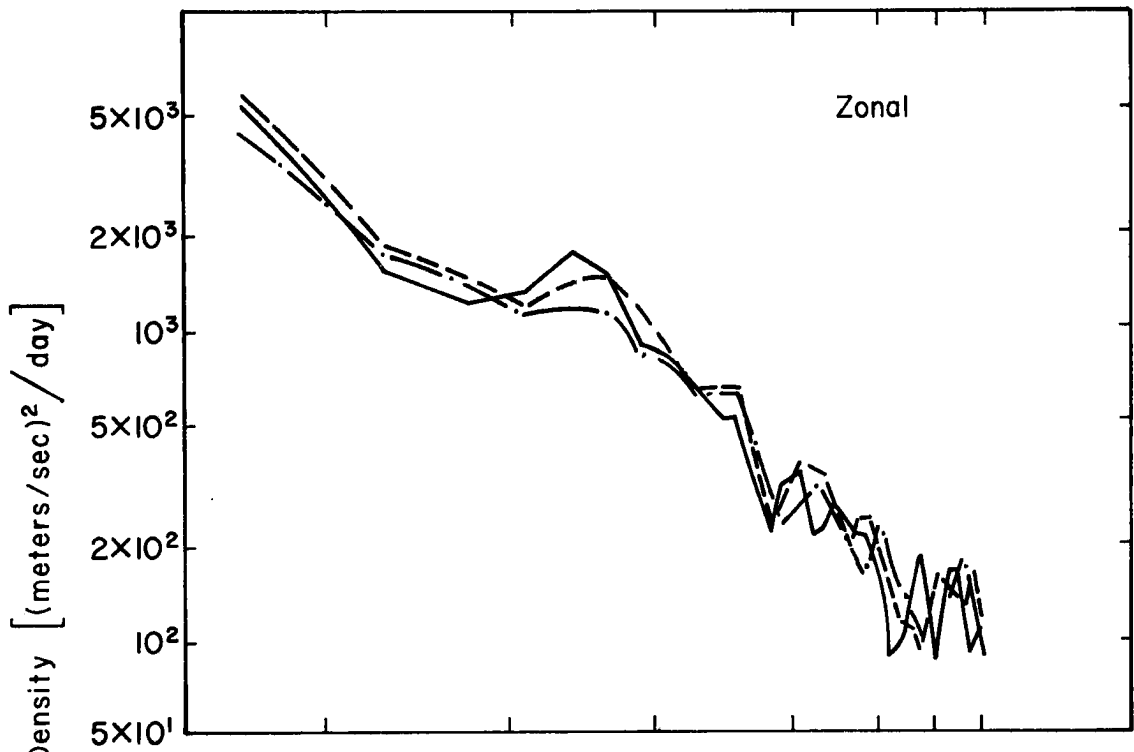


Fig. 4.6-7 Height variations in the (a) 1958 and (b) 1961 zonal and meridional spectra for Eagle Farm (Brisbane): 30,000 ft. (solid line), 35,000 ft. (dashed line), and 40,000 ft. (dash-dot line).

(b)



constant pressure levels. In this case, if the analogy holds, the peak at 9.25 days would be the result of small pressure fluctuations in the constant height fields.

In Weinert's (1968) analysis of the subtropical jet stream over Australia for the years 1958-1961, he found that the year 1959 was one of great fluctuations in the month-to-month latitudes of the STJ (Fig. 4.6-4). Thus, despite this wide latitudinal variation, the spectra of the three levels remained unchanged relative to each other.

The same general conclusions derived from examining the Townsville spectra are also true of the 1958 and 1961 annual spectra for Eagle Farm (Fig. 4.6-7). The agreement in shape among the spectra in Fig. 4.6-7a of the meridional component is almost exact. Each spectra displays four definite peaks at 10.6-, 4.9-, 3.1- and 2.3-days. With the exception of the high frequency end of the spectrum where the 35,000 foot spectral values exceed the others, the 40,000 foot level possesses the highest spectral densities.

The Eagle Farm spectrum for 1961 is presented in Fig. 4.6-7b to provide a check on the above conclusions regarding the relative magnitudes of the spectral densities at the three constant heights. The only deviation from the above results occurs in the meridional spectra where the 35,000 foot spectral values become greater than the 40,000 foot values at a much lower frequency than in the previously analyzed year, 1958. A predominant meridional spectral peak exists at 5.7 days in the 1961 spectra whereas this spectral peak was not prevalent in the 1958 spectra. It can be concluded, however, that the spectra agree quite well in shape and general magnitude regardless of height; this result

then allows a comparison of spectra between stations and wind components to be made at one level.

One further noteworthy result concerns the 30,000 foot spectra of the above stations. In all of the previous examples, the spectra at this level were characterized by two facts: (1) it had generally the lowest spectral densities of the three heights examined, and (2) it generally exhibited the widest fluctuations in number of spectral peaks and in the range of maximum and minimum spectral values. These observations indicate that the winds at the lower levels were much more variable than those in the upper levels near the tropopause. The same conclusion was also derived from the spectral analyses of the North American winds.

#### 4.7 Interhemispheric Comparisons

Interhemispheric comparisons of the upper tropospheric wind patterns cannot be made on a latitudinal basis. Perhaps this result should be expected in light of the different climatic regimes which are determined mainly by the variations in the land-sea distribution between the hemispheres and from different orographic features. Guildford (31°56'S) and Midland, Texas (31°56'N) are located at the same latitude in the Southern and Northern Hemispheres, respectively. Their spectra are presented in Fig. 4.7-1. Obviously neither the zonal nor the meridional spectra agree in general shape or in positions of spectral peaks. To verify the above conclusion in more general terms, the Guildford spectra were compared with the nine other spectra of stations aligned along 32°N.

It would be redundant to reproduce all the spectra merely to verify that no agreement was found between them and their Southern Hemisphere counterpart. The fact that little similarity existed between

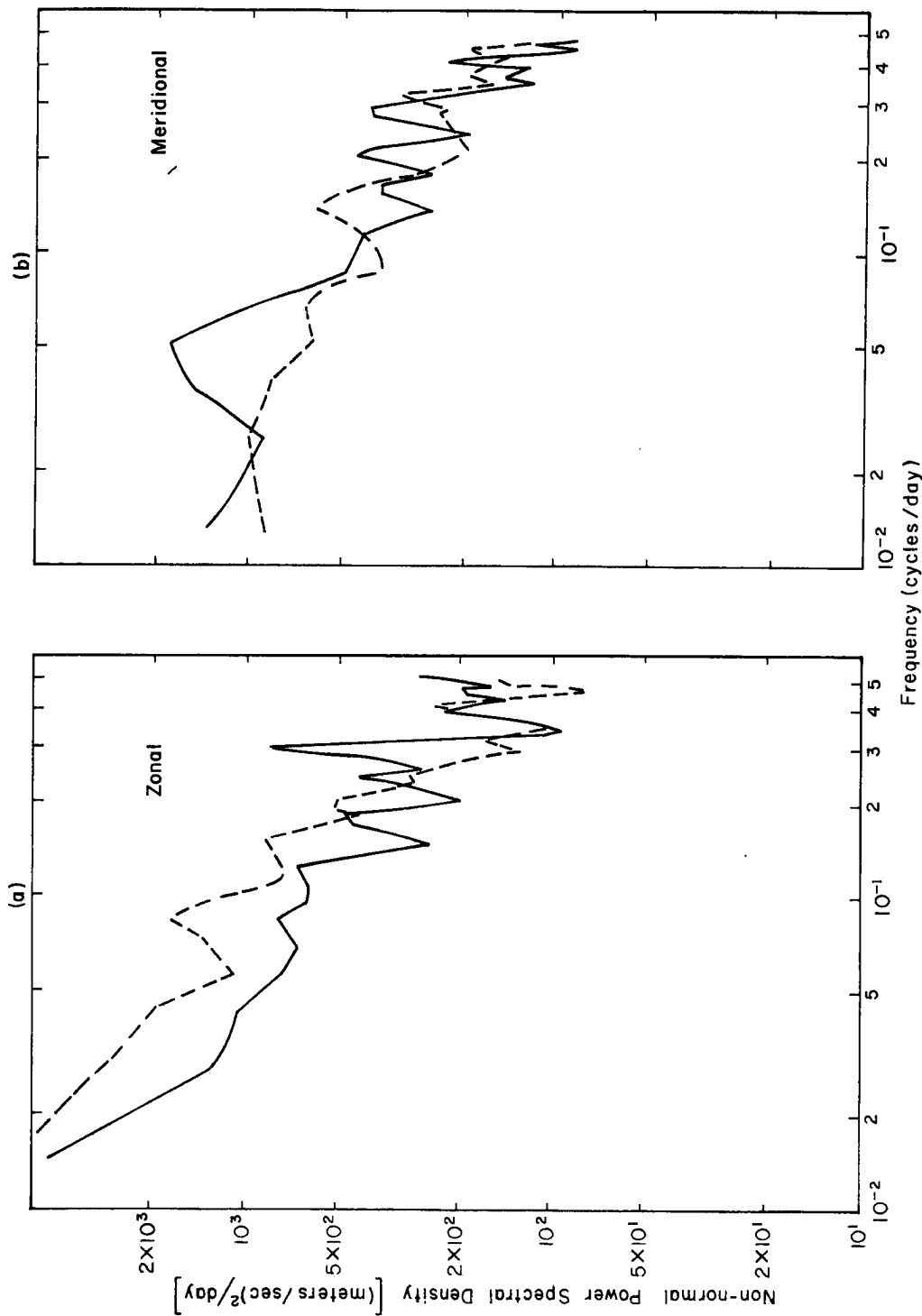


Fig. 4.7-1 Comparison of the (a) zonal and (b) meridional spectra between the 200 mb level at Midland, Texas (31°56'N), (solid line) and the 40,000 ft. level at Guildford (31°56'S) (dashed line).

either the zonal or the meridional spectra of the respective stations leads to the conclusion that different upper-tropospheric wind patterns occur at the corresponding latitudes in the respective hemispheres.

In light of the above conclusion, the next logical choice in order to more adequately compare the hemispheric wind systems would be along "natural" coordinates. Since Australia lies too far equatorward to be influenced by a polar front jet stream system and since the subtropical jet stream extends over Australia as well as over Mexico and the southeastern United States, the STJ axis in the respective hemispheres may serve as the reference line.

Many studies have been done specifically on the Subtropical Jet Stream over Australia (Gibbs, 1952; Hutchings, 1950; Loewe and Radok, 1950; Muffatti, 1963; Phillipot, 1959; Porter, 1953; Radok and Grant, 1957; Spillane, 1968; Weinert, 1968). Reiter (1963), and to a limited extent Riehl (1962), discussed the Southern Hemispheric jet streams from a more general point of view. Muffatti (1963), Spillane (1968) and Wienert (1968) dealt with the same six year period, 1956-1961; four years during this period were also examined in the present investigation (1958-1961). The mean positions and behavior of the Northern Hemispheric STJ have been deduced generally from Reiter (1963), Riehl (1962) and specifically from Krishnamurti (1961a; 1961b).

Spillane (1968) discerned the height of the Southern Hemispheric strongest mean wind to be very close to the 200-mb (40,000 foot) level; this was the only level analyzed by Muffatti (1963) and Weinert (1968). Consequently, only the 40,000 foot level spectra were used in this paper. Krishnamurti (1961a) and Reiter (1963) located the core of the Northern Hemispheric STJ at approximately 200-mb. Krishnamurti (1961a)

found that the mean latitude of the STJ for the 1955-1956 winter was  $27.5^{\circ}\text{N}$  with a wave-like distribution of  $12.5^{\circ}$  in magnitude. Muffatti (1963) determined the average position of the Southern Hemispheric STJ core to be  $28.5^{\circ}\text{S}$  with a standard deviation of  $3.7^{\circ}$  latitude in longitudes  $120^{\circ}$  to  $140^{\circ}\text{E}$ ; the standard deviation decreased to  $2.9^{\circ}$  latitude at  $160^{\circ}\text{E}$ .

Due to the orographic influences on the wind systems over North America, zonal perturbation motions, expressed as maxima embedded in the main current, are prevalent. Lack of such orographic features over Australia would then tend to shift the burden in transport processes to the meridional perturbations in the main current. Table 4.7-1 lists the spectral densities of the 200-mb (40,000 foot) zonal spectra for stations located along the STJ axis in the two hemispheres. Variations exist along the jet axis over the North American stations. These variations can be accounted for by the fact that the STJ in the Northern Hemisphere only persists during winter (Reiter, 1963). This allows factors in other seasons to influence the annual spectra; thus, at similar frequencies different spectral densities may result in the annual spectra of the stations located along the STJ axis. Charleville and Eagle Farm are the only two stations which might be considered to actually lie along the Australian STJ axis; the axis as determined by Spillane (1968) actually passes over Eagle Farm. Guildford lies south and Alice Springs is located north of said axis (Spillane, 1968). The STJ over Australia is much more persistent than its Northern Hemispheric counterpart. Thus some of the differences in the spectral densities can be accounted for by the location of stations and by characteristics of the STJ itself. The analysis of a larger data sample would prove

Table 4.7-1

Zonal spectral densities at selected periodicities  
for stations located along the Northern Hemispheric  
subtropical jet stream and the Southern Hemispheric STJ

	1/14.8 Days	1/6.17 Days	1/3.52 Days
Empalme (255)	882 m <sup>2</sup> sec <sup>-2</sup> Day	266	261
Chihuahua (225)	534	272	203
Del Rio (261)	508	203	276
Lake Charles (240)	664	358	240
Burwood (232)	809	252	105
Jacksonville (211)	562	741	296
Tampa (206)	526	600	85
Guildford (Perth)	1040	538	138
Alice Springs	868	415	98
Charleville	1164	363	165
Eagle Farm (Brisbane)	1007	373	149

beneficial in the determination of a mean spectrum but would lend little insight in the attempt to understand a spectrum of any given year or season. The extreme variability of the Southern Hemispheric winds have already been noted previously.

Wooldridge and Reiter (1970) contend that the spectral densities of the zonal component over the synoptic scale range in the Southern Hemisphere are less than the corresponding spectral densities in the Northern Hemisphere by a factor of two. Their analysis was based upon results obtained from two New Zealand stations, Christchurch and Invercargill, and one North American station, Washington, D.C. The inaccuracies inherent in such a comparison have already been pointed out and need not be reiterated now. However, despite the limitations of their study, the general conclusion which they reached has some merit.

The most notable feature in Table 4.7-1 concerns the zonal spectral densities at 1/3.52 days. The spectral values of the Australian stations are lower, generally by half, than the values of the North American stations. This is the same result which was derived by Wooldridge and Reiter (1970). Regarding the relative magnitudes of the zonal spectral densities at lower frequencies, their results differ from those obtained in this analysis. As shown in Table 4.7-1 the zonal spectral densities of Australia are greater than those of North America at the period of 14.8 days. Wooldridge and Reiter (1970) listed the New Zealand spectral values as being less than half of the Washington, D.C. value at this periodicity. Their meridional values compared favorably with ours. Their result was based on three stations with

widely varying wind characteristics; consequently a great deal of emphasis cannot be placed on this particular result of their study.

#### 4.8 Conclusions

The conclusions and results of this study may be briefly summarized as follows:

1. The variances and spectral densities at particular periodicities show distinct geographical variations related to positions of jet streams and tracks of traveling cyclones and anticyclones. Maximum spectral energies occur at frequencies  $1/4.9$  and  $1/3.4$  days. The peak at a periodicity of 8-10 days may be associated with small height fluctuations in pressure fields.
2. Meridional spectral densities are shown to be greater than zonal values.
3. The effect of lengthening or shortening the time periods defined as a "season" may significantly alter the resulting seasonal spectra.
4. Wide variations in spectra for different years occur over Australia; however, the spectra of the height levels were remarkably similar.
5. Corresponding latitudes in the Northern and Southern Hemispheres do not have the same spectral representations. Consequently, inter-hemispheric comparisons of spectra should be made along a "natural coordinate axis, e.g., subtropical jet stream axis.
6. Interhemispheric spectral comparisons indicate that cyclones with periodicities of 3-6 days account for relatively more meridional transport of energy in the Southern than in the Northern Hemisphere; this is probably the result of the lack of orographic features in the Southern Hemisphere which could anchor the wind regimes.
7. Spectrum analysis properties show geographical differences

between 200- and 300-mb related to the sloping of the tropopause with latitude as shown in the Appendix.

## 5.0 SPECTRA OF WIND COMPONENTS - THEORETICAL CONSIDERATIONS

In this chapter, a critical review of analytical and numerical work is presented. Observational and theoretical results which will be helpful in the interpretation of the conclusions presented in Chapter 4 have been emphasized. Also, studies which refer to the determination of atmospheric spectra by other investigators are briefly reviewed in order to check the consistency of the results presented in this study.

### 5.1 Numerical and Analytical Models

In this section a review of numerical and analytical models is presented to offer an explanation for the periodicities found in the atmosphere and discussed in Chapter 4.3 and presented in Fig. 4.3-1. Simplified versions of the equations of motion have been analyzed in these models either by means of numerical integrations or by linearized theories. The present object is to examine available theories which are sufficiently simplified to be readily interpreted with respect to their predictions for the observed flows. Toward this purpose barotropic and baroclinic theories will be reviewed independently. They are summarized in Table 5.1-1.

Lorenz (1961) considered a two-dimensional, homogeneous, incompressible inviscid flow with no variation of the Coriolis parameter. This motion is governed by a barotropic vorticity equation of the form

$$\frac{\partial}{\partial t} \nabla^2 \psi = -\vec{k} \cdot \nabla \psi \nabla (\nabla^2 \psi) .$$

This equation approximately governs the vertically averaged flow in the tropical atmosphere and therefore can be used to interpret its behavior in the middle levels.

Table 5.1-1

Categorization and synthesis of barotropic and baroclinic  
theoretical models. (Modified from Paegle, 1969)

Author	System of Equations	Other Specifications	Method	Pertinent Results
Lorenz (1960)	Nonlinear barotropic no $\beta$ -effect	Vorticity represented $\nabla^2 \psi = A \cos ly + B \cos kx + C \sin ly \sin kx$	Initial value numerical integration	Minor fluctuations 5.5 days. Major fluctuations 6.5 days
Aihara (1961)	Nonlinear barotropic $\beta$ Plane	Initial representation $u = u \cos ny$ $\psi(x,y) = A \cos ly \cos kx$	Numerical integration	Periods from 8-15 days
Arakawa (1961)	Linear barotropic $\beta$ effect, mean flow		Numerical integration using atmospheric data as initial state	Periods around 9 days
Baer (1964)	Nonlinear barotropic	19 $\psi = \sum_{k=1} \psi_K e^{iKx} \frac{\phi p}{K} x(\sin \phi)$	Numerical integration	Exchange between mean flow and wave number 1: Period = 3 days 3: Period = 6 days
Kenyon (1966)	Nonlinear barotropic $\beta$ Plane	$\psi = \sum_{\vec{k}} \psi_{\vec{k}} e^{i\vec{k}x + \omega t}$ Weak nonlinear integration	Asymptotic expansions	Fore-equilibrium conditions $E(k) \propto k^{-2}$
Gambo (1966)	2-level quasi-geostrophic model with variable mean shear flow and static stability	One initial wave (only one considered) through integration	Numerical integration	With variable mean shear flow only - 20 days with variable static stability also - 10 days

Table 5.1-1 (Continued)

Author	System of Equations	Other Specifications	Method	Pertinent Results
Arakawa (1969)	$\beta$ level quasi-geostrophic flow with variable mean shear flow	Solution obtained in terms of elliptic functions	Analytic results	Periods from 10-30 days
Brown (1969)	Quasi-geostrophic model	Initial wave was most unstable baroclinic wave	Numerical integration	Periods from 3-4 days

Solutions to this equation are given by

$$\nabla^2 \psi = \sum_{\vec{n}} e^{i\vec{n}\cdot\vec{x}}$$

$$\psi = \sum_{\vec{n}} \frac{1}{nn} \psi_{\vec{n}} e^{i\vec{n}\cdot\vec{x}}$$

where  $\vec{x}$  represents the position vector and  $\vec{n}$  the horizontal wave number vector. The system is characterized by conservation of the mean energy and mean vorticity. This system does not allow a cascade of vorticity or energy towards smaller scales.

Solutions of this system are expressed in terms of elliptic functions which depend upon the ratios  $k_x/k_y$  and  $V/E$  where  $V$  is the mean vorticity and  $E$  is the mean energy. For convenience Lorenz proceeded to integrate the system numerically.

Periodicities of 5.5 days were found which is slightly greater than the predominant peak of 4.9 days found in Fig. 4.3-1. In these five day cycles momentum is initially transported from the zone of the easterlies to the zone of the westerlies, thus increasing the zonal index. As the zonal index builds to greater values it eventually breaks down after 66 hours with the flow regaining its initial appearance after 5.5 days.

For the linear case in which the Fourier coefficient of the cosine term is constant the following results are obtained: for  $k_x/k_y > 1$  the flow is stable and harmonic solutions can be obtained; for  $k_x/k_y < 1$  the flow is unstable and the disturbances grow, drawing their energy from the kinetic energy of the mean flow. Upon attainment of sufficiently large amplitudes the interactions with the zonal flow determine the decay of the disturbances. In this model the zonal index should undergo some fluctuation in order that the disturbances propagate.

The integration for the case of a large disturbance resulted in a periodicity of 6.5 days. In this case the zonal index changes signs so the easterlies occupy the regions where westerlies were originally present. The disturbances do not propagate in one direction but move back and forth depending upon the zonal index. This was called by Lorenz "large amplitude disturbance" phenomenon.

Though this model is overly simplified and no lateral boundaries are allowed in it, it is interesting to note that this behavior corresponds to that observed in the atmosphere for the very long waves which often fluctuate about a mean position with a period determined by Eliassen and Machenhauer (1965) to be about five days.

Aihara (1961) carried numerical integrations for a non-divergent barotropic atmosphere including a  $\beta$  effect:

$$\frac{\partial}{\partial t} \nabla^2 \psi + \beta \frac{\partial \psi}{\partial x} + J(\psi, \nabla^2 \psi) = 0 .$$

Different linear initial conditions were used. They consisted of a cosine wave in the meridional direction for the zonal flow, with a given amplitude and a disturbance consisting of the product of two cosine waves in the zonal and meridional directions. Rigid lateral boundary conditions were used. The kinetic energy of the zonal flow and the kinetic energy of the disturbance presented oscillations of the same period and of opposite phase. The mean flow kinetic energy presented a weak damping effect associated with the generation of new waves due to the non-linear interactions. Periods for the kinetic energy oscillation found in these computations are presented in Table 5.1-2.

Table 5.1-2

Periods for the kinetic energy oscillation found in the computations by Aihara (1961).

Zonal Wave Number	Zonal Wind Speed (m/sec)	Disturbance North-South Wind Speed Max. (m/sec)	Period of Mean Kinetic Energy Oscillation (day)
1	15	10	12
1	30	10	8
2	15	10	9.5
3	15	10	15

A larger number of degrees of freedom were introduced by Baer (1964), for the spectral representation of the barotropic vorticity equation:

$$\frac{d\psi_{\vec{k}}}{dt} + ik_x \omega_k \psi_{\vec{k}} = A_{\vec{k}} = \frac{dR_{\vec{k}}}{dt}; R_{\vec{k}} = \psi_{\vec{k}} e^{ik_x \omega_k t}$$

where  $\omega_k$  represents the phase speed of Rossby waves on a spherical earth, also known as Rossby-Haurwitz phase speed. The advection term

is given by  $A_{\vec{k}} = \sum_{\vec{m}, \vec{n}} \psi_{\vec{m}} \psi_{\vec{n}} I_{\vec{k}, \vec{m}, \vec{n}}$

where  $\psi_{\vec{m}}$  are the expansion coefficients for the stream function which is represented by  $\psi = \sum_{\vec{k}} \psi_{\vec{k}} e^{ik_x \lambda} P_{\vec{k}}(\sin \phi)$  where  $P_{\vec{k}}(\sin \phi)$  are the

associated Legendre polynomials. The interaction coefficients

$I_{\vec{k}, \vec{m}, \vec{n}}$  are not time dependent.

The equations were truncated at wave number 19 and only odd polynomials were allowed to maintain symmetry of the velocity field with respect to the equator. The initial condition allowed power only in the mean flow and wave numbers one and three. Each wave underwent fluctuations in phase and amplitude. Part of the phase fluctuations were due to the linear characteristics of the system which may be exactly determined. The rest of the fluctuations in phase and all changes in amplitude were due to the nonlinear interactions.

It was noted that: 1) The waves with which the integration was started contained over 91% of the total energy throughout the integration period. 2) Wave number three contributed most of the energy in the initially inactive waves, and in one case also gave energy to wave number one and the mean flow. 3) There was a three-day periodicity in the energy exchange between wave number one and the mean flow and a six day periodicity between wave number three and the mean flow. 4) There was a general exchange of energy between the mean flow and all the waves; when the mean flow was gaining energy most of the waves were losing it and vice-versa. 5) In each of the planetary waves the lowest mode in the y-direction dominated the energy. 6) Truncating the system where Baer (1964) did energy exchanges similar to the ones found by Lorenz (1960) resulted, with three and six day periodicities.

Thus far in the analysis of theoretical studies possible explanations for the peaks in the spectra presented in Fig. 4.3-1 have been presented. The periodicity between 5 and 6 days could be accounted for by the exchange of momentum between the westerlies and easterlies (Lorenz, 1960). The 8-15 day periodicities observed in Chapter 4 may be explained by a kinetic energy oscillation as determined by Lorenz (1960). The 3-6 day periods found by Baer (1964) may correspond with the energy exchanges between wave numbers one and three and the mean flow. It is within this frequency range that the greatest number of stations examined in Chapter 4 possessed their largest spectral values (Fig. 4.3-1).

Up to this point the barotropic vorticity equation was numerically integrated to determine the behavior and periodicities related to non-linear mechanisms. These periodicities might be related to some of the

periodicities observed at a single station in the atmosphere in addition to the periodicities related to the propagation of waves. When the wave number and frequency of the disturbances are related or connected it is possible to explain some of the features observed in a single station frequency spectrum in terms of the characteristics of the instantaneous wave number spectrum. This conversion has been discussed by Reiter (1972) and Vinnechenko (1970). It is therefore of interest to review some theories about the characteristics of the wave number spectrum which might be helpful for the understanding of the observed time behavior at a single station. In the case when the scales under consideration extend all around the globe as considered up to here, an expansion in discrete modes is only possible since an integral number of waves should fit around the earth. When the wavelength becomes smaller, this concept loses significance and a continuous spectrum of waves can be found in the system.

For the case in which a continuous spectrum of waves is possible wave bands instead of discrete modes should be considered in the analysis. Wave bands occur in a dispersive medium, such as the atmosphere. In a dispersive medium, the phase speed is a function of wavelength. This must be done since it has been shown by Benney and Newell (1967) that energy might be transferred to the side bands of a discrete wave in the same time scale as energy goes to the discrete mode itself by the resonant mechanism. The side bands of a discrete mode are the adjacent modes extending on either side of the discrete mode. Therefore if these resonant interactions are responsible for the preferred development of certain wave numbers in the atmosphere a spectral analysis of relevant atmospheric variables will reveal the

presence of a finite bandwidth peak or wave package rather than discrete wave number contributions (Newell, 1969). Amplitudes of these wave packages may be periodic functions of time along their group velocity lines. The group velocity results from considering finite bandwidth wave packages, its effect being to introduce an amplitude modulation of the waves in a time scale longer than the oscillations of the waves themselves. When the nonlinear effects are neglected the amplitude of the wave will remain constant and no modulation of the amplitude will occur when moving along group velocity lines (Reiter, 1963).

For wave numbers five through seven and prevailing conditions at mid-latitudes barotropic non-divergent and divergent models predict group velocities of the order of 26 meters per second towards the east; twice as fast as their respective phase speeds. When no mean flow is considered the group velocity turns out to be approximately equal to the phase speed propagating in the opposite direction, to the west.

The main effects of the nonlinear interactions are two-fold: new modes are created and resonant modes are excited.

An idea for the time scales of the nonlinear interactions can be obtained from Kenyon's (1967) computations of energy transfer rates. It was observed that energy was transferred from waves with lower wave numbers to waves with higher wave numbers with a time scale of interactions of approximately ten days. This is to be compared with the pronounced peak evident in both the zonal and meridional spectra presented in Fig. 4.3-1. Kenyon (1967) compared this to a wave period of 7.4 days. Wave numbers five to seven, those with wavelengths of four to five thousand km in mid-latitudes, are believed to be the result of baroclinic instability. In effect these wavelengths

correspond to the ones which would amplify first in a two-level quasi-geostrophic model. A non-divergent barotropic model would predict for such wavelengths a phase speed towards the west of approximately 6.6 m/sec and if a mean flow of 20 m/sec is considered a phase speed of 13.4 m/sec results towards the east. For these short waves a divergent barotropic model predicts essentially the same phase speed, 12.7 m/sec. Phase speeds from 5 to 15 m/sec were numerically found by Brown (1969) for wavelengths from 6,000 to 3,000 km in his numerical investigation of atmospheres with lateral and vertical shears. These values correspond to eastward moving waves with periods around four days. The periodicity lies between the two major energy peaks found in Chapter 4, 3.36 days and 4.9 days. Though Kenyon's (1967) results are obtained from a model in which the mean flow is at rest it might be more realistic to interpret his results in terms of eastward moving waves in the presence of the mean flow which are those observed in the atmosphere. In this case the nonlinear interactions occur on time scales at least 2.5 times larger than the wave periods.

Newell (1969) determined that for waves with characteristic time scale of four days in which the nonlinear interactions are occurring on time scales of ten days, the excitation of the zonal flow from the neighborhood of resonant waves will occur at time scales of the order of 20-25 days. This may be one explanation for the peaks in the energy spectra for the zonal flow found at approximately 18 days in our data (Fig. 4.3-1).

Each of the models considered in detail up to this point have been barotropic. One of the simplest baroclinic models which could be applied with some generality to the atmosphere consists in a two-level

linearized quasi-geostrophic model where a disturbance periodic in the x and y directions is allowed to exist superimposed in a basic zonal flow independent of y. Arakawa (1969) developed such a system.

A period of about 20 days is obtained from this development. The process responsible for this cycle is characterized by the growing baroclinic disturbances transporting heat northwards. The northward heat transport will decrease the thermal wind, both of them controlling the growth of the disturbance, which in turn controls the behavior of the northward heat transport. The result is that the disturbances will reach a maximum value. From then on southward heat transport occurs, thus increasing the thermal wind. In this fashion a cycle is completed.

Gambo (1966) considered essentially the same problem as Arakawa (1969) except that the variation of static stability with time is also allowed and discussed. The numerical integration of his system for a wavelength of 5,000 km showed that when only the vertical shear of the mean flow is considered a function of time, a period of around 17 days is obtained. If the static stability is also considered a function of time, smaller fluctuations are introduced and a period of approximately ten days resulted. The 17 day periodicity is produced by the same effects discussed in connection with Arakawa's (1969) work. The 10 day periodicity may be better examined considering the case when only the static stability is allowed to be time dependent and the mean vertical shear is kept constant in time (Arakawa, 1962). Then heat is transported upwards and northward by the growing baroclinic disturbances thus increasing the static stability as the wave becomes of finite amplitude. This increase of the static stability has in turn an effect

in modifying the meridional heat transport, which in turn controls the growth of the disturbance. Thus, maximum values are obtained for the disturbance and the meridional heat transport. As the latter changes sign, the static stability decreases and the disturbance transports heat downwards. A full cycle is completed in this way.

Brown (1969) considered a quasi-geostrophic numerical model in order to study the instabilities of a small amplitude wave for cases where both the lateral and vertical shears were included. For the case when the lateral shear presented vorticity maxima at various latitudes it was found that the system produced two wavelengths of maximum instability, the shorter one amplifying through a prominent baroclinic mechanism, drawing its energy from the available potential energy of the basic flow and through a conversion of available eddy potential energy to eddy kinetic energy. A weaker barotropic stabilizing mechanism existed also where the kinetic energy of the disturbance was transferred to the kinetic energy of the basic flow. The relatively long unstable waves have as energy sources both available potential and kinetic energy of the basic flow. These results were obtained for the case in which typical values of the atmosphere for the vertical variation of the zonal winds (mean January winds at  $45^{\circ}\text{N}$ ) and static stability (winter, Gates, 1961) were used.

As the kinetic energy of the zonal flow was increased the wavelength of maximum instability shifted towards lower values, from values of 6,000 km down to 3,000 km, with phase speeds from 5 to 15 m/sec for the longer wave; and from values of 3,500 to 3,000 km for the shorter wave with phase speed around 15 m/sec. As the zonal available potential energy increased the wave of maximum instability shifted towards higher wavelengths.

Comparing these cases to the pure baroclinic case it was noted that the effect of the lateral shear acted in destabilizing the shorter waves, shifting the value of maximum instability towards smaller wavelengths, decreasing the phase speed and stabilizing the longer waves. In comparison to the barotropic case it was noted that the effect of the vertical shear was to increase the growth rate of the unstable wave.

The zonal flow was made time dependent in order to study the non-linear interactions between an initially unstable eddy with the zonal flow. A wavelength of 4,500 km was chosen which at first grew primarily through a baroclinic mechanism. The overall rapid weakening of the zonal flow which occurred as the disturbance amplified obscured at first the barotropic pulsation of the jet stream. This consisted in splitting the jet in the middle of the channel traveling towards the side walls, weakening and being reflected, a jet in the center of the channel reforming in the meantime. This effect became apparent after 1.5 days. An energy source was included to represent the gross effects of diabatic heating. The solution in time approached an oscillation about a steady state. For this case periods obtained from Brown's Graphs are listed below for different quantities:

- 1) Conversion from zonal kinetic energy to eddy kinetic energy occurred in 3 to 4 days.
- 2) Conversion from available zonal potential energy to available eddy potential energy in 4 to 5 days.
- 3) Eddy and zonal kinetic to available potential energy in 4 to 5 days.

The previous results determined in Chapter 4 may then be thought of in connection with the aforementioned determinations of periodicities

by Brown (1969). It appears that the energy conversions which occur within the 3 to 6 day periodicities may account for, at least in some part, the peaks observed in Fig. 4.3-1.

## 5.2 Horizontal Wave-number Spectra

In this section previous works associated with the determination of the horizontal wave number spectrum and the time variability of the larger scales are reviewed. Table 5.2-1 depicts some of the basic characteristics of the work done by previous investigators.

Eliassen and Machenhauer (1965, 1969) represented the height field of the 1000- and 500-mb surfaces using spherical harmonics. It was seen that the wave numbers associated with the greatest large scale meridional fluctuations exhibit a periodic fluctuation about a mean position corresponding to a period of five days. The ones associated with the second largest scales exhibit mean propagation towards the west, their speed decreasing with decreasing scale, for example

(k,n) = (1,4) Phase speed =  $20^{\circ}$  long/day; period = 18 days

(k,n) = (2,5)  $12^{\circ}$  long/day; 14 days

(k,n) = (3,6)  $8^{\circ}$  long/day; 14 days

where k,n indicates the number of zero points between the North and South Poles in the associated Legendre functions of the first kind. These values are in agreement with the predictions from the divergent barotropic model which essentially gives a modified Rossby-Haurwitz phase speed especially for the moderately large scales.

These ideas were confirmed in their later paper (Eliassen and Machenhauer, 1969), though the relative contribution of the zonal flow, long and ultra-long waves to the total variance, changed somewhat. It was also found through the investigation of phase angles that the mean

Table 5.2-1

Categorization and synthesis of previous studies done in the wave-number or space domain. (Modified from Paegle, 1969)

Author	Period Covered	Latitudes ( $^{\circ}$ N)	Levels (MBS)	Wave Number	Assumptions
Saltzman and Peixoto (1950)	1950	30, 45, 60	500	1-12	Real Wind Data
Win-Nielson (1959)	1/1954-4/1954	13 to North Pole	600	1-15	Quasi-Geostrophic Model
Peixoto (1960)	1950	0 to 80	800 to 300	Stationary and Transient Eddies	Real Data
Saltzman and Fleischer (1962)	1951	15 to 80	500	0-15	Geostrophic
Shapiro and Ward (1960)	1/1945-1/1953	30, 45, 60	500	1-12	Geostrophic
Messineer (1963)	1/21/58-8/28/58	15 to 88	500	1 < k < 15-1 < n < 11	Balance
DeLand (1963)	10/1951-3/1952	40, 50, 60	500	1-3	Height Data
Hurn and Bryson (1963)	10/1951-4/1952	24, 45, 65	300, 500, 700	1-12	Geostrophic
Saltzman and Teweles (1964)	1955-1964	15-80	500	1-15	Geostrophic

Table 5.2-1 (Continued)

Author	Period Covered	Latitudes ( $^{\circ}$ N)	Levels (MBS)	Wave Number	Assumptions
Eliassen and Machenhauer (1965)	12/1956-2/1957	10-85	500-1000	1<k<18 N-k<20	Balance
Eliassen and Machenhauer (1969)	1957-1958	Northern and Southern Hemispheres	500-1000	1<k<9 0<n<18	Geostrophic

velocities, except for the largest scale, were quite well in agreement with the non-divergent Rossby model. It has been known that the largest scale waves usually fluctuate about a mean position or a slowly changing position, with amplitudes relatively large during the westward motion and relatively small during the eastward motion. This has been interpreted by Deland (1964) as being due to the presence of a westward traveling planetary wave superimposed upon a stationary wave. Since the cosine and sine components of a traveling wave fluctuate in such a way that the cosine component is always a quarter period ahead of the sine component for westward displacement this hypothesis could be tested with a quadrature spectrum (Jenkins and Watts, 1969) applied to the cosine and sine components. Deland (1964) made this analysis for the zonal harmonics one, two and three for latitudes  $40^{\circ}$ ,  $50^{\circ}$ , and  $60^{\circ}$ N. For the first and second harmonics the quadrature was large and positive for periods between 2.5 and 6 days. From the position of the spectral maximum the following values were obtained:

$k = 1$	speed = $90^{\circ}$ long/day	period of 4 days
$k = 2$	speed = $60^{\circ}$ long/day	period of 3 days

### 5.3 Conversion from Frequency to Wave-number Domain

The data available in our case consists in time series at a certain point. Therefore our results are obtained in terms of a frequency distribution. Nevertheless, frequency and wave number spectra can be related to each other when certain characteristics about the waves are known.

When the waves are non-dispersive such that they propagate with a certain phase speed,  $c$ , independent of the wave number the transformation from frequency to wave number domains is straightforward. In

such a case we are just observing in time at a certain point fixed in space the characteristics of the waves along a line parallel to their direction of propagation. For the case in which dispersive effects are present the nature of this dispersion should be included.

The typical situation in the atmosphere is characterized by long waves which fluctuate about a mean position as noted previously. This has been interpreted by some authors (Eliassen and Machenhauer, 1965; 1969; Deland, 1964) as produced by the presence of westward moving waves superimposed upon a stationary wave. The tracking of these waves in order to determine their phase speed is not a simple matter since they are characterized by undergoing strong displacements when their amplitude is small. Special care has been taken on this point in the observational studies reviewed previously to determine their speeds of propagation. The phase speeds of the westward components, except for the case of the longest scales, seems to be quite well explained by values obtained from a divergent barotropic model.

In such a case the westward phase speeds are larger for larger waves. In Table 5.3-1 the values predicted by this model whose phase speed is given by

$$c = \bar{u} - \frac{\beta'}{k^2 + \alpha^2} ; \alpha^2 = \frac{f^2}{gH} ; \beta' = \alpha^2 \bar{u} + \beta$$

are depicted corresponding to a latitude of  $45^\circ$  and a typical wind speed of 20 m/sec for increments in wavelength of 2,000 km. In the above equation,  $c$  is the phase speed,  $\bar{u}$  represents the mean wind speed,  $\alpha$  is the wave number,  $f$  is the Coriolis parameter,  $g$  is gravity,  $H$  is the depth of the layer being considered and  $\beta$  is the variation of the Coriolis parameter with latitude. Though at longer waves only some of these wavelengths will appear in the representation of the field under

Table 5.3-1

Phase speed from a divergent and non-divergent  
Barotropic model, and group velocity from a divergent barotropic  
model for different wavelengths (after Paegle, 1969)

L (10 <sup>3</sup> km)	C <sub>ND</sub> (m/sec)	C <sub>D</sub> (m/sec)	Period (days)	C <sub>GD</sub> (m/sec)
2	18.4	18.2	1.3	21.4
4	13.4	12.7	3.6	26.3
6	5.6	4.6	15.2	32.6
8	-6.3	-5.1	-18.3	34.6
10	-21.4	-15.2	-7.6	35.3
12	-39.1	-25.3	-5.5	32.3
14	-60.5	-34.7	-4.1	27.3

consideration, since only some of them will fit a discrete number of times around the earth, this representation is convenient to obtain an idea of the variation of the phase speed with wave length when a continuous spectrum is considered. Actually for smaller scales these restrictions become less important.

The present aim is to convert a frequency spectrum at a certain point in space to an instantaneous wave number spectrum in space. Since a random function in time is being considered which supports a continuous spectrum in frequency, continuous wave number spectra will have to be considered for the conversion to be valid.

From Table 5.3-1 it is seen that the smaller the wavelengths are the smaller the dispersion effects become and the particular wave number can be considered to be advected by the mean wind. This behavior arises from the nature of dispersion. It is just group velocity,  $c_g$ , which is defined as  $c_g = \frac{d(kc)}{dk}$ . If  $c = \bar{u} - \frac{\beta}{k^2}$ , then  $c_g = \bar{u} + \frac{\beta}{k^2} = \bar{u} + \frac{\beta L}{4}$ . Thus  $c_g$  approaches  $\bar{u}$  for decreasing wavelength,  $L$ . It has been demonstrated that waves with wave numbers larger than seven basically move the same distance in a month, the value corresponding to a propagation speed of 9 m/sec or  $10^0$  long/day. Similar tendencies for smaller waves to have smaller typical periods were found by Shapiro and Ward (1960) in their time series analysis of individual Fourier components.

Therefore the atmospheric motions are assumed to be characterized by very long waves propagating with the divergent barotropic phase speed and smaller waves which are essentially carried by the wind. The

first ones are mainly zonal in their nature and the second ones are primarily related with the direction of the mean wind.

From Table 5.3-1 we see that periods associated with the long waves propagating towards the west are of the same order as the ones we would expect from waves propagating towards the east mainly advected by the mean wind, or with phase speeds slightly smaller, from 5 to 15 m/sec. Since the difference in direction of propagation is not considered in the power spectra and the assumption of a continuous wave number is valid only for a smaller wavelength, for wave numbers 6 or 7 or larger, the correspondence between wave number and frequency spectra is considered to be determined by phase speeds given by the mean wind. This is essentially Taylor's hypothesis as applied to micro-turbulence.

These relationships can then be used to interpret the obtained results in the frequency domain in terms of the corresponding values in the wave number domain, and thus interpret them as observations of the nonlinear mechanisms acting in the atmosphere.

## 6.0 SUMMARY AND CONCLUSIONS

In general the results obtained indicate the presence of peaks and characteristic slopes in the spectra for the different horizontal wind components. These peaks and slopes can be explained through the theories reviewed previously. It is seen that nonlinear barotropic mechanisms may be considered partly responsible for periodicities found from 5 to 15 days. This may help in the interpretation of the peaks shown in Fig. 4.3-1 which were determined using actual data. Interaction of baroclinic disturbances with the thermal structure of the mean flow may be considered responsible for periodicities found from 10 to 20 days.

As noted previously, the study of a case of high resolution in frequency shows the importance of the mechanisms acting on the side bands of a peak. Therefore, finite band widths, rather than discrete modes should be considered to exist for the atmosphere at synoptic scales. This is in line with the problem discussed in Chapter 2.2. If these peaks are considered to arise from the effects of instabilities as discussed earlier, the possibility of the excitation of a finite bandwidth instead of just the most unstable mode should be considered.

It has been shown that spectra obtained for the same station and level differ from year to year, but the general features in the time scales of synoptic interest, periods from a day to a month, are essentially the same and statistically significant. These time scales are of interest since they are associated with changes of weather patterns which we would like to predict. True periodicities present in these time scales can be compared with periodicities found through idealized numerical and analytical models to gain dynamical insight of the

processes causing them. Also the existence of such periodicities in the atmosphere may be taken as an indication of the validity of the models in predicting atmospheric features.

Dynamic theories, including barotropic models, apply most directly to the kinetic energy spectra. The most important findings for these spectra are as follows:

- 1) The large power in periods from 2 weeks to a month might be associated with a) the generation of zonal currents on long time scales produced by the spectral side bands in the neighborhood of resonant modes, or b) by the oscillations resulting from the interaction of the zonal flow with finite-amplitude waves, which started as baroclinically-unstable waves.
- 2) Two-week periodicities may also be explained through barotropic exchanges between the zonal flow and disturbances. Planetary waves passing over a station may be responsible for periodicities found between 14 and 20 days.
- 3) Barotropic nonlinear interchanges may explain periodicities between three and ten days. The longer scales associated with periods larger than three or four days are mainly responsible for the nonlinear interactions. The ten-day period may be explained by the interaction of the mean flow with finite amplitude waves which started as baroclinically-unstable waves for the case when the mean static stability is considered variable in time.
- 4) The range of periods found between two days and ten days may be explained by the passage of synoptic and planetary waves.

- 5) Previous works in the wave number domain indicate the existence of periodicities between three and ten days associated with the various wave-number modes.

In summary, there exists evidence for preferred scales of motion in the atmosphere. The presence of these scales may be justified on the basis of linear instability theories when the disturbances are small. For larger time scales, when the disturbances become of finite amplitude, and nonlinear interactions become important, barotropic and baroclinic theories and theories of resonant growth of interacting modes offer explanations of the observed peaks.

REFERENCES

- Aihara, M., 1961: Time dependent behavior of parallel flows in a non-divergent barotropic atmosphere. J. Met. Soc. Japan, 39, 157-174.
- Anderssen, E. C., 1965: A study of atmospheric long waves in the southern hemisphere. Notos, 14, 57-65.
- Arakawa, A., 1962: Non-geostrophic effects in the baroclinic prognostic equations. Proc. Internat. Symposium Numerical Weather Prediction, Tokyo, 161-175.
- Baer, F., 1964: Integration with the spectral vorticity equation. J. Atmos. Sci., 21, 260-276.
- Bendat, J. S. and A. G. Piersol, 1968: Measurement and Analysis of Random Data, New York, John Wiley.
- Benney, D. J., and A. C. Newell, 1967: The propagation of non-linear envelopes. J. Math. and Phys., 46, 133.
- Benton, G. S. and A. B. Kahn, 1958: Spectra of large-scale atmospheric flow at 300 millibars. J. of Meteor., 15, 404-410.
- Blackburn, J. A., ed., 1970: Spectral Analysis: Methods and Techniques. New York, Marcel Dekker.
- Blackman, R. B. and J. W. Tukey, 1959: The Measurement of Power Spectra. New York, Dover.
- Bolin, B., 1950: On the influence of the earth's orography on the general character of the westerlies. Tellus, 2, 184-195.
- Brooks, C. E. P., C. S. Durst, N. Carruthers, et. al., 1950: Upper Winds Over the World. Geophysical Memoirs No. 85, Fifth Number, Volume X, London.
- Brown, J., 1969: A numerical investigation of hydrodynamic instability and energy conversion in the quasi-geostrophic atmosphere. J. Atmos. Sci., 26, 352-375.
- Chiu, W.-C., 1960: The wind and temperature spectra of the upper troposphere and lower stratosphere over North America. J. Meteor., 17, 64-77.
- Crutcher, H. L., and D. K. Halligan, 1967: Upper Wind Statistics of the Northern Western Hemisphere, ESSA Technical Report, EDS-1, Silver Spring Maryland.
- Deland, R. J., 1964: Traveling planetary waves. Tellus, 16, 271-273.
- Dickson, R. R., 1968: The weather and circulation of March 1968. Monthly Weather Review, 96, 399-404.

- Eliassen, E., and B. Machenhauer, 1965: A study of the fluctuations of the atmospheric planetary patterns represented by spherical harmonics. Tellus, 17, 220-238.
- \_\_\_\_\_, 1969: Large scale atmospheric wave motions. Tellus, 21, 149-165.
- Essenwanger, O. M., 1970: Elements of Statistical Analysis in Atmospheric Science, Redstone, Alabama, U. S. Army Missile Command.
- Gambo, K., 1966: Some remarks on the treatment of finite amplitude disturbances in the baroclinic atmosphere. J. Meteor. Soc. Japan, 44, 109-121.
- Gates, W. L., 1961: Static stability measures in the atmosphere. J. Meteor., 18, 526-533.
- Gibbs, W. J., 1952: Notes on the mean jet-stream over Australia. J. Meteor., 9, 279-284.
- \_\_\_\_\_, 1953: A comparison of hemispheric circulations with particular reference to the western Pacific. Quart. J. Royal Meteor. Soc., 79, 121-136.
- \_\_\_\_\_, 1965: Jet streams over high southern latitudes. Austral. Meteor. Mag., 49, 14-27.
- Goodman, N. R., 1957: On the joint estimation of the spectra, cospectrum and quadrature spectrum of a two-dimensional stationary Gaussian process. Scientific Paper No. 10, Engineering Statistics Laboratory, New York Univ.
- Grenador, V., and M. Rosenblatt, 1957: Statistical Analysis of Stationary Time Series, New York, John Wiley and Sons.
- Haltiner, G. J., and F. L. Martin, 1957: Dynamical and Physical Meteorology. New York, McGraw-Hill.
- Hannan, E. J., 1970: Multiple Time Series. New York, John Wiley.
- Heastie, H., and P. M. Stephenson, 1960: Upper Winds Over the World. Parts I and II. Geophysical Memoirs No. 103, London.
- Henry, R. M., and S. L. Hess, 1958: A study of the large-scale spectra of some meteorological parameters. J. Meteor., 15, 397-403.
- Holloway, J. L., 1958: Smoothing and filtering of time series and space fields. Advances in Geophysics, 4, 351-189.
- Horn, L. H., and R. A. Bryson, 1963: An analysis of the geostrophic kinetic energy spectrum of large-scale atmospheric turbulence. J. Geophys. Res., 68, 1059-1064.

- Hutchings, J. W., 1950: A meridional atmospheric cross section for an oceanic region. J. Meteor., 7, 94-100.
- Jenkins, G. M., and D. G. Watts, 1969: Spectral Analysis and Its Applications. San Francisco, Holden-Day.
- Julian, P. R., W. M. Washington, L. Hembree and C. Ridley, 1970: On the spectral distribution of large-scale atmospheric kinetic energy. J. Atmos. Sci., 27, 376-387.
- Kahn, A. B., 1962: Large-scale atmospheric spectra at 200 mb. J. Atmos. Sci., 19, 150-158.
- Kao, S.-K., and W. S. Bullock, 1964: Lagrangian and Eulerian correlations and energy spectra of geostrophic velocities. Quart. J. Royal Meteor. Soc., 90, 166-174.
- Kendall, M. G., 1946: Contributions to the study of oscillatory time series. Occasional Papers IX, National Institute of Economic and Social Research, Cambridge, England, Cambridge University Press.
- Kenyon, K., 1966: A discussion on non-linear theory of wave propagation in dispersive systems. Proc. Royal Soc., A 299, 141-144.
- Klein, W. H., 1957: Principal Tracks and Mean Frequencies of Cyclones and Anticyclones in the Northern Hemisphere. Research Paper No. 40. U. S. Dept. of Commerce, Weather Bureau, Washington, D. C.
- Krishnamurti, T. N., 1961a: The subtropical jet stream of winter. J. Meteor., 18, 172-191.
- \_\_\_\_\_, 1961b: On the role of the subtropical jet stream of winter in the atmospheric general circulation. J. Meteor., 18, 657-670.
- Kubota, S., and M. Iida, 1954: Statistical characteristics of the atmospheric disturbances. Papers in Meteorology and Geophysics, 5, 22-34.
- \_\_\_\_\_, 1959: Numerical analysis of the energetical structure of the atmosphere over the Northern Hemisphere. Papers in Meteorology and Geophysics, 10, 1-33.
- Lahey, J. F., R. A. Bryson, H. A. Corzine and C. W. Hutchins, 1960: Atlas of 300 mb Wind Characteristics for the Northern Hemisphere. Final Report Part I. USAF Contract AF19(604)-2278. AFCRC-TR-59-270. Madison, Univ. of Wisconsin Press.
- Loewe, F., and U. Radok, 1950: A meridional aerological cross section in the southwest Pacific. J. Meteor., 7, 58-65.
- Lorenz, E. N., 1960: Maximum simplification of the dynamic equations. Tellus, 12, 243-254.

- Muffatti, A. H. J., 1963: Aspects of the subtropical jet stream over Australia. Symposium on Tropical Meteorology, Rotura, New Zealand, New Zealand Meteorological Service, 72-88.
- Muller, F. B., 1966: Notes on the Meteorological Application of Power Spectrum Analysis. Meso-Meteorology and Short Range Forecasting-- Rept. 1. Canadian Meteorological Memoirs, No. 24, Dept. of Transport, Toronto.
- Munn, R. E., 1970: Biometeorological Methods. New York, Academic Press.
- Newell, A. C., 1969: Rossby wave packet interactions. J. Fluid Mech., 35, 255-271.
- Oort, A. H., and A. Taylor, 1969: On the kinetic energy spectrum near the ground. Monthly Weather Review, 97, 623-636.
- Paegle, J. E. N., 1969: The Spectral Behavior of the Atmosphere in the Frequency Domain. Unpublished Ph.D. dissertation, U.C.L.A.
- Panofsky, H. A., and R. A. McCormick, 1954: Properties of spectra of atmospheric turbulence at 100 metres. Quart. J. Royal Meteor. Soc., 80, 546-564.
- Radok, U., and A. M. Grant, 1957: Variations in the high tropospheric mean flow over Australia and New Zealand. J. Meteor., 14, 141-149.
- Reiter, E., 1963: Jet-Stream Meteorology. Chicago, Univ. of Chicago Press.
- \_\_\_\_\_, 1969: Atmospheric Transport Processes, Part 1: Energy Transfers and Transformations. Atomic Energy Commission Critical Review Series, Oak Ridge, Tennessee.
- \_\_\_\_\_, 1972: A multivariate treatment of kinetic energy. (To be published in memorial volume for Flohn.)
- Riehl, H., 1962: Jet streams of the atmosphere. Technical Report No. 32, Dept. of Atmospheric Science, Colorado State Univ., Fort Collins, Colorado.
- Rosenthal, S. L., 1960: Some estimates of the power spectra of large-scale disturbances in low latitudes. J. Meteor., 17, 259-263.
- Rubin, M. J., and H. van Loon, 1954: Aspects of the circulation of the Southern Hemisphere. J. Meteor., 11, 68-76.
- Saltzman, B., 1958: Some hemispheric spectral statistics. J. Meteor., 15, 259-263.
- \_\_\_\_\_, and A. Fleisher, 1962: Spectral statistics of the wind at 500 mb. J. of Atmos. Sci., 19, 195-204.

- Serebreny, S. M., E. J. Wiegman, and R. G. Hadfield, 1957a: A Study of the Jet Stream Conditions in the Northern Hemisphere During Winter. Pan American World Airways, Inc., Pacific-Alaska Division, Meteorology Dept. Tech. Rept. No. 5. Project Arowa Contract No. N600 (188)40835, NWRP 20-1057-0086, San Francisco.
- 
- \_\_\_\_\_, 1957b: A Study of the Jet Stream Conditions in the Northern Hemisphere During Summer. Pan American World Airways, Inc., Pacific-Alaska Division, Meteorology Dept. Tech. Rept. No. 6. Project Arowa Contract No. N600(188)44188, NWRP 20-1057-007, San Francisco.
- 
- \_\_\_\_\_, 1958a: A Study of the Jet Stream Conditions in the Northern Hemisphere During Spring. Pan American World Airways, Inc., Pacific-Alaska Division, Meteorology Dept. Tech. Rept. No. 7. USNWRP Contract No. N600(188)44188, NWRP 0658-008, San Francisco.
- 
- \_\_\_\_\_, 1958b: A Study of the Jet Stream Conditions in the Northern Hemisphere During Fall. Pan American World Airways, Inc., Pacific-Alaska Division, Meteorology Dept. Tech. Rept. No. 8. UNSWRF Contract No. N189(188)-39691A, NWRP 20-1258-021, San Francisco.
- Shapiro, R., and F. Ward, 1960: The time-space spectrum of the geostrophic meridional kinetic energy. J. Meteor., 17, 621-626.
- 
- \_\_\_\_\_, 1963: The kinetic energy spectrum of meridional flow in the mid-troposphere. J. Atmos. Sci., 20, 353-358.
- Spillane, K. T., 1968: The winter jet stream of Australia and its turbulence. Austral. Meteor. Mag., 16, 64-71.
- Taljaard, J. J., 1967: Development, distribution and movement of cyclones and anticyclones in the Southern Hemisphere during the IGY. J. Appl. Meteor., 6, 973-987.
- Van der Hoven, I., 1957: Power spectrum of horizontal wind speed in the frequency range from 0.0007 to 900 cycles per hour. J. Meteor., 14, 160-164.
- van Loon, H., 1965: A climatological study of the atmospheric circulation in the Southern Hemisphere during the IGY, Part I: July 1957-31 March 1958. J. Appl. Meteor., 4, 479-491.
- 
- \_\_\_\_\_, 1967: A climatological study of the atmospheric circulation in the Southern Hemisphere during the IGY, Part II. J. Appl. Meteor., 6, 803-815.
- van Mieghem, J., P. Defrise and J. van Isacker, 1959: On the selective role of the motion systems in the atmospheric general circulation. Rossby Memorial Volume, 230-239.

- Vinnichenko, N. K., and J. A. Dutton, 1969: Empirical studies of atmospheric structure and spectra in the free atmosphere. International Symposium on "Spectra of Meteorological Variables," Stockholm, Sweden, 9-19 June 1969.
- \_\_\_\_\_, 1970: The kinetic energy spectrum in the free atmosphere--1 second to 5 years. Tellus, 22, 158-166.
- Visher, S. S., 1954: Climatic Atlas of the United States. Cambridge, Mass., Harvard Univ. Press.
- Wallace, J. M., and C.-P. Chang, 1969: Spectrum analysis of large-scale wave disturbances in the tropical lower troposphere. J. Atmos. Sci., 26, 1010-1025.
- Weinert, R. A., 1968: Statistics of the subtropical jet stream over the Australian region. Austral. Meteor. Mag., 16, 137-148.
- White, R. M., and D. S. Cooley, 1956: Kinetic-energy spectrum of meridional motion in the mid-troposphere. J. Meteor., 13, 67-69.
- Wiin-Nielsen, A., 1967: On the annual variation and spectral distribution of atmospheric energy. Tellus, 19, 540-559.
- Woolridge, G., and E. R. Reiter, 1970: Large-scale atmospheric circulation characteristics as evident from ghost balloon data. J. Atmos. Sci., 27, 183-194.
- Yanai, M., T. Maruyama, T. Nitta and Y. Hayashi, 1968: Power spectra of large-scale disturbances over the tropical Pacific. J. Meteor. Soc. Japan, 46, 308-323.
- \_\_\_\_\_, and M. Murakami, 1970: A further study of tropical wave disturbances by the use of spectrum analysis. J. Meteor. Soc. Japan, 48, 185-197.

APPENDIX

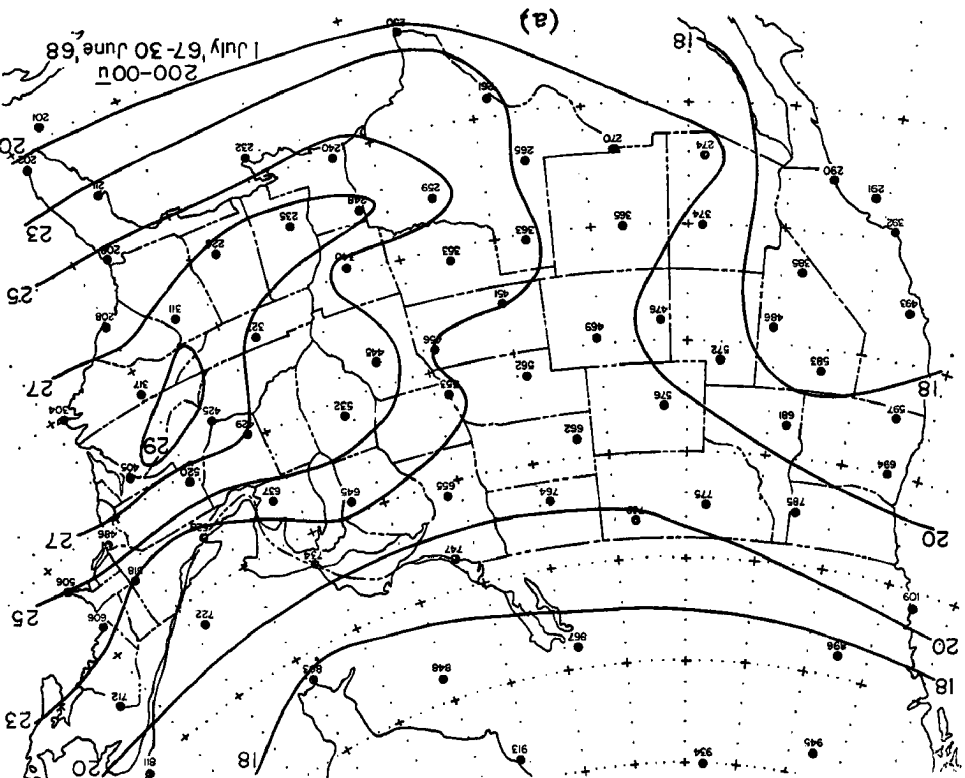
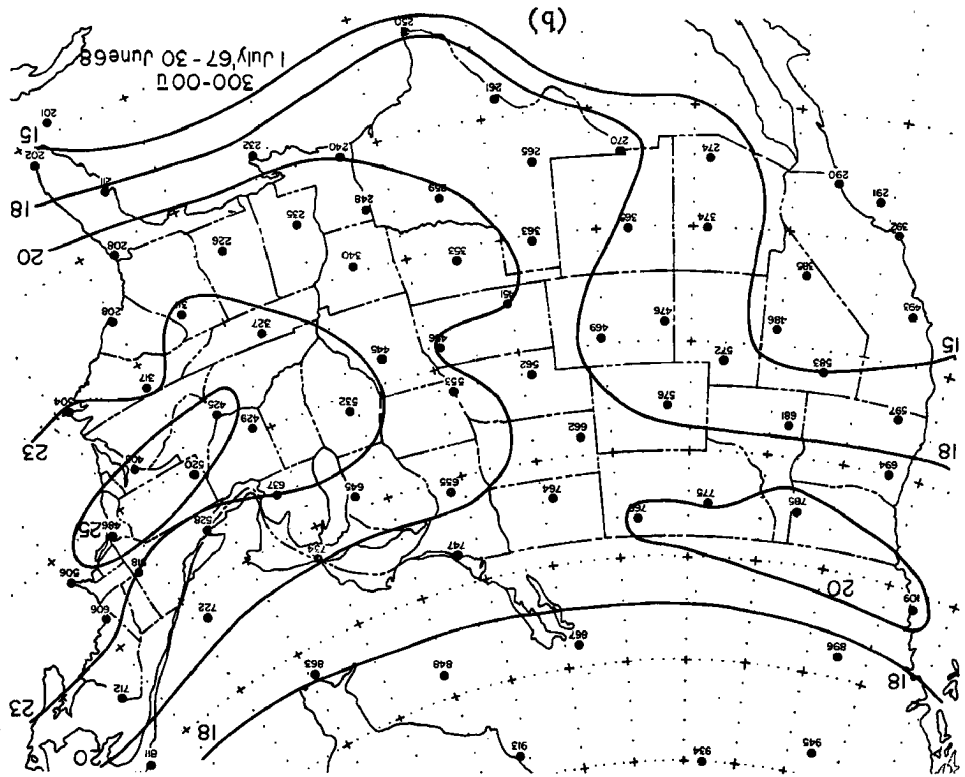
A.1 Mean Zonal and Meridional Wind Speeds

Figure A.1-1 portrays the geographical distribution of the mean zonal wind component for the twelve month period July 1, 1967, through June 30, 1968; Figure A.1-2 shows the mean meridional wind component. Since an increase in wind speed would be expected to increase the frequency of oscillations, the correspondence between the variance values and the mean wind speeds should indicate the consistency of the results presented in the main body of the text. A dependence of the spectral densities on the square of the mean wind speed should be expected since both are quadratic quantities (Chapter 2.1).

Maximum values of the mean zonal wind component occur over the Middle Atlantic states and extend generally southwestward from that region. This region of maximum  $\bar{u}$  values can be attributed to the frequent merging of the subtropical jet stream with the polar front jet stream (Reiter, 1963; Reiter and Whitney, 1969); this area also corresponds with a primary storm track as shown by Visher (1954) in Figure 4.2-3. In general, the higher zonal variances (Fig. 4.2-1) occur in the same regions as the higher mean zonal wind speeds (Fig. A.1-1).

The correspondence between the values of the mean meridional wind speeds and meridional variances is more difficult to ascertain. As the absolute values of  $\bar{v}$  become greater, the variance values become less. This relationship may be explained by considering the high degree of variability of the meridional wind component. If the mean meridional wind is near zero, then one of two things must have happened: (1) the wind regime was predominantly zonal, or (2) there were wide variations in the values of  $v$  produced by transient eddies which cancelled

Fig. A.1-1 Geographic distributions of the mean zonal wind speeds at the (a) 200 mb and (b) 300 mb constant pressure levels for 7/1/67 - 6/30/68.



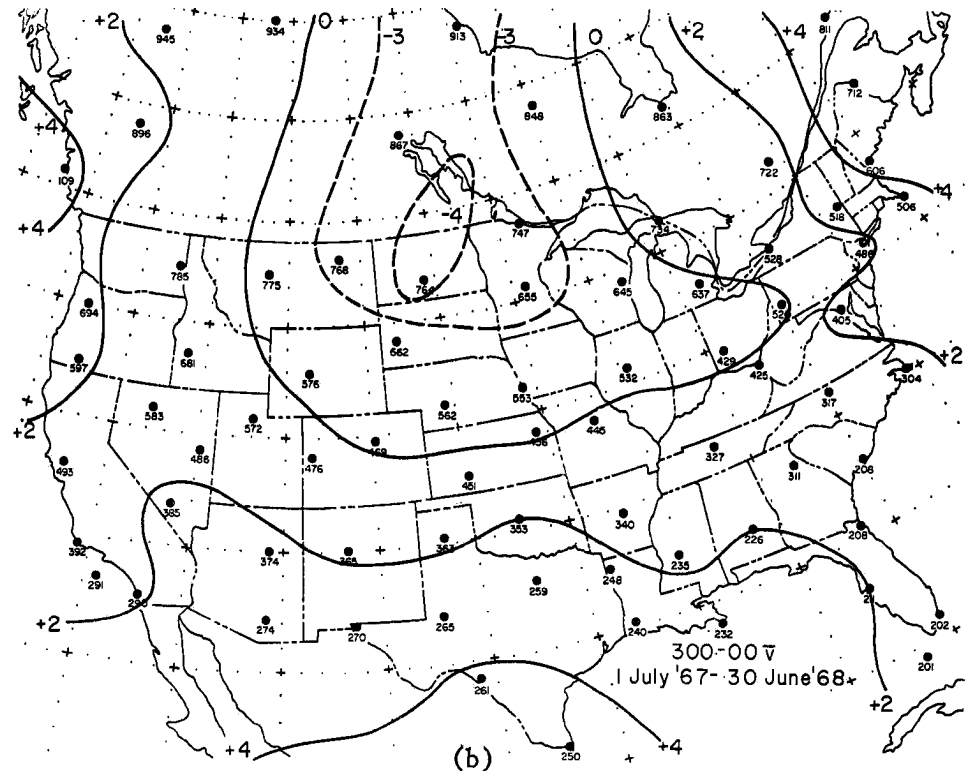
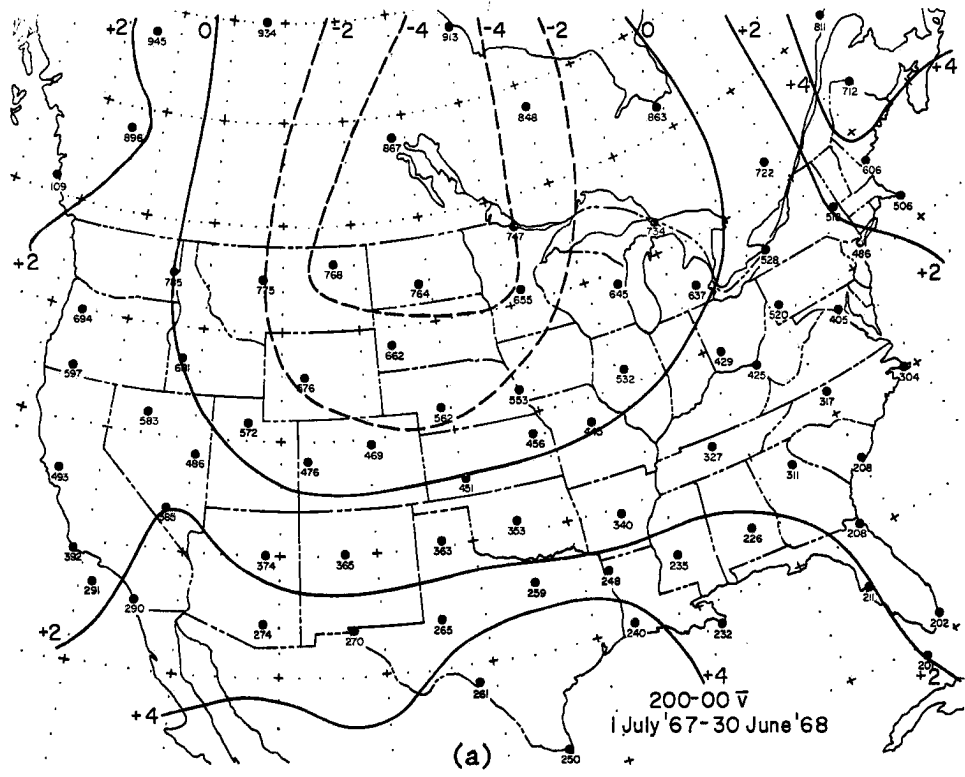


Fig. A.1-2 Geographic distributions of the mean meridional wind speeds at the (a) 200 mb and (b) 300 mb constant pressure levels for 7/1/67 - 6/30/68.

each other out in the averaging process (Munn, 1970). The latter reason is more plausible because the majority of instantaneous wind values contribute significantly to the total variance of the v-component.

### B.1 Periodicity of 18.5 Days

Both the zonal and meridional spectra displayed a tendency to peak at a period of 18.5 days (Fig. 4.3-1). Approximately 50% of the 127 North American stations examined exhibited a peak in the zonal spectrum and 65% possessed a peak in the meridional spectrum within the 15-24 day periodicity range. Figures B.1-1 and B.1-2 indicate the geographical distribution of the spectral densities at a period of 18.5 days for the zonal and meridional spectra respectively. The stations which had a peak in their spectra at this frequency are indicated by a square. Only the spectral values derived from data collected at the 00 GMT observation time at the 200 mb and 300 mb constant pressure levels are reproduced.

Whereas the spectral densities associated with this particular period were high, the kinetic energies were not. As noted in Chapter 2.2, the value of  $S(f)$  at any given frequency must be multiplied by that frequency,  $f$ , to obtain a value representative of kinetic energy. In the case of an 18.5 day period, multiplication of  $S(f)$  by a frequency 0.0541 cycles/day rendered the value of  $fS(f)$  small. The value of  $fS(f)$  for each isoline of constant spectral density is shown in parentheses in each figure in Part B of the Appendix.

Evident from Figure B.1-1, the stations which have a peak at 18.5 days are grouped regionally. Four significant patterns emerge in the distribution of the zonal spectral densities. The Pacific Northwest region exhibited a number of stations which possessed a peak at 18.5 days and also formed an area of maximum spectral values. Perhaps the easiest explanation for this orientation of maximum spectral values along  $47^{\circ}\text{N}$  is that this is the mean position of the polar front jet stream (Reiter, 1963); the PFJ does not lie continually along this

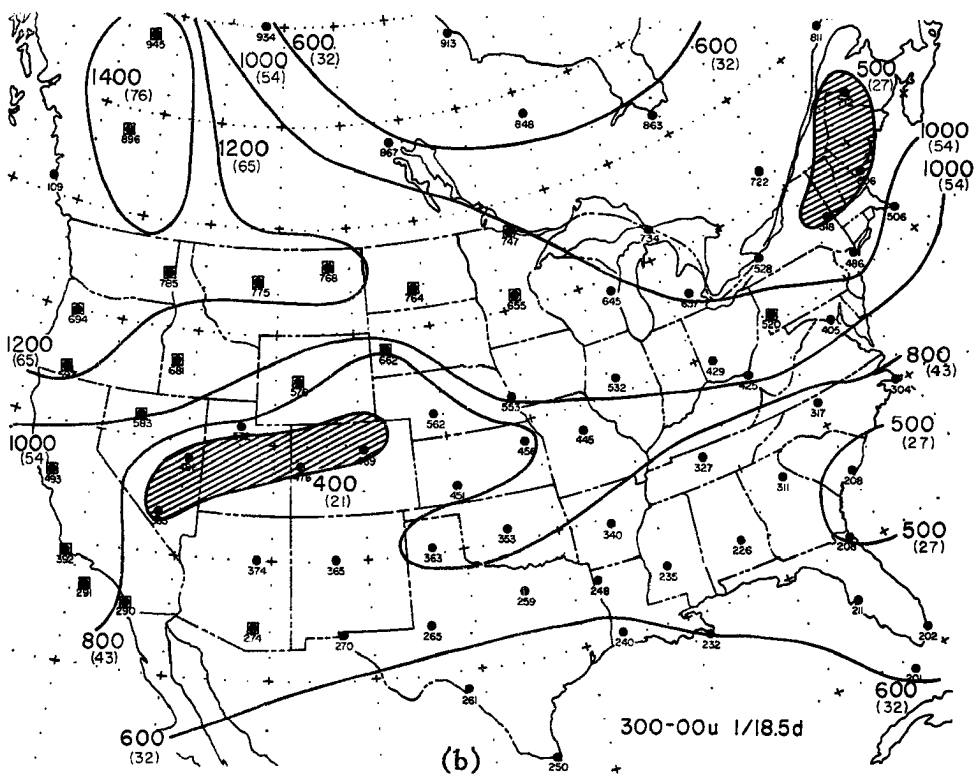
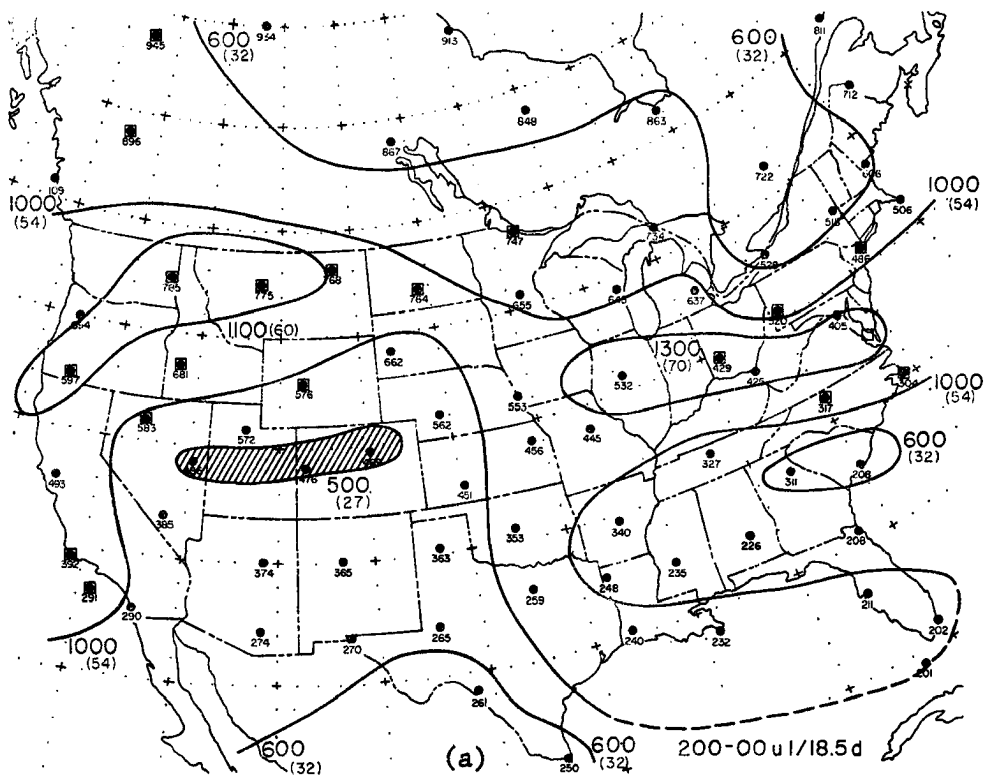


Fig. B.1-1 Geographic distributions of the zonal spectral densities at a period of 18.5 days at the (a) 200 mb and (b) 300 mb constant pressure levels.

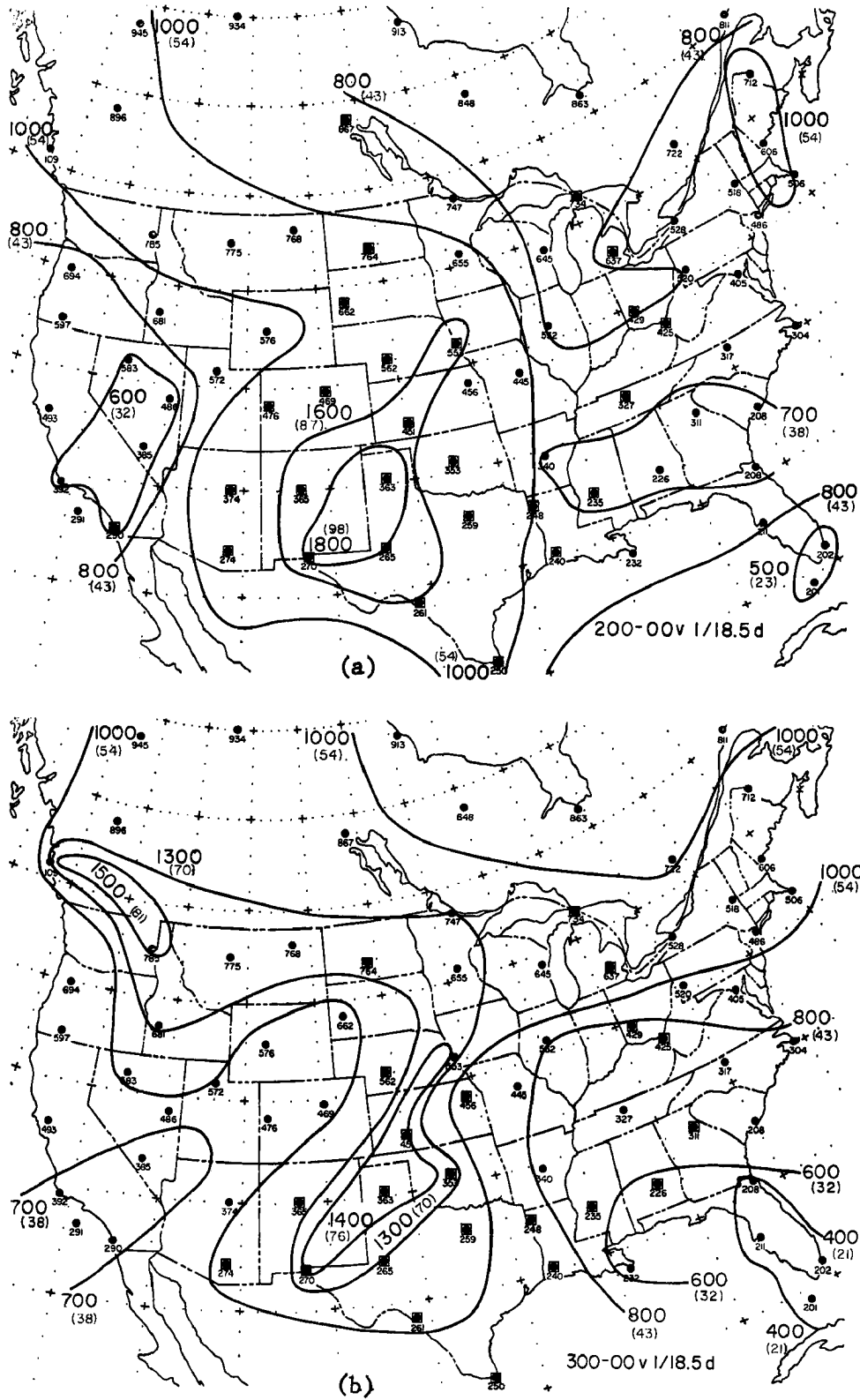


Fig. B.1-2 Geographic distributions of the meridional spectral densities at a period of 18.5 days at the (a) 200 mb and (b) 300 mb constant pressure levels.

latitude, but the north-south migration of the PFJ is centered along this latitude circle over North America.

The zonal spectral values at 300 mb are greater than the ones at 200 mb along  $47^{\circ}\text{N}$ . At this latitude, the PFJ is located closer to the 300 mb than to the 200 mb level due to the downward sloping of the tropopause from equator to pole. Another reason which could account for the higher spectral densities at the 300 mb level is that the vertical shear of the horizontal wind above the jet core is greater than that below it (Reiter, 1963).

According to Figure B.1-lb, there appears to be a decrease in the spectral values when progressing eastward. The eastermost station in the  $45^{\circ}\text{N}$ - $50^{\circ}\text{N}$  band to exhibit a peak at 18.5 days was International Falls ( $93^{\circ}\text{W}$ ). The above discussion demonstrates that spectral characteristics of individual stations along a latitude circle vary widely; thus, the spectra of no one station can be considered as being representative of the spectra along any given latitude circle. Furthermore, by averaging spectra along a latitude circle, these differences become smoothed out and the results thus derived become suspect.

The second pattern which is evident from Figure B.1-lb is the orientation of stations with a peak at 18.5 days along  $122^{\circ}\text{W}$ , extending from San Nicolas in southern California to Fort Nelson, Canada. The physical reason for this pattern is unknown. An area of minimum spectral densities occurred in the region of the Mojave Desert and from the Great Basin eastward to Denver. This region coincided with an area of minimum zonal wind variability (Fig. 4.2-1).

Evident on the 200 mb, but not on the 300 mb distribution, is an area of maximum spectral density in the Peoria-Dayton-Huntington region.

This area might be accounted for by the merging of the PFJ with the STJ near or in this region (Reiter, 1963). This maximum spectral density area could also be associated with the meridional spectral density maximum in this region.

An area of maximum meridional spectral energies at 18.5 days is located in the south-central states and oriented longitudinally along  $100^{\circ}\text{W}$ - $105^{\circ}\text{W}$  (Fig. B.1-2). This is also an area dominated by stations whose meridional spectra peaked at an 18.5 day period. The spectral values at 200 mb exceeded those values at the 300 mb level in this region. The reason the zonal spectra did not peak in this region might be explained by the uniformity of the zonal wind in this area; the major disturbances in the flow pattern, then, might have resulted in meridional modifications of the wind regime.

A second area of maximum spectral energies exists in the Pacific Northwest. Since these values are not associated with a peak at 18.5 days, they may be the result of association with the high zonal spectral densities in this region (Fig. B.1-1). The above observation might be related to the originally zonal current impinging perpendicular to the Rocky Mountains and being modified cyclonically to the lee (Bolin, 1950; Reiter, 1963). This behavior would introduce greater variations in the meridional wind component which would be reflected in the higher meridional spectral densities east of the Rocky Mountains.

## B.2 Periodicities of 10.6 and 9.25 Days

As noted in Chapter 4.3, the zonal spectra revealed a tendency to peak at the 10.6 day period while the meridional spectra generally peaked at 9.25 days (Fig. 4.3-1). Figure B.2-1 illustrates the distribution of zonal spectral values and peaks associated with a period of 10.6 days. A

large band of relatively high spectral densities is oriented from the southwest to the northeast regions of the United States. With the exception of the southwest, this band of high spectral values coincides with the belt of high zonal variances as shown in Figure 4.2-1. The area of maximum energy concentration in the Green Bay-Flint region might be accounted for by its association with the extremely high meridional spectral densities in that area (not shown).

Curiously, the stations which possessed peaks at 10.6 days are aligned in the same direction as the spectral energy gradient. This alignment suggests that this peak is associated with particular regions and does not depend on the magnitude of the disturbances with this periodicity which contribute to high spectral densities.

Referring to Figure 4.4-4 and the analysis of the spectra of the 200 mb and 500 mb heights at Amarillo, Texas, a peak in the 200 mb spectrum is evident at a period of 10.6 days. A significant peak at 9.25 days occurs in the spectrum of the 500 mb heights. As noted above, the zonal spectra tend to peak near 10.6 days and the meridional spectra near 9.25 days in this region.

The meridional spectra behave quite differently than the zonal spectra as can be seen from Figure B.2-2. No stations west of Denver ( $105^{\circ}\text{W}$ ) have peak meridional spectral densities at 9.25 days, whereas few stations east of Dodge City ( $100^{\circ}\text{W}$ ) possessed a peak in their respective zonal spectra. Quite apparent, especially at the 300 mb level, is the influence of the Rocky Mountains which are discussed previously in conjunction with the period of 18.5 days. The area of maximum intensity is oriented southwest-northeast, though more zonally than the u-component spectral densities which was shown in Figure B.2-1. This frequency peak may be

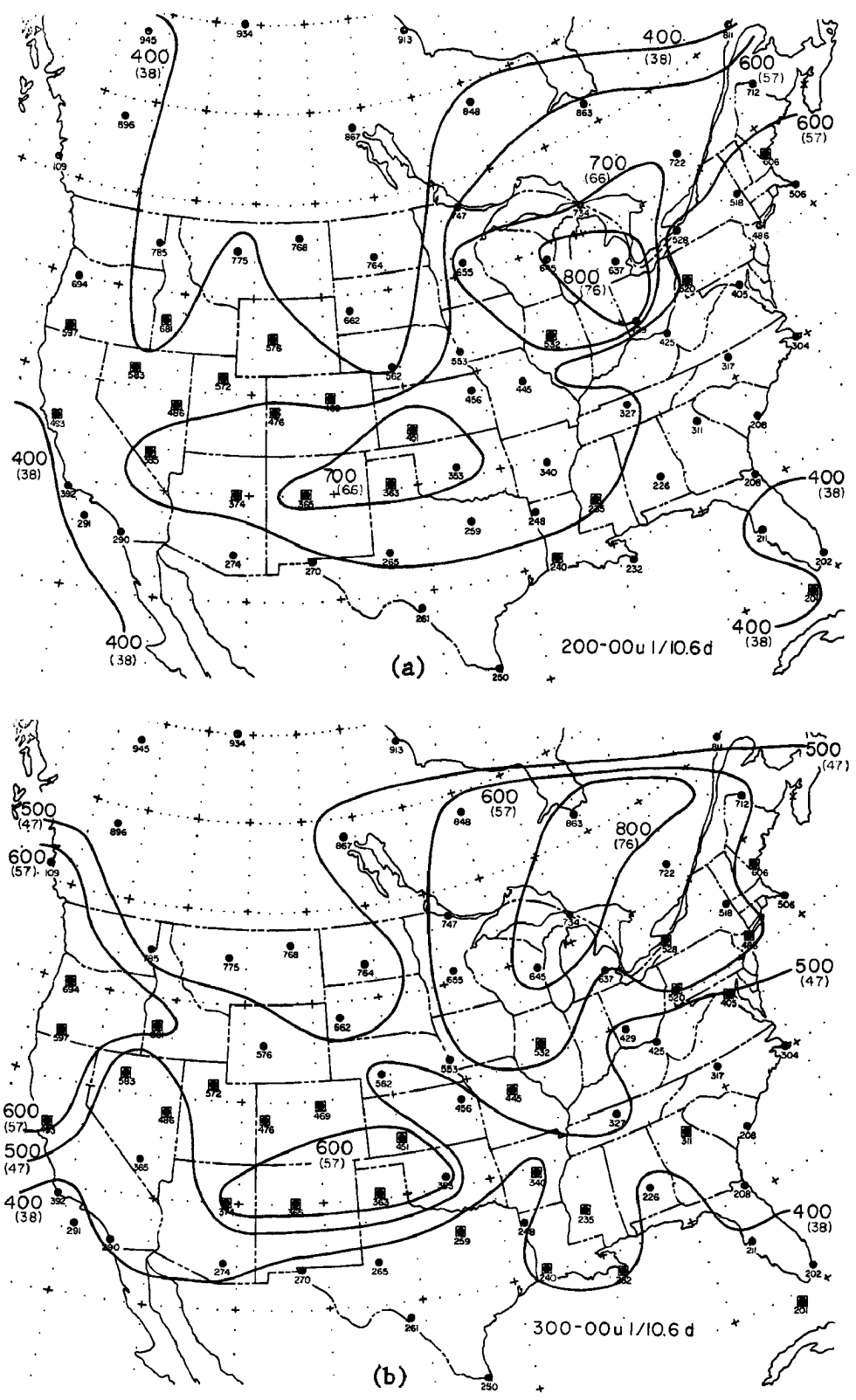


Fig. B.2-1 Geographic distributions of the zonal spectral densities at a period of 10.6 days at the (a) 200 mb and (b) 300 mb constant pressure levels.

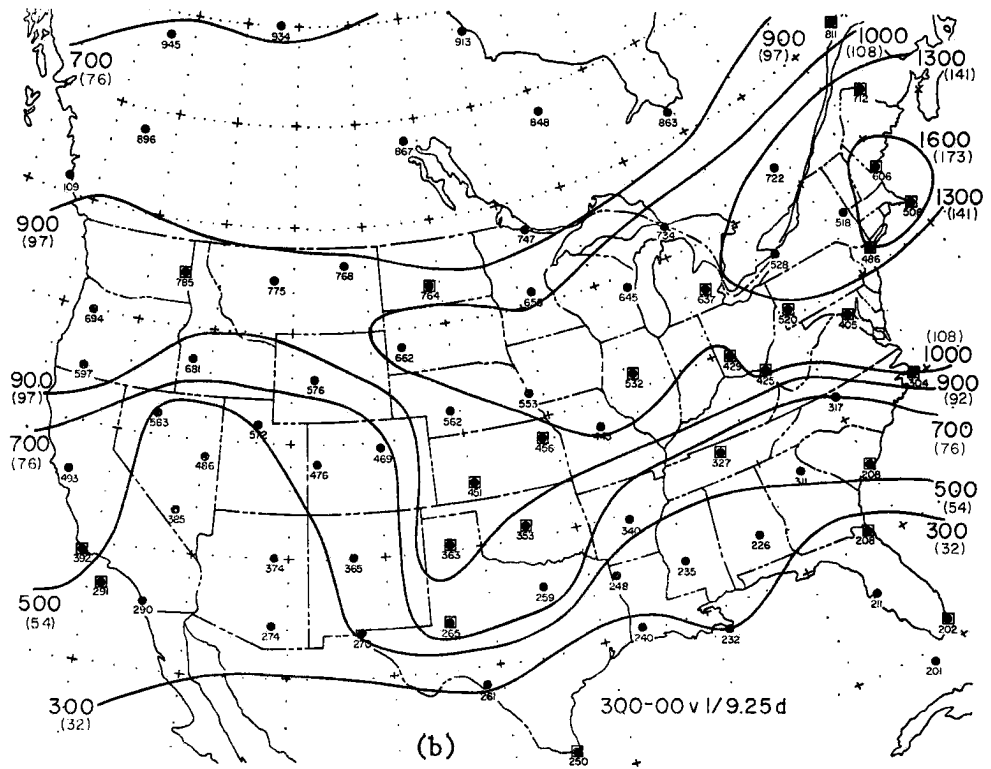
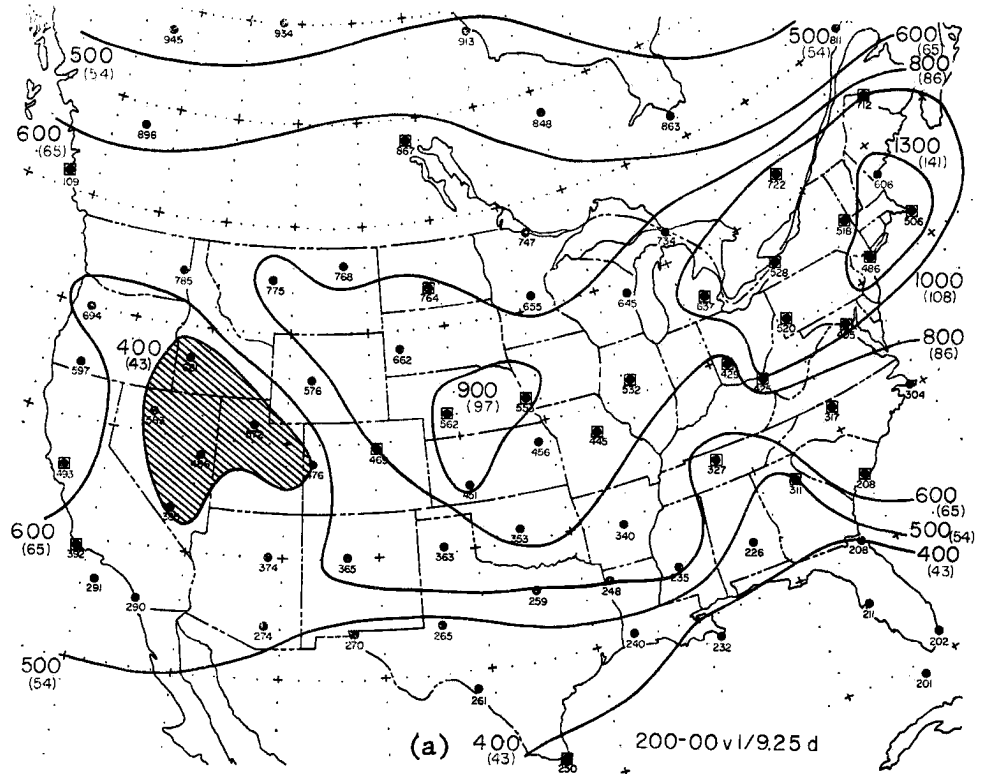


Fig. B.2-2 Geographic distributions of the meridional spectral densities at a period of 9.25 days at the (a) 200 mb and (b) 300 mb constant pressure levels.

maintained by the long-wave features intruded by the Rocky Mountains. Altering the zonal current, the orographical effect of the mountains introduce a meridional component into the wind systems. The greatest spectral band in the geographic distribution of the meridional spectral densities is situated along the position of the PFJ ( $40^{\circ}\text{N}$ - $50^{\circ}\text{N}$ ). As discussed in Chapter 4.5, the major portion of the spectral energies at this frequency occurred during the winter and spring seasons.

Whereas the zonal spectra demonstrated peaks in the Great Basin, the meridional spectra show a distinct minimum there; the same was true for the distribution at 18.5 days. Evidently, the flow in this area is predominantly zonal with little north-south variation.

### B.3 Periodicity of 6.17 Days

In addition to the two previously analyzed periods, the next significant period to be presented occurs at 6.17 days. Figure B.3-1 presents the geographic distribution of zonal spectral densities at this periodicity; the meridional spectral energies are shown in Figure B.3-2. When spectral densities associated with this period were converted to values proportional to kinetic energy, this peak did not contribute significantly to the total variances; this was also true of the two previous frequencies. Furthermore, the stations exhibiting a peak at 6.17 days were generally scattered and disorganized.

The peaks in the zonal spectra at 300 mb were established from Grand Junction ( $108.5^{\circ}\text{W}$ ) eastward along  $40^{\circ}\text{N}$  with a few isolated peaks in the western Louisiana-Fort Worth-Little Rock area. However, at the 200 mb level (not shown) the spectral peaks were clustered in the Gulf Coast states. Curiously, the peaks at 5.69 days (not shown) at the 300 mb level were centered in the southwest coinciding with a relative maximum

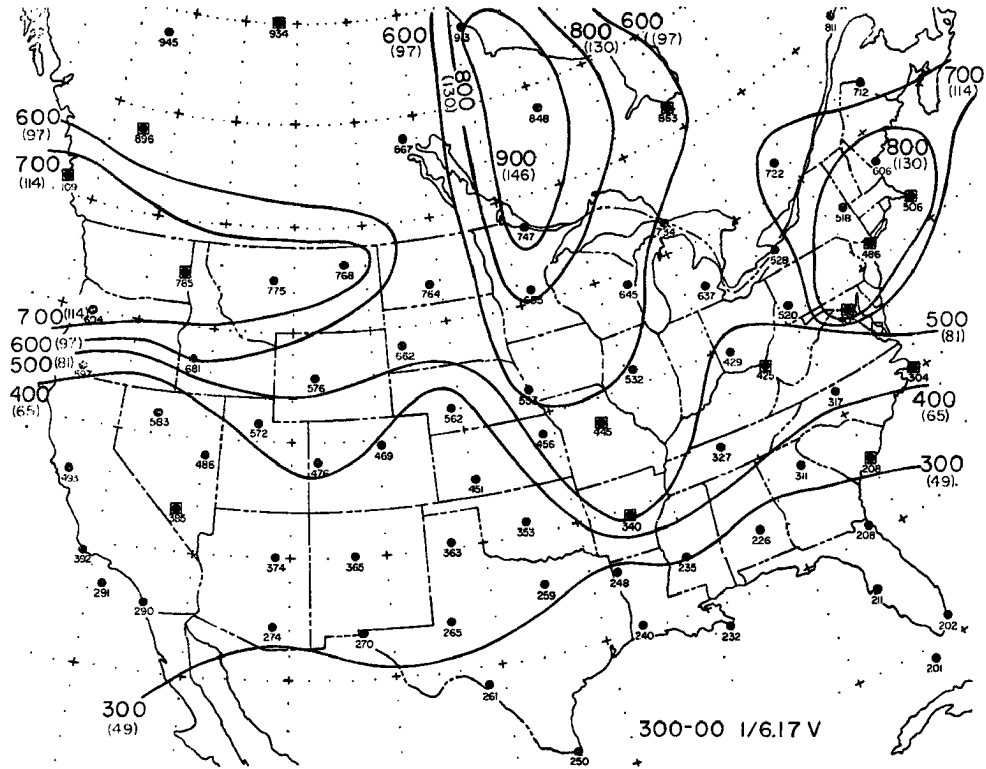


Fig. B.3-1 Geographic distributions of the zonal spectral densities at a period of 6.17 days at the 300 mb constant pressure level.

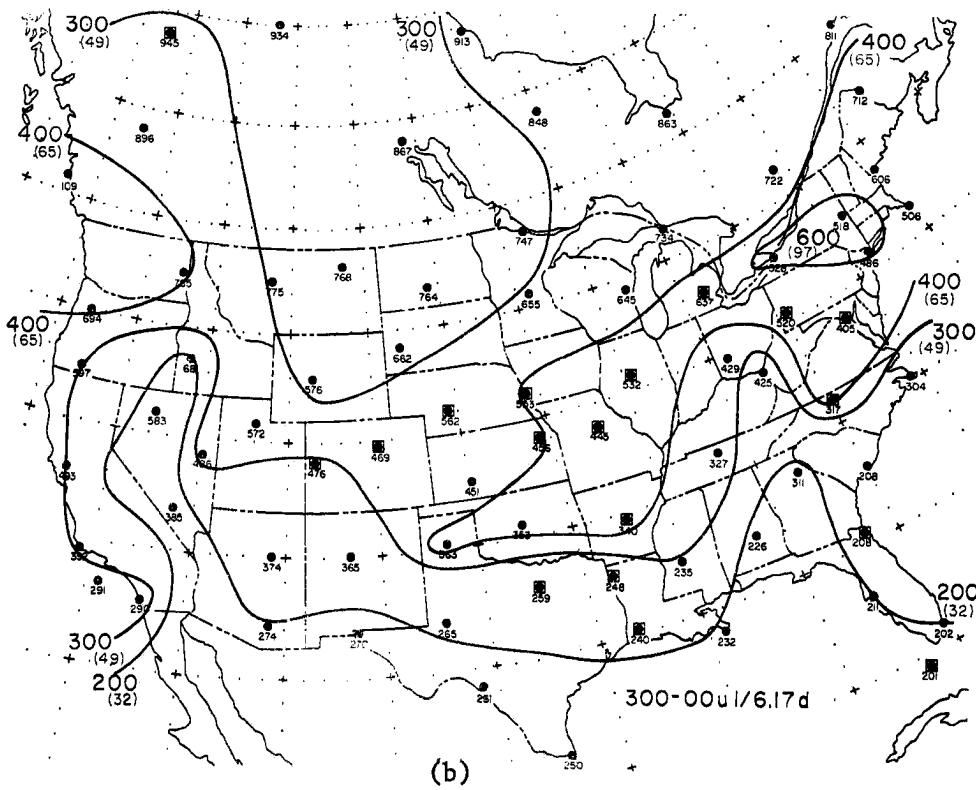
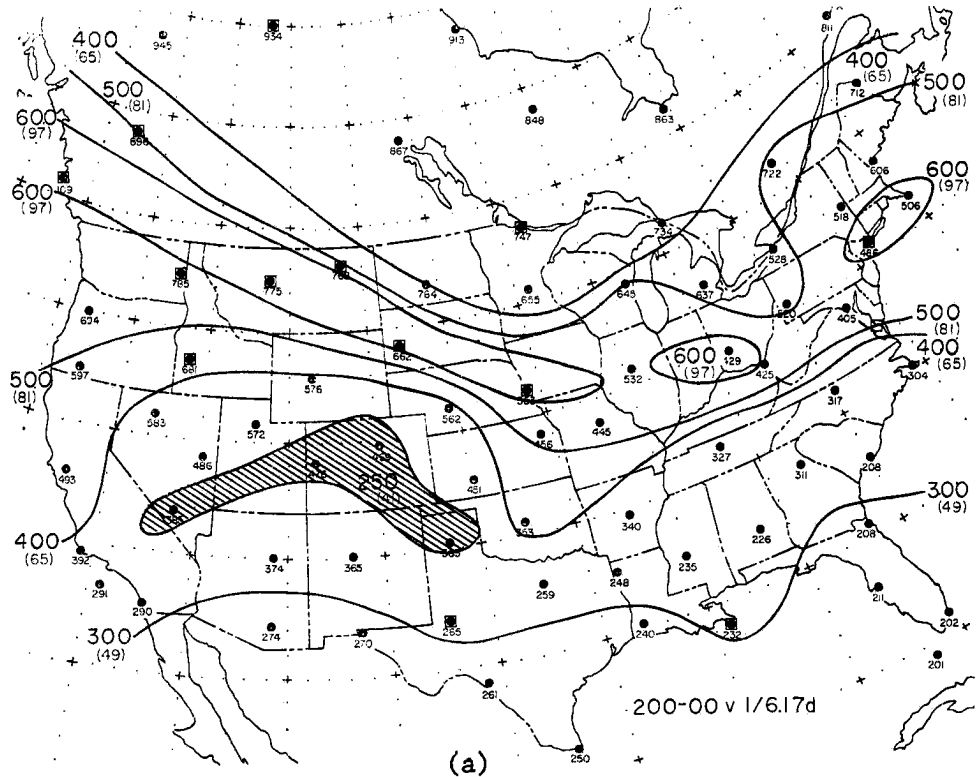


Fig. B.3-2 Geographic distributions of the meridional spectral densities at a period of 6.17 days at the (a) 200 mb and (b) 300 mb constant pressure levels.

Northwest, oriented east-west; central Canada-Minnesota, oriented north-south; and the Washington, D.C.-New England area. Evident, again, is the influence of the Rocky Mountains with the north-south oriented maximum possibly representing the cold air outbreaks so familiar to the central Canadian-United States prairies (Visher, 1954). Especially notable is the fact that the twelve month period under investigation was quite cold east of the Rocky Mountains.

#### B.4 Periodicity of 4.93 Days

The most significant peak to appear, especially in the meridional spectra, occurred at a period of 4.93 days. Over 50% of the stations analyzed exhibited a peak in their respective meridional spectra at this periodicity (Fig. 4.3-1b). The geographic distribution of the zonal spectral values at the 4.93 day period is shown in Figure B.4-1; the meridional spectral values are presented in Figure B.4-2.

The pronounced tendency to peak at 4.93 days is not as strong nor as evident in the zonal spectral distribution (Fig. 4.3-1a). The meridional spectral values are greater by almost a factor of two over the zonal spectral densities. The 300 mb spectral values are generally greater everywhere than the 200 mb values. All maxima were oriented from Texas to Main which indicated the most favored position of a mean storm track (Fig. 4.2-3).

This frequency is in the time interval of the "cyclone rise" and is well substantiated by other investigators, e.g., Oort and Taylor (1969). Lahey, et al. (1960), computed the kinetic energy per unit volume and plotted these monthly mean values across the United States. Figure B.4-3 presents the kinetic energy diagrams for January, April, July and October. The close resemblance between these diagrams and the distributions shown

shown in Figures B.4-1 and B.4-2 is not surprising since the greatest amount of variance is contributed by the cyclone-anticyclone perturbation.

An area not shown on the previous distributions but also analyzed was the Alaskan peninsula. The most significant feature of the Alaskan spectra was the predominance of a spectral peak at or near the period of 4.93 days for most of the stations. This region corresponded to a location of "maximum number of days with a cyclone within its borders" as defined by Klein (1957). According to Klein (1957), the Gulf of Alaska-Alaska region represents an area with a high frequency of cyclone passage. In addition, this is also an area of frequent cyclogenesis which is more noticeable in the Gulf of Alaska rather than the land mass proper. It is probably for this latter reason that many of the Alaskan stations did not exhibit a frequency peak near 3.36 days. The Alaskan spectra confirmed what was known from weather map analyses (Klein, 1957).

#### B.5 Periodicity of 3.70 Days

Although several stations possessed a peak of 3.70 days in their respective zonal and meridional spectra, this peak was not considered generally significant. The stations indicating this peak were widely scattered and disorganized patterns emerged in the geographical distributions of spectral values for both the zonal and meridional spectra. The general distribution of spectral densities at this period conformed to the gross features described in the previous sections. Little new information was found from an examination of the characteristics of the geographic distributions corresponding to this periodicity.

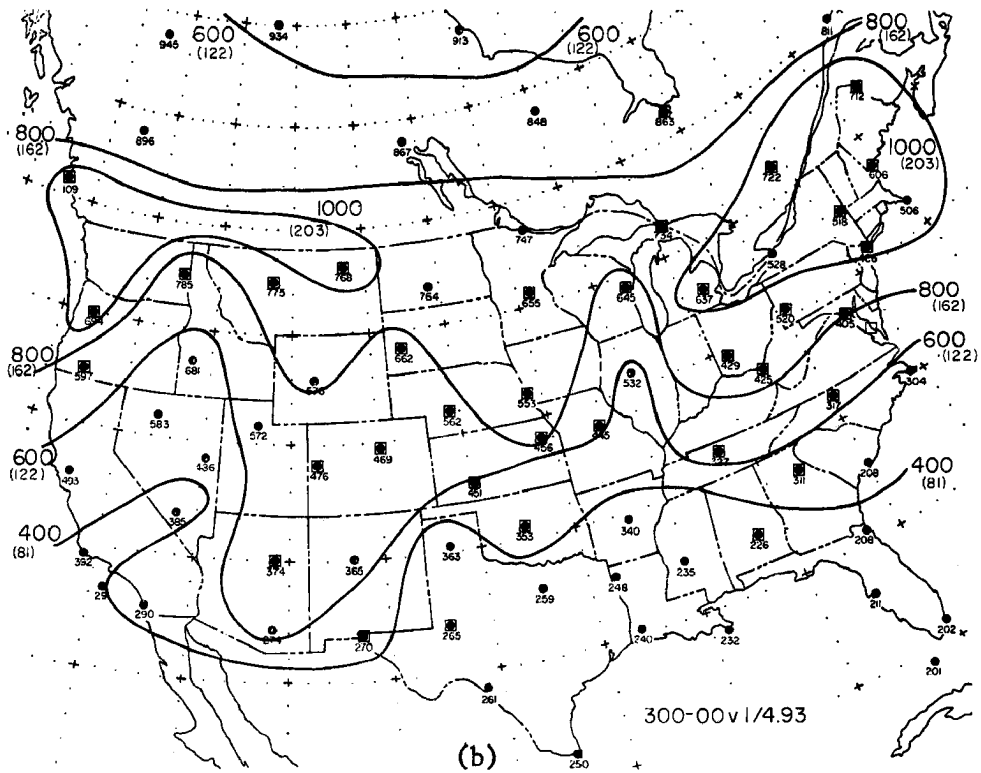
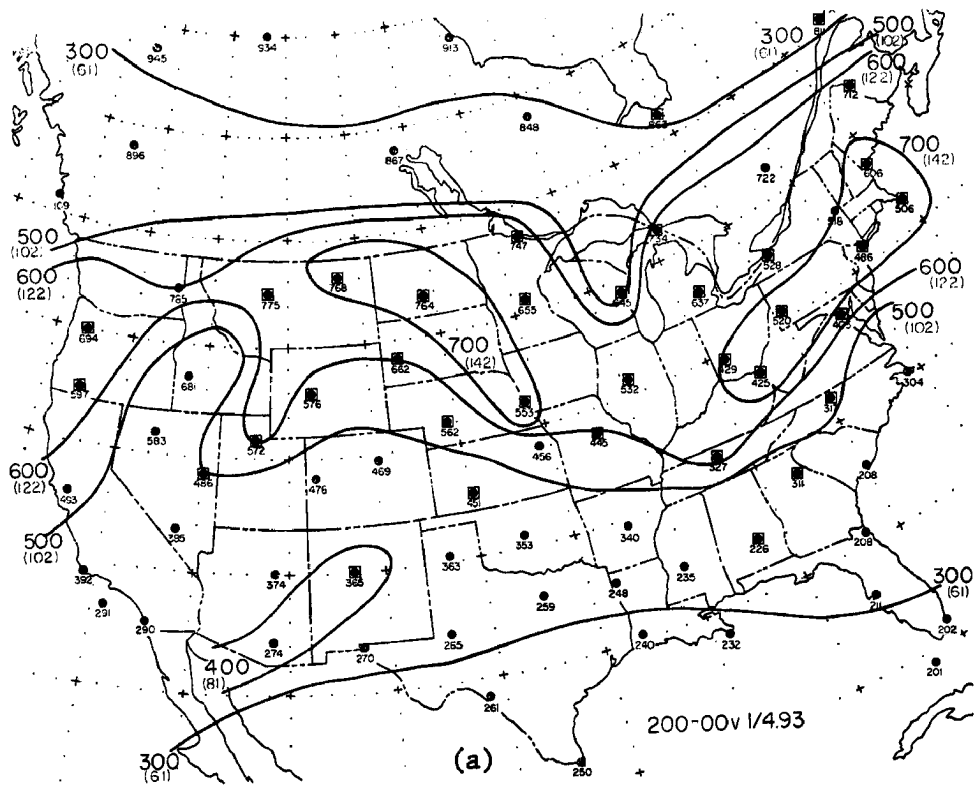


Fig. B.4-1 Geographic distributions of the zonal spectral densities at a period of 4.93 days at the (a) 200 mb and (b) 300 mb constant pressure levels.

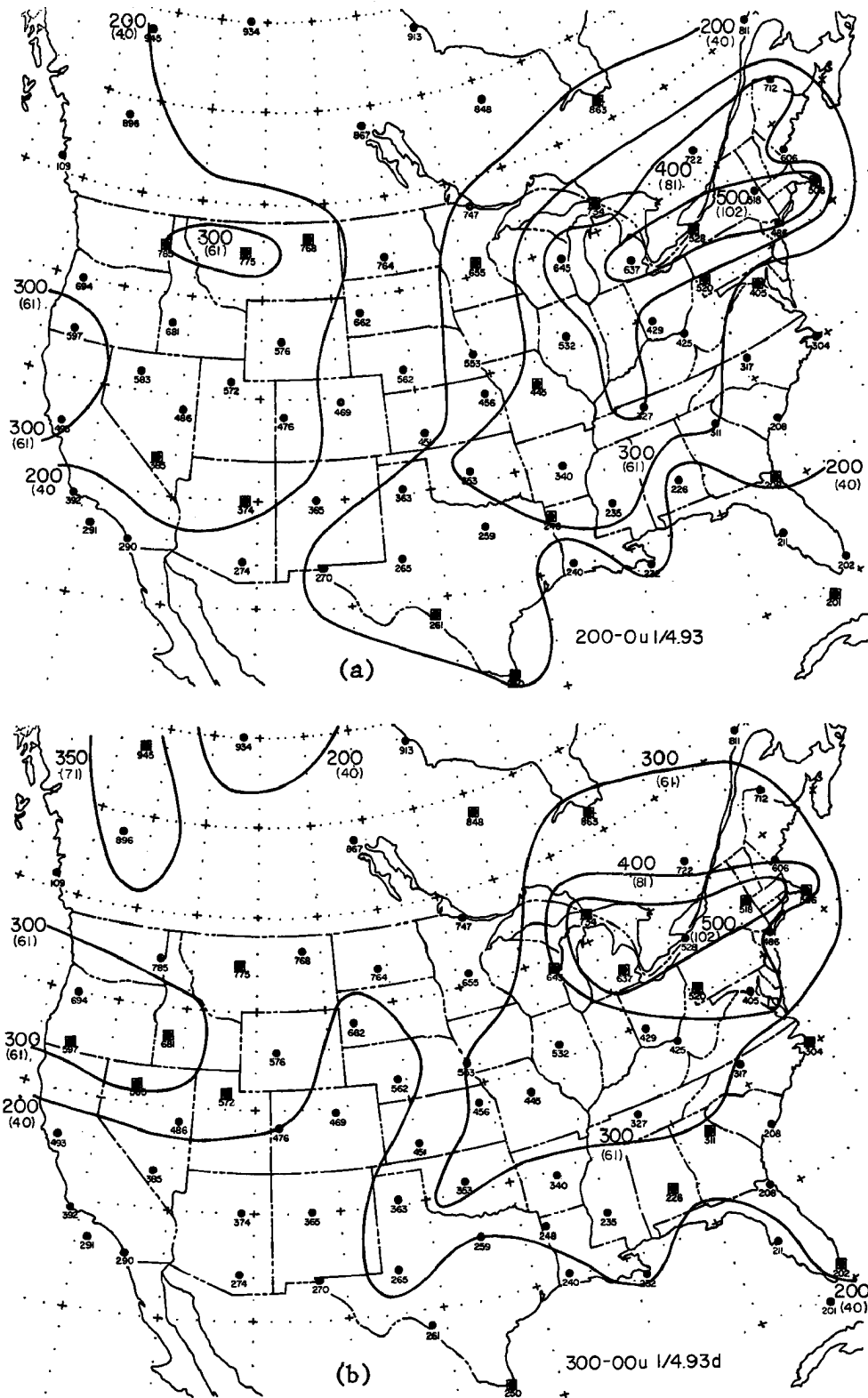
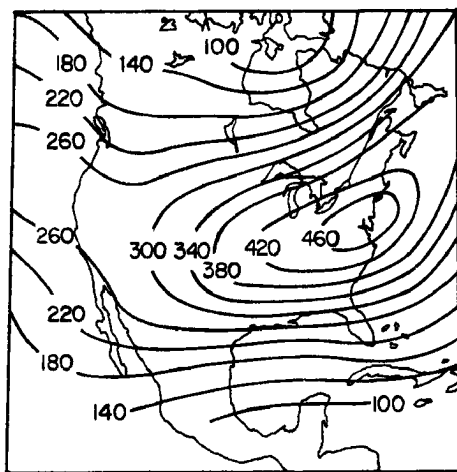
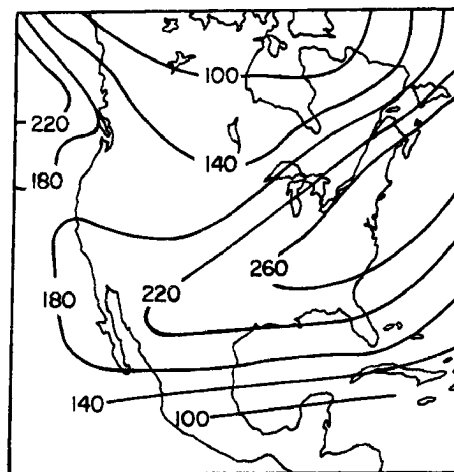


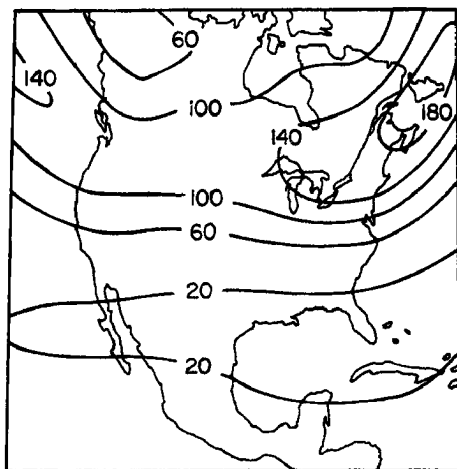
Fig. B.4-2 Geographic distributions of the meridional spectral densities at a period of 4.93 days at the (a) 200 mb and (b) 300 mb constant pressure levels.



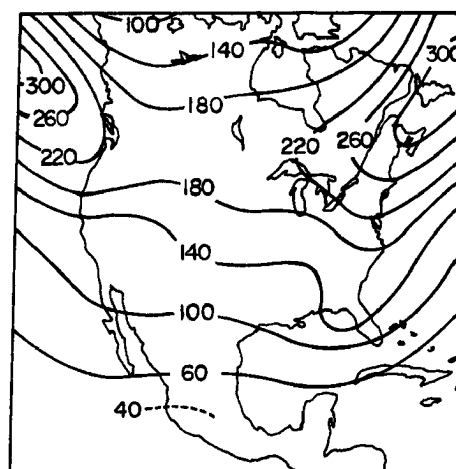
(a)



(b)



(c)



(d)

Fig. B.4-3 Mean kinetic energies per unit volume [ $\text{kg m}^{-1} \text{sec}^{-2}$ ] for (a) January, (b) April, (c) July and (d) October. (After Lahey, et al., 1960)

of spectral densities in this area. The influence of the STJ in these regions is possibly the cause of this peak at 6.17-5.69 days.

The seasonal spectra of Jackson aids in analyzing this period (Chapter 4.5). At both the 200 mb and 300 mb levels during the spring-long season (Chapter 3.1), a definite major peak in the zonal spectra existed at a period of 5.4 days as shown in Figure 4.5-5a. As far as the seasonal breakdown was concerned, this represented a major peak at a frequency contributing significantly to the total variance. This is in contrast to the general trend which, as pointed out earlier, has just been the opposite.

However, this is the only season which possessed such a peak at or near the period of 6 days. It may be inferred from the above analysis that the contribution to the annual spectra near this frequency was due primarily to the appearance of this spectral peak in the spring season.

The 300 mb geographic distribution of zonal spectral densities shows a band of relatively high values oriented southwest-northeast in much the same way as the 9.25 day pattern. Two tongues of minimum spectral energy exist, one in the lee of the Sierra Nevadas and the second in the lee of the Appalachians.

Meridional spectral density geographic distributions also show a considerable difference between the 200 mb and 300 mb constant pressure levels (Fig. B.3-2). At 300 mb the stations which possessed a peak at a period of 6.17 days were located along the east coast of the United states from Nantucket to Charleston; the 200 mb meridional spectral density distribution had stations with peaks at this period in the eastern Washington-Idaho-Montana-Western South Dakota area. Three areas of maximum spectral density clearly stand out in Figure B.3-2b: the Pacific

### B.6 Periodicity of 3.36 Days

Figures B.6-1 and B.6-2 represent the zonal and meridional spectral energy geographic distributions for the period of 3.36 days at the 200 mb and 300 mb levels. With the exception of the 300 mb meridional spectral distribution, an area of minimum values persisted in the Rocky Mountain region. Most notable was the widespread minimum west of the Rockies which extended into the northern Plains and throughout Canada. The maximum zonal spectral energy densities existed in the eastern and central states whereas the maximum in the meridional spectral distribution occurred in the North Dakota-Minnesota-Wisconsin region.

The 300 mb spectral values exceeded the values at 200 mb for both spectra demonstrating that the phenomena causing this peak is more easily discernable at the lower constant pressure level. It could be that at the 200 mb level only the strongest features of the wind regimes persist. The disturbances occurring in the regions below the level of maximum winds are probably more erratic and would, therefore, produce greater variances. At both levels, the Great Basin area is no longer a region of minimum meridional spectral values; in fact, this region is now characterized by having maximum spectral densities at the 3.36 day period. Thus a phenomenon with a period near 3.36 days was affecting the wind pattern in that area which was not true at the longer periods.

The phenomena causing this spectral behavior might be the cyclogenesis and anticyclogenesis occurring in this region. Klein (1957) presented the general patterns of the occurrence of cyclones and anticyclones by analyzing each month individually by region and averaging around latitude circles. As can be seen from his study, the Great Basin

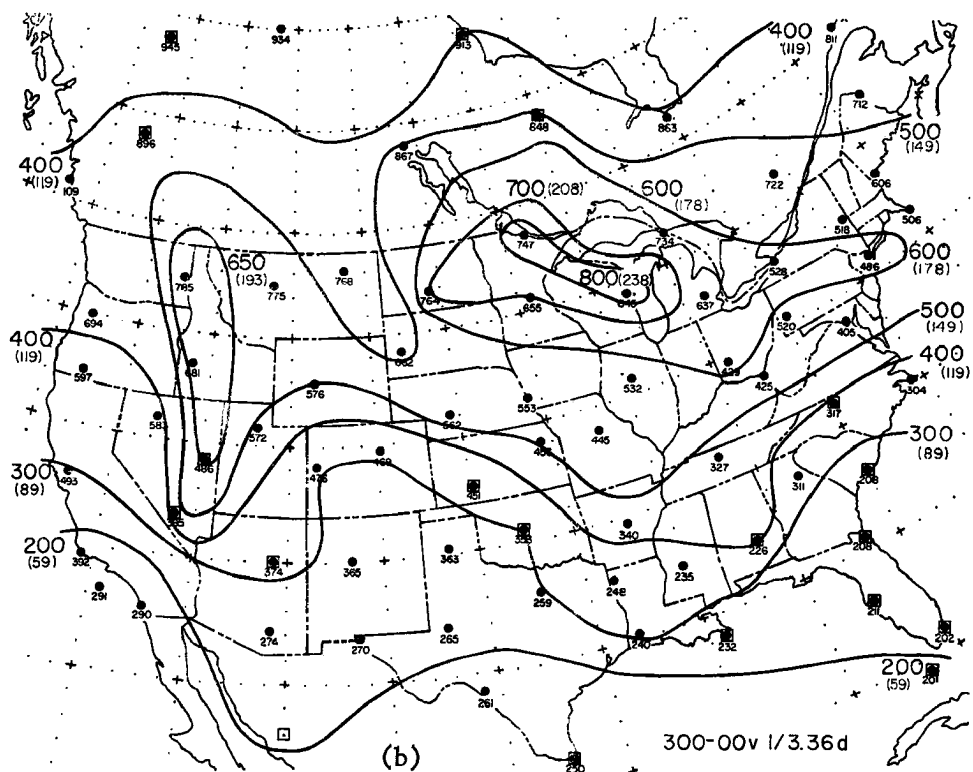
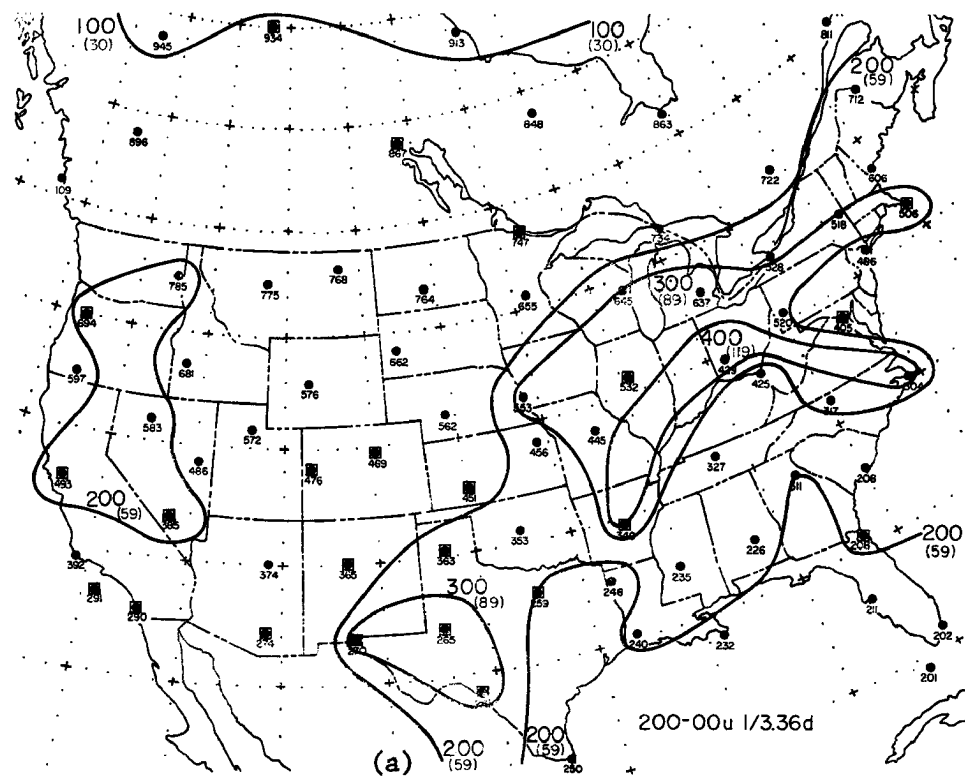


Fig. B.6-1 Geographic distributions of the zonal spectral densities at a period of 3.36 days at the (a) 200 mb and (b) 300 mb constant pressure levels.

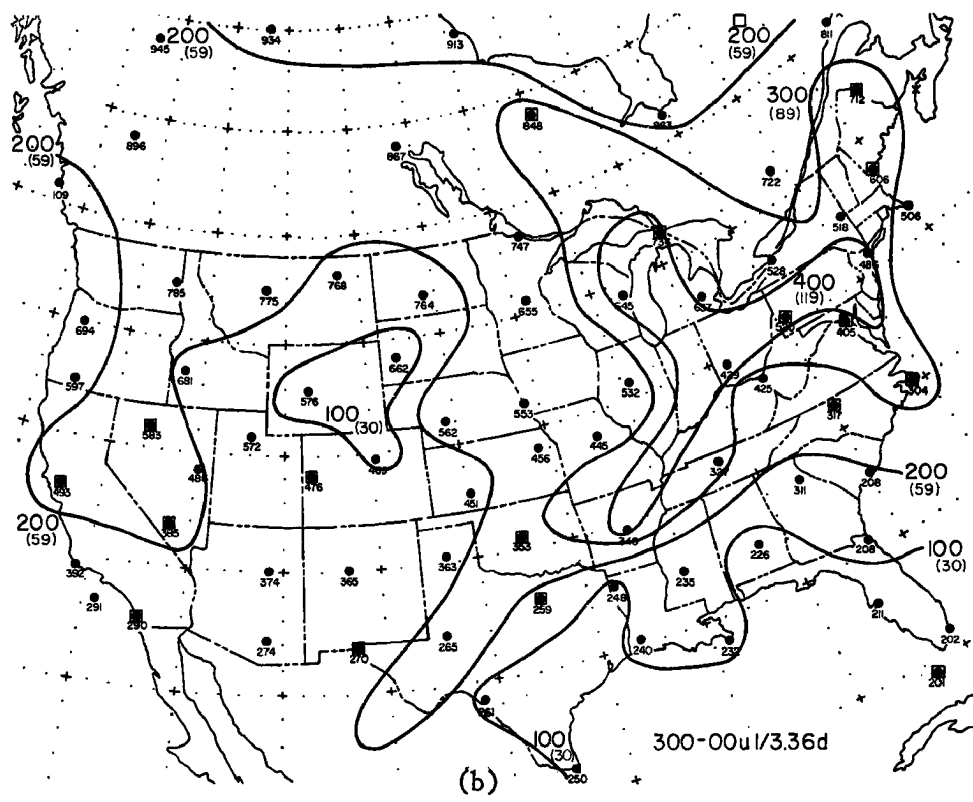
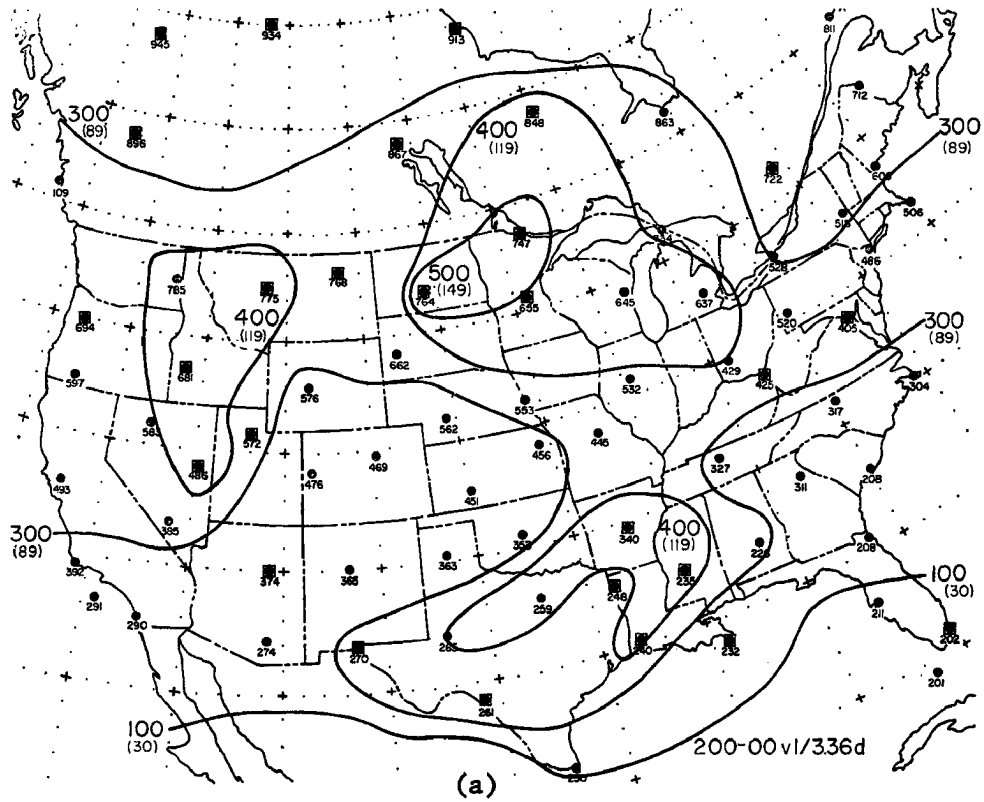


Fig. B.6-2 Geographic distributions of the meridional spectral densities at a period of 3.36 days at the (a) 200 mb and (b) 300 mb constant pressure levels.

is an area of maximum cyclogenesis and anticyclogenesis in most of the months.

Also portrayed on the geographic distributions were the relative kinetic energy values,  $fS(f)$ . In addition to the energies at 4.93 days, the highest kinetic energy values were associated with the 3.36 day period. This was true for both the zonal and meridional spectra as well as for both constant pressure levels. The reason for this is not difficult to understand. The above results demonstrate that the major portion of the energy associated with atmospheric motions occurs within the cyclone frequency range, both in passage of cyclones and in cyclogenesis. The same generalization also applies to anticyclones, though to a lesser extent.

### C.1 General Conclusions from Periodicity Distributions

A few general conclusions might now be summarized. Maximum spectral densities occurred in the Washington, D.C.-Huntington-New York City region in almost all of the geographic distributions for the periods examined. However, these high spectral values do not imply that a peak in the spectra of the respective stations existed. As pointed out previously, this area coincides with the maximum mean kinetic energy region at 300 mb as calculated by Lahey, et al. (1960). Energy values seem to decrease poleward of  $45^{\circ}\text{N}$  and equatorward of  $35^{\circ}\text{N}$ ; this indicates (1) a region of high activity associated with the polar front jet stream, (2) the merging of the PFJ with the STJ over the eastern United States, and (3) the greatest fluctuations in wind regimes due to short wave long wave pattern changes.

Additional areas which had maximum spectral values existed in the Pacific Northwest, often extending along a latitude circle as far eastward as Bismarck, and in the southwest, extending to El Paso, Midland, Dodge City and Omaha. A definite minimum in spectral densities, but not necessarily lacking in significant spectral peaks, was the Great Basin region with the area extending westward to San Diego and southward to Yucca Flats. This behavior can partially be explained by cyclogenesis.

The spectral values of the zonal wind component were usually less than those associated with the meridional wind component which was expected due to the predominantly zonal nature of the upper-tropospheric and lower-stratospheric wind regimes over North America. Since spectrum analysis places more emphasis on the larger or more frequent variations and since there exists more variation in the meridional than in the

zonal component of the wind, the meridional spectral values would be greater than the zonal spectral densities.

In general, the spectral values at the 300 mb level were greater than those at the 200 mb constant pressure level. If one assumes that the mean height of the level of maximum wind lies at or near the 250 mb level (Reiter, 1963), then the above observation indicates that the shear of the horizontal wind below the LMW is less than the shear above it. Reiter (1963) found this to be the situation.

Finally, a major portion of the kinetic energy associated with atmospheric motions was shown to occur within the 3-5 day period. This can easily be accounted for by the passage and generation of cyclones and anticyclones. Thus, the spectra analyzed provided new insights into the upper-tropospheric and lower-stratospheric wind regimes and flow patterns over North America.